

Cosmological gravitational particle production and its implications for cosmological relics

Edward W. Kolb^{1,*} and Andrew J. Long^{2,†}

¹*Kavli Institute for Cosmological Physics and Enrico Fermi Institute,
The University of Chicago,
5640 S. Ellis Ave., Chicago,
Illinois 60637 USA*

²*Department of Physics and Astronomy,
Rice University, Houston,
Texas 77005 USA*

(Dated: December 14, 2023)

Cosmological gravitational particle production (CGPP) is the creation of particles in an expanding universe due solely to their gravitational interaction. These particles can play an important role in the cosmic history through their connection to various cosmological relics including dark matter, gravitational wave radiation, dark radiation, and the baryon asymmetry. This review explains the phenomenon of CGPP as a consequence of quantum fields in a time-dependent background, catalogs known results for the spectra and cosmological abundance of gravitationally produced particles of various spins, and explores the phenomenological consequences and observational signatures of CGPP.

CONTENTS

I. Introduction	1	L. Observational: laboratory tests	38
II. Historical development	3	M. Observational: dark matter isocurvature	39
III. Theoretical framework	4	N. Observational: non-Gaussianity	40
A. Quantum scalar field in an FLRW spacetime	5	O. Observational: small-scale structure	40
B. Mode functions and Bogolubov transformations	6	P. Observational: signatures of late time decay	41
C. Energy, renormalization, and observables	10	VII. Outlook	41
IV. CGPP for spin-0 particles	13	Acknowledgments	42
A. Inflationary cosmology	13	A. General relativity	42
B. Mode evolution and spectrum	17	B. FLRW spacetime	45
C. Resultant particle abundance	21	C. de Sitter spacetime	47
D. Inhomogeneity	22	D. JWKB Method	48
V. Extension to fields with spin	23	References	51
A. CGPP requires conformal symmetry breaking	23		
B. Massive spin-1/2 field	24		
C. Massive spin-1 field	25		
D. Massive spin-3/2 field	27		
E. Massive spin-2 field	28		
F. Numerical comparison	30		
G. Higher-spin particles	30		
VI. Recent and ongoing activity	31		
A. Modeling: nonminimal gravitational interaction	31		
B. Modeling: scale and shape of inflaton potential	31		
C. Modeling: gravity-mediated thermal freeze-in	32		
D. Modeling: gravity-mediated inflaton annihilation	33		
E. Modeling: interference effects	34		
F. Relics: dark matter	35		
G. Relics: gravitational reheating	36		
H. Relics: baryogenesis	36		
I. Relics: dark radiation	37		
J. Relics: gravitational wave radiation	37		
K. Relics: primordial black holes	38		

I. INTRODUCTION

The hot early universe as a potential site for production of elementary particles has been proposed as an explanation for the origin of dark matter, to limit the properties of known elementary particles, and to explore the consequences of new hypothetical particle species. The universe is also a convenient laboratory to study the properties of known particle species with very long lifetimes and very weak interactions. It is usually stated that an important feature of the big-bang laboratory for particle physics is that the high temperatures of the early universe are capable of producing particles of mass far beyond the reach of terrestrial accelerators. However there are two caveats to this statement.

1. Utilizing the hot primordial plasma as a source of new particles usually assumes that the particles have interactions with standard-model (SM)

* rocky.kolb@uchicago.edu

† andrewjlong@rice.edu

particles. But what about a new particle species without interactions with SM particles? (When we speak of interactions with SM particles we do not include gravitational interactions.) Indeed, many ideas for beyond the standard model (BSM) physics involve “hidden” sectors, “secluded” particles, the “shadow” world, or reclusive particle species with interactions too weak to be populated in the primordial plasma. In the extreme, these new particles may *only* interact with SM particles via the gravitational force, and their cosmological origin must have been through gravity. That is the possibility we explore in this review, although many of our results would remain unchanged if the interactions of the new species with SM particles are sufficiently weak.

2. For a particle species to be produced from the primordial plasma, the temperature of the universe must have been high enough to produce the particles. But in inflation models the maximum temperature of the radiation-dominated universe may be as low as a few MeV without coming into conflict with observations (de Salas *et al.*, 2015). But we focus on the mechanism of Cosmological Gravitational Particle Production (CGPP) that may produce particles of mass comparable to the scale of inflation, possibly as large as 10^{14} GeV, even if the reheat temperature is much less than the mass of the particle or the mass scale of inflation.

There are several proposed scenarios for CGPP. This review focus on gravitational particle production from the vacuum as the result of a time evolution of the background gravitational field due to the expansion of the universe. (When we refer to CGPP, we refer to this mechanism.) Cosmological Gravitational Particle Production is an example of a “semiclassical” process in the sense that the external gravitational field is not quantized, but a “spectator” field *is* quantized, and the production of the spectator field is a quantum effect. We will assume that the background geometry is rigid: the spectator field has no backreaction on the geometry. This is justified *ex post facto* by the result that particle production is a small effect; the energy density contributed by produced particles does not dominate the mass-energy density until possibly late in the history of the universe when a classical description of the spectator field is appropriate. Although CGPP will be a tiny effect in the early universe, if the mass of the produced particle is large enough, the spectator species may come to dominate the mass density of the universe at late times when they behave classically.

The most familiar example of particle production in an external field is the “Schwinger Effect,” in which a sufficiently strong external electric field leads to the emergence of electron-positron pairs from the vacuum. The effect, first predicted by Heisenberg and Euler (Heisen-

berg and Euler, 1936) based upon work of Sauter (Sauter, 1931), was completely understood in 1951 by Schwinger (Schwinger, 1951), with a complete theoretical description using quantum electrodynamics (QED). The basic idea is that an external electric field interacts with virtual particles, accelerating electrons in one direction and positrons in the opposite direction. If the external field is strong enough to accelerate particles to energies greater than its mass over a distance smaller than or equal to the Compton wavelength of the particle, $|\vec{E}| > |\vec{E}_{\text{crit}}| = m_e^2 c^3 / e \hbar$, then virtual particles can be “pulled” out of the vacuum and propagate as real particles. The rate for this is proportional to $\exp(-\pi |\vec{E}_{\text{crit}}| / |\vec{E}|)$.

We can use the Schwinger effect as an exemplar to envision pair production in the expanding universe (Audreetsch and Schaefer, 1978; Martin, 2008). Imagine a pair of virtual particles being pulled apart due to the expansion of the universe. As space expands the recession velocity of the particles increases with distance ($v = Hd$; Hubble’s law). At a distance equal to m^{-1} , the velocity would be H/m . In order for this to be of order unity requires H to exceed a critical value $H_{\text{crit}} \sim m$. So if $H \gtrsim m$, the particles will obtain relativistic velocities within a Compton wavelength and particle creation is possible. In analogy with the Schwinger effect, one might expect particle production proportional to $\exp(-\pi H_{\text{crit}}/H) \sim \exp(-\pi m/H)$. Indeed, although we will discuss exceptions and details, this will serve as a good guide.

The important aspects of CGPP, as opposed to standard scenarios for cosmological particle production, is that CGPP operates even when the spectator particle does not couple directly to standard model particles or the inflaton, it is possible to produce particles of mass in excess of the largest temperature of the radiation-dominated universe, and CGPP does not depend on coupling of the spectator particle to the particle physics standard model.

Early-universe production from the plasma of SM particles is the most common assumption for the origin of particle dark matter. However, to date, dark matter has stubbornly evaded detection through interactions with Standard Model particles via direct detection, indirect detection, or accelerator production/detection. Perhaps nature is telling us that dark matter may not interact with SM particles other than by gravity. If this is so, presumably the primordial origin of dark matter must be through the gravitational force. Dark matter is significant motivation to study early-universe production of particles solely through gravitational interactions. It is an especially natural mechanism to explain the origin of dark matter, which is only known to interact gravitationally, and may not have any non-gravitational interactions with visible matter. CGPP provides a compelling explanation for the origin of stable relics, and may play a role in other phenomena such as the matter-antimatter asym-

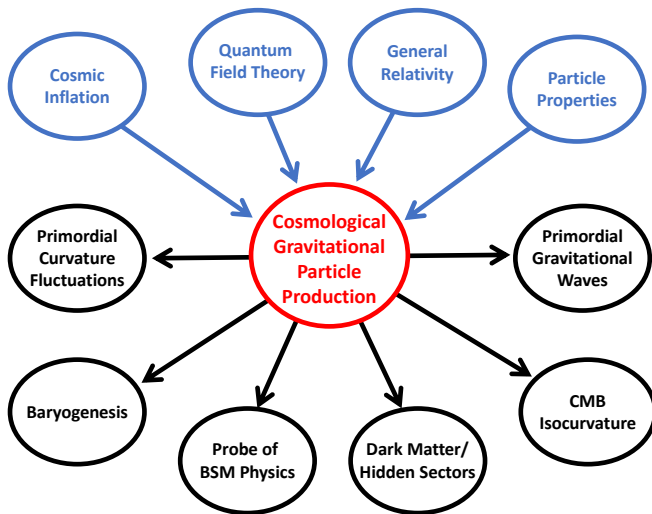


FIG. 1 CGPP takes as input cosmic inflation, quantum field theory, general relativity, and the properties of a particle, and outputs observable or potentially observable consequences.

metry.

Inflationary cosmology is a remarkable success of modern cosmology, with spectacular agreement between theory and observation. Inflation provides a connection between cosmological inhomogeneities measured by Cosmic Microwave Background (CMB) anisotropies and Large-Scale Structure (LSS) observations, and predicts a gravitational-wave background. The origin of the inhomogeneities and gravitational waves traces to CGPP of the inflaton field(s) and the metric field. It is natural to consider the possibility of quantum production of other fields.

Although there has been a lot of recent work on CGPP, it is a phenomenon that has yet to be fully exploited, so we present this review to provide a summary of key results, both classic and recent, and to present a top-to-bottom overview of how the CGPP calculation is performed, so as to provide the reader with the tools they need to exploit the results of CGPP for new applications in cosmology.

The input to CGPP is inflation, quantum field theory, general relativity, and the properties of the spectator particle. The output of CGPP includes the generation of primordial temperature fluctuation, primordial gravitational waves, a possible arena for baryogenesis, a probe of BSM physics, the origin of dark matter and particles in a hidden sector, and CMB isocurvature fluctuations. The CGPP input and output are illustrated in Fig. 1.

The remainder of the article is outlined as follows. Section II contains a short summary of CGPP’s long history. In Sec. III we establish the theoretical framework for CGPP using scalar field theory to develop the extension of quantum field theory (QFT) to curved spacetime. Following that, after reviewing some salient features of

inflationary cosmology, in Sec. IV we present numerical results and analytic approximations for CGPP of spin-0 particles. Section V contains a discussion of CGPP for particles with non-zero spin. Then, in Sec. VI we review some recent work involving CGPP for the production of cosmological relics and observational signatures. Appendix A contains a brief refresher on GR, including the frame-field formalism needed for CGPP of fermions, and establishes the sign choices employed in the main body of the paper. In Appendix B we summarize key results for Friedmann-Lemaître-Robertson-Walker (FLRW) spacetimes. In Appendix C we present the solutions to the mode equation in de Sitter space. Finally, Appendix D reviews the Jeffreys-Wentzel-Kramers-Brillouin (JWKB) method for solving wave equations of the form encountered in CGPP calculations.

II. HISTORICAL DEVELOPMENT

The phenomenon of cosmological gravitational particle production has been explored through various studies over the course of nearly a century. CGPP provides a robustly calculable and practically testable prediction of quantum field theory in curved spacetime. The most well-studied application of CGPP is the study of inflationary quantum fluctuations in the scalar inflaton field and metric, which lead to inhomogeneities in the spatial distribution of matter and radiation that imprint onto the anisotropies of the cosmic microwave background radiation and large scale structure of the Universe. Other work on CGPP has sought to apply this phenomenon in explaining the origin of cosmological relics such as dark matter. In this short section we offer a brief overview of the key historical developments in the study of CGPP.

The first paper discussing the creation of particle pairs in the expanding universe was Schrödinger’s 1939 paper *The Proper Vibrations of the Expanding Universe* (Schrödinger, 1939). In this prescient paper Schrödinger was the first to realize that the expansion of the universe can mix positive- and negative-frequency mode solutions of the wave equation. Schrödinger described this as “mutual adulteration” of positive and negative frequency modes in what he regarded as an “alarming phenomenon.” He recognized mutual adulteration as production (or annihilation) of matter “merely by the expansion of the universe.” He stated that this was a phenomenon of “outstanding importance,” although he did not make clear why. The paper certainly does not contain a full field theoretical calculation (it was, after all, in 1939), and there are a few technical stumbles. Notably, Schrödinger suggested that CGPP should occur for photons, but in the Einstein–Maxwell theory (massless photons minimally coupled to gravity) the presence of conformal (Weyl) invariance prohibits CGPP.

Research on particle creation in a background gravita-

tional field did not restart in earnest until the thesis of Leonard Parker in 1965 (Parker, 1965) and papers following his thesis. Parker’s treatment was the first field-theoretical analysis. In the conclusion of a 1968 paper (Parker, 1968), Parker wrote “...for the early stages of a Friedmann expansion it [particle creation] may well be of great cosmological significance, especially since it seems inescapable if one accepts quantum field theory and general relativity.” Parker does not speculate what the great cosmological significance might be. Parker continued to develop the concept, first alone (Parker, 1969, 1971, 1972), and then with collaborators including Fulling, Ford, and Hu (Ford and Parker, 1977a,b, 1978; Fulling and Parker, 1974; Fulling *et al.*, 1974; Parker and Fulling, 1974). At the same time Hawking (Hawking, 1974) was developing the theory of particle creation by black holes, another example of gravitational particle production in a curved spacetime, albeit not *cosmological* gravitational particle production resulting from the expanding universe. The Birrell and Davies (1984) textbook includes an excellent review of this early literature.

Soon after Parker’s 1968 paper, in the Soviet Union Ya. B. Zel’dovich (Zel’dovich, 1970) considered particle production in a cosmological setting with a background Kasner metric, a homogeneous, anisotropic metric of the form $(ds)^2 = (dt)^2 - \sum_{i=1}^3 t^{2p_i} (dx^i)^2$. It is a vacuum solution of Einstein’s equation if the Kasner exponents p_i satisfy $\sum_{i=1}^3 p_i = \sum_{i=1}^3 p_i^2 = 1$. Zel’dovich appreciated cosmological particle creation, and he used the Kasner model to explore whether particle creation could isotropize an initially anisotropic universe, and by extension, explain how physical processes could turn an initial anisotropic/inhomogeneous universe into the observed homogeneous/isotropic universe. Zel’dovich continued this line of research in a series of papers, both alone and with Alexei Starobinski (Zel’dovich and Starobinski, 1977; Zeldovich and Starobinsky, 1972). Zel’dovich indeed identified a problem of great significance that is now generally assumed to be solved by inflation. Others, such as Starobinski, Grib, Frolov, Mamaev, and Mostepanenko turned to calculations of particle creation in homogeneous and isotropic cosmologies (Frolov *et al.*, 1976; Grib *et al.*, 1976; Mamaev *et al.*, 1976). A more complete set of references to work from the Soviet Union may be found in the book *Quantum Effects in Strong External Fields* by Grib, Mamaev, and Mostepanenko (Grib *et al.*, 1994).

In the 1980’s CGPP found a new home in the recently proposed theory of cosmological inflation. This early period of accelerated expansion was initially lauded for efficiency at simultaneously solving the horizon, flatness, and monopole problems that had confounded early efforts to connect cosmology with elementary particle physics. Before long, studies of quantum fluctuations in the scalar inflaton field and the metric led to predictions for density perturbations (as well as gravitational-wave radia-

tion) that provided an explanation for the inhomogeneity of the large scale structure of the Universe and the subtle anisotropies in the cosmic microwave background radiation. The first papers explicitly to link density perturbations to particle creation were by Mukhanov and Chibisov (1981), Mukhanov (1988) and Sasaki (1983); see also Kodama and Sasaki (1984). This early literature is summarized well in the review by Mukhanov, Feldman, and Brandenberger (Mukhanov *et al.*, 1992). Precision measurements of the large scale structure and cosmic microwave background have furnished a wealth of information about the composition and evolution of the Universe, and their connections with the epoch of inflation are made possible through the phenomenon of CGPP.

Besides generating primordial density perturbations, and possibly also gravitational-wave radiation, the phenomenon of CGPP during inflation may have served another purpose of great significance. Namely, it may have provided an origin for cosmological relics such as dark matter, the matter-antimatter asymmetry, or the primordial plasma itself through gravitational reheating. This idea was first explored by Ford (1987) and Turner and Widrow (1988) who sought to explain the origin of light scalar (axion) dark matter via CGPP. A series of studies in 1998 (Chung, 2003; Chung *et al.*, 1998a,b; Kuzmin and Tkachev, 1998, 1999) emphasized the novel role of CGPP for creating superheavy dark matter with mass comparable to the inflationary Hubble scale $m \approx H_{\text{inf}}$. They also expanded the scope of interest to include CGPP for fermionic dark matter. A natural candidate for CGPP is the gravitino that arises in theories of supergravity (Giudice *et al.*, 1999a,b; Kallosh *et al.*, 2000; Kolb *et al.*, 2021a), since it may couple very weakly to ordinary matter and may not thermalize with the plasma.

The last several years have seen a growing interest in the phenomenon of CGPP and its implications for cosmological relics. Several recent developments are discussed throughout the article, particularly in Sec. VI. These include: the production of ultralight spin-1 particles and connections to isocurvature-free dark photon dark matter; the enhanced production of massive spin-3/2 particles due to instabilities associated with a vanishing effective sound speed; the production of particles via thermal freeze-in with a gravitational mediator; the reinterpretation of CGPP at the end of inflation as inflaton annihilations; and efforts to detect dark matter’s gravitational interactions in the laboratory.

III. THEORETICAL FRAMEWORK

In this section we offer a detailed review of the theoretical framework underlying CGPP, including aspects of quantum field theory in curved spacetime. Complementary discussions can be found in classic textbooks, such as

Birrell and Davies (1984), Mukhanov (2005), Mukhanov and Winitzki (2007), and Parker and Toms (2009), as well as more recent reviews (Armendariz-Picon and Diez-Tejedor, 2023; Ford, 2021) and books, *e.g.*, (Baumann, 2022). Our goals here are (1) to illuminate how the framework of quantum field theory in curved spacetime is employed to derive the equations of motion for the time-dependent Fourier mode amplitudes $\chi_k(\eta)$, (2) to clarify how the cosmological expansion induces a mixing of positive- and negative-frequency mode functions, (3) to explain why this mixing can be interpreted as particle production, and (4) to address the emergence of ultraviolet divergences in the calculation of observables. In this section we will use scalar quantum field theory to develop formalism and illustrate notation.

A. Quantum scalar field in an FLRW spacetime

Covariant action for a scalar field. Let $\Phi(x)$ be a real scalar field, which has spin-0 particles as its quantum excitations, and let the classical spacetime metric be denoted by $g_{\mu\nu}(x)$. We consider a massive scalar that only interacts with gravity. See Appendix A for a refresher on general relativity and an explanation of our conventions. We consider a theory defined by the action

$$S[\Phi(x), g_{\mu\nu}(x)] = \int d^4x \sqrt{-g} \left[\mathcal{L} - \frac{1}{2} M_{\text{Pl}}^2 R \right] \quad (1)$$

$$\mathcal{L} = \frac{1}{2} g^{\mu\nu} \nabla_\mu \Phi \nabla_\nu \Phi - \frac{1}{2} m^2 \Phi^2 + \frac{1}{2} \xi \Phi^2 R .$$

This theory has three model parameters: the reduced Planck mass $M_{\text{Pl}} = (8\pi G)^{-1/2}$, the scalar field's mass m , and the scalar field's coupling to the Ricci scalar, ξ . In the context of inflationary cosmology Φ is not the inflaton, but rather an additional scalar spectator field.

Nonminimal coupling to gravity. The dimensionless parameter ξ is the coefficient of the dimension-4 operator coupling Φ to the Ricci scalar. For $\xi = 0$ we say that the scalar field is minimally coupled to gravity, and for $\xi = 1/6$ it is conformally coupled to gravity; and for other nonzero values of ξ it is merely nonminimally coupled to gravity. From the perspective of effective field theory, $\Phi^2 R$ is just one of many possibly operators that parametrize Φ 's gravitational interactions; see Sec. VI A for an extended discussion. The motivation for focusing on the $\Phi^2 R$ operator is primarily pedagogical. The theory of a conformally coupled scalar ($\xi = 1/6$) leads to equations of motion that are similar to the ones arising in theories of minimally-coupled fermions and vectors. We seek to build intuition for these equations and their solutions by first investigating the simpler scalar context.

FLRW spacetime. We seek to study the phenomenon of

CGPP in cosmological spacetimes, which are approximately homogeneous, isotropic, and expanding. Such spacetimes are described by the Friedmann-Lemaître-Robertson-Walker (FLRW) metric:

$$g_{\mu\nu}^{\text{FLRW}}(x) = a^2(\eta) \text{diag}(1, -1, -1, -1) \quad (2)$$

where the spacetime coordinate 4-vector $x^\mu = (\eta, \mathbf{x})$ has been written in terms of the conformal time coordinate η , related to coordinate time t by $a d\eta = dt$, and the comoving spatial coordinate 3-vector $\mathbf{x} = (x, y, z)$. The time-dependent function $a(\eta)$ is called the scale factor, and the spatial expansion rate $H(\eta) = a'(\eta)/a^2(\eta)$ is called the Hubble parameter. Primes denote derivatives with respect to conformal time, and $\nabla = (\partial_x, \partial_y, \partial_z)$ denotes derivatives with respect to comoving spatial coordinates. One can evaluate the usual tensors that arise in GR, finding for the Ricci scalar $R(\eta) = -6a''/a^3 = -12H^2 - 6H'/a$. See Appendix B for a refresher on the FLRW spacetime.

Canonical kinetic term in FLRW spacetime. In the FLRW spacetime the scalar field kinetic term is not canonical, since $\sqrt{-g} g^{\mu\nu} \propto a^2$. Upon performing a change of variables $\Phi(\eta, \mathbf{x}) = a^{-1}(\eta) \phi(\eta, \mathbf{x})$, the kinetic term is rendered canonically normalized, and the action becomes

$$S^{\text{FLRW}}[\phi(\eta, \mathbf{x})] = \int d\eta \int d^3\mathbf{x} \left[\frac{1}{2} (\phi')^2 - \frac{1}{2} |\nabla \phi|^2 - \frac{1}{2} a^2 m_{\text{eff}}^2 \phi^2 - \frac{1}{2} \partial_\eta (a H \phi^2) \right], \quad (3)$$

$$m_{\text{eff}}^2(\eta) = m^2 + \left(\frac{1}{6} - \xi \right) R(\eta) .$$

Notice that the canonically normalized field variable $\phi(\eta, \mathbf{x})$ acquires a time-dependent effective squared mass $a^2(\eta) m_{\text{eff}}^2(\eta)$, which may be either positive or negative.

Hamiltonian. The scalar field's dynamics are equivalently captured in the Hamiltonian formalism. Denoting the field and its conjugate momentum density by $\phi(\eta, \mathbf{x})$ and $\pi(\eta, \mathbf{x})$, the Hamiltonian may be written as

$$H(\eta) = \int d^3\mathbf{x} \left[\frac{1}{2} \pi^2 + \frac{1}{2} |\nabla \phi|^2 + \frac{1}{2} a H (\pi \phi + \phi \pi) + \frac{1}{2} (a^2 m_{\text{eff}}^2 + 2a^2 H^2 + a H') \phi^2 \right]. \quad (4)$$

We write $\pi \phi + \phi \pi$ because after quantization $[\pi, \phi] \neq 0$.

Canonical quantization. We work in the Heisenberg picture in which operators evolve subject to the Heisenberg equations of motion $i \partial_\eta \mathcal{O} = [\mathcal{O}, H]$ and states are static $i \partial_\eta |\psi\rangle = 0$. Now ϕ and π will be regarded as quantum operators. Canonical quantization is accomplished by imposing equal-time commutation relations

$$\begin{aligned} [\phi(\eta, \mathbf{x}), \pi(\eta, \mathbf{y})] &= i \delta(\mathbf{x} - \mathbf{y}) \\ [\phi(\eta, \mathbf{x}), \phi(\eta, \mathbf{y})] &= [\pi(\eta, \mathbf{x}), \pi(\eta, \mathbf{y})] = 0 . \end{aligned} \quad (5)$$

The operator equations of motion are

$$\begin{aligned}\pi' &= \nabla^2 \phi - aH\pi - (a^2 m_{\text{eff}}^2 + 2a^2 H^2 + aH')\phi \\ \phi' &= \pi + aH\phi ,\end{aligned}\quad (6)$$

and they combine to give

$$\phi'' - \nabla^2 \phi + a^2 m_{\text{eff}}^2 \phi = 0 , \quad (7)$$

which takes the form of a second-order linear wave equation with a time-dependent effective mass. For any solution of this equation, the corresponding conjugate momentum density is simply $\pi = \phi' - aH\phi$, so we are free to focus on solving the wave equation.

Evolution equations. Solutions of the linear wave equation take the form

$$\begin{aligned}\phi(\eta, \mathbf{x}) &= \int \frac{d^3 \mathbf{k}}{(2\pi)^3} \left[a_{\mathbf{k}} U_{\mathbf{k}}(\eta, \mathbf{x}) + a_{\mathbf{k}}^\dagger V_{\mathbf{k}}(\eta, \mathbf{x}) \right] \\ \text{with } U_{\mathbf{k}}(\eta, \mathbf{x}) &= \chi_k(\eta) e^{i\mathbf{k} \cdot \mathbf{x}} \quad \text{and} \quad V_{\mathbf{k}} = U_{\mathbf{k}}^* .\end{aligned}\quad (8)$$

The complex fields $U_{\mathbf{k}}(\eta, \mathbf{x})$ and $V_{\mathbf{k}}(\eta, \mathbf{x})$, called the mode functions, are labeled by a comoving wavevector \mathbf{k} with comoving wavenumber $k = |\mathbf{k}|$. The mode functions are orthonormal basis functions that span the space of solutions of the wave equation. The complex functions $\chi_k(\eta)$ are called the Fourier mode amplitudes (or sometimes also the mode functions). A ladder operator is assigned to each mode function: $a_{\mathbf{k}}$ are paired with $U_{\mathbf{k}}(\eta, \mathbf{x})$ and $a_{\mathbf{k}}^\dagger$ are paired with $V_{\mathbf{k}}(\eta, \mathbf{x})$. The ladder operators are required to obey the usual algebra of commutation relations

$$\begin{aligned}[a_{\mathbf{k}}, a_{\mathbf{q}}^\dagger] &= (2\pi)^3 \delta(\mathbf{k} - \mathbf{q}) \\ [a_{\mathbf{k}}, a_{\mathbf{q}}] &= [a_{\mathbf{k}}^\dagger, a_{\mathbf{q}}^\dagger] = 0 .\end{aligned}\quad (9)$$

Since the wave equation is second order, for each \mathbf{k} it admits a two-dimensional space of solutions, and much of the analysis of CGPP is based on identifying a ‘good’ basis of mode functions to span this space such that $U_{\mathbf{k}}(\eta, \mathbf{x})$ corresponds to positive-frequency modes and $V_{\mathbf{k}}(\eta, \mathbf{x})$ corresponds to negative-frequency modes. We discuss this issue at length in the next subsection. In lieu of specifying explicit expressions for the mode functions at this point, we assume for the moment that they form a complete and orthonormal basis, which is expressed by the Wronskian conditions

$$\begin{aligned}\int d^3 \mathbf{x} (U_{\mathbf{k}} V_{\mathbf{q}}' - V_{\mathbf{q}} U_{\mathbf{k}}') &= i (2\pi)^3 \delta(\mathbf{k} - \mathbf{q}) \\ \text{implying: } \chi_k \chi_k'^* - \chi_k^* \chi_k' &= i .\end{aligned}\quad (10)$$

The wave equation leads to equations of motion for the Fourier mode amplitudes, called the mode equation:

$$\chi_k''(\eta) + \omega_k^2(\eta) \chi_k(\eta) = 0 . \quad (11)$$

For each k this is a harmonic oscillator equation with time-dependent comoving squared angular frequency

$$\omega_k^2(\eta) = k^2 + a^2(\eta) m^2 + \left(\frac{1}{6} - \xi\right) a^2(\eta) R(\eta) . \quad (12)$$

Note that $\omega_k^2(\eta)$ need not be positive. The next subsection is dedicated to discussing the solutions of Eq. (11).

The equation of motion presented here (11) resembles the Mukhanov-Sasaki equation (Baumann, 2022), and they capture similar physics: the evolution of scalar field perturbations during an inflationary phase. However, they differ insofar as the Mukhanov-Sasaki equation accounts for the backreaction of the inflaton perturbations on the scalar metric perturbations through the Einstein equation, whereas our derivation neglects this backreaction since our scalar spectator field does not dominate the energy density of the universe.

B. Mode functions and Bogolubov transformations

The mode functions $\chi_k(\eta)$ evolve according to the mode equation (11). We are interested in solving these equations for cosmologically relevant spacetimes, characterized by a quasi-de Sitter (qdS) phase of inflation followed by reheating, radiation-domination, and so on. To understand how such solutions are obtained, we begin by focusing on the conceptually and computationally simpler cases of Minkowski spacetime and general asymptotically-flat spacetimes. After discussing Bogolubov transformations and CGPP in this context, we move on to address cosmologically relevant spacetimes.

Minkowski spacetime. In Minkowski spacetime the FLRW scale factor is constant $a(\eta) = \bar{a}$ and there is no cosmological expansion, $H(\eta) = \bar{H} = 0$ and $R(\eta) = \bar{R} = 0$. The squared angular frequency is also constant, $\omega_k^2(\eta) = \bar{\omega}_k^2 = k^2 + \bar{a}^2 m^2$. For each wavevector \mathbf{k} , the mode equation (11) is a linear, second-order differential equation in a complex variable, and its solutions form a four-dimensional vector space.¹ Every solution can be written as a linear combination of a pair of basis functions with complex coefficients normalized to satisfy Eq. (10). The canonical basis functions, $e^{-i\bar{\omega}_k \eta} / \sqrt{2\bar{\omega}_k}$ and $e^{i\bar{\omega}_k \eta} / \sqrt{2\bar{\omega}_k}$, are called the positive- and negative-frequency modes, respectively. The positive-frequency mode functions are

$$\chi_k(\eta) = \frac{e^{-i\bar{\omega}_k \eta}}{\sqrt{2\bar{\omega}_k}} \quad \text{or} \quad U_{\mathbf{k}}(\eta, \mathbf{x}) = \frac{e^{-i(\bar{\omega}_k \eta - \mathbf{k} \cdot \mathbf{x})}}{\sqrt{2\bar{\omega}_k}} , \quad (13)$$

and they correspond to plane waves propagating in the direction of \mathbf{k} with phase velocity ω_k/k . When this set

¹ Solutions of the wave equation (7) form only a two-dimensional vector space per Fourier mode, since $\phi \in \mathbb{R}$, but the parametrization in Eq. (8) introduces a two-fold redundancy.

of mode functions are used to construct the field operator via Eq. (8), the associated ladder operators $a_{\mathbf{k}}$ define a vacuum state $|0\rangle$ such that $a_{\mathbf{k}}|0\rangle = 0$ for all \mathbf{k} . Minkowski spacetime is privileged insofar as all inertial observers agree on the absence of particles in this vacuum state, and the presence of particles in excited states (Birrell and Davies, 1984). In other words, there is no CGPP in Minkowski spacetime.

Building intuition. Minkowski spacetime is special, because it is static. Therefore, it has time translations as an isometry, and there is an associated Killing vector field $i\partial/\partial\eta$ that has the positive-frequency mode functions (13) as its positive-eigenvalue eigenfunctions. For cosmological spacetimes that expand or contract, it is not generally possible to specify positive-frequency mode functions that hold for all time. This leads to the situation whereby observers at different times may decompose the field operator onto different bases of mode functions and ladder operators. Consequently, the vacuum state at some initial time can be an excited state at another time. These concepts are illustrated in the following discussion.

Another way of illustrating this point is to recognize that (nonconformal) fields on a time-dependent spacetime background develop a time-dependent Hamiltonian. For instance each Fourier mode of the scalar field $\phi_{\mathbf{k}}(\eta) = a_{\mathbf{k}} \chi_{\mathbf{k}}(\eta)$ has the dynamics of a quantum simple harmonic oscillator (QSHO) with time-dependent natural frequency $\omega_{\mathbf{k}}^2(\eta)$. If the frequency were constant, the ground state wavefunction would be a Gaussian. If the frequency were varied slowly, the wavefunction would adjust so as to track the adiabatically-varying ground state, and the system would remain almost unexcited. Alternatively, if the frequency were varied rapidly, the wavefunction would be unable to keep up, and the system would find itself in an excited state with respect to the new Hamiltonian. When these concepts are carried over to quantum field theory, the excited state corresponds to particle production.

Asymptotically flat spacetimes. Next we consider spacetimes that are only asymptotically flat (Minkowski-like) toward early and late time. Suppose that the scale factor $a(\eta)$ limits to a^{IN} as $\eta \rightarrow -\infty$ and to a^{OUT} as $\eta \rightarrow \infty$. Denote the corresponding limits of the comoving angular frequency by

$$\lim_{\eta \rightarrow -\infty} \omega_{\mathbf{k}}(\eta) = \omega_{\mathbf{k}}^{\text{IN}} \quad \text{and} \quad \lim_{\eta \rightarrow \infty} \omega_{\mathbf{k}}(\eta) = \omega_{\mathbf{k}}^{\text{OUT}}, \quad (14)$$

which are assumed to be real and positive. In the asymptotic regimes where the spacetime is approximately Minkowski, the positive-frequency mode functions take the form appearing in Eq. (13) with $\bar{\omega}_{\mathbf{k}}$ replaced by $\omega_{\mathbf{k}}^{\text{IN}}$ or $\omega_{\mathbf{k}}^{\text{OUT}}$. This observation motivates us to identify solutions of the mode equations, denoted by $\chi_{\mathbf{k}}^{\text{IN}}(\eta)$ and $\chi_{\mathbf{k}}^{\text{OUT}}(\eta)$, that are asymptotic to the Minkowski positive-frequency

mode functions at either early or late times:

$$\begin{aligned} \chi_{\mathbf{k}}^{\text{IN}}(\eta) &\sim \frac{1}{\sqrt{2\omega_{\mathbf{k}}^{\text{IN}}}} e^{-i\omega_{\mathbf{k}}^{\text{IN}}\eta} \quad \text{as } \eta \rightarrow -\infty \\ \chi_{\mathbf{k}}^{\text{OUT}}(\eta) &\sim \frac{1}{\sqrt{2\omega_{\mathbf{k}}^{\text{OUT}}}} e^{-i\omega_{\mathbf{k}}^{\text{OUT}}\eta} \quad \text{as } \eta \rightarrow \infty. \end{aligned} \quad (15)$$

Using either set of mode functions and a corresponding set of ladder operators, denoted by $a_{\mathbf{k}}^{\text{IN}}$ and $a_{\mathbf{k}}^{\text{OUT}}$, one can construct the field operator as in Eq. (8):

$$\begin{aligned} \phi(\eta, \mathbf{x}) &= \int \frac{d^3\mathbf{k}}{(2\pi)^3} \left(a_{\mathbf{k}}^{\text{IN}} \chi_{\mathbf{k}}^{\text{IN}}(\eta) + a_{-\mathbf{k}}^{\text{IN}\dagger} \chi_{\mathbf{k}}^{\text{IN}*}(\eta) \right) e^{i\mathbf{k}\cdot\mathbf{x}} \\ &= \int \frac{d^3\mathbf{k}}{(2\pi)^3} \left(a_{\mathbf{k}}^{\text{OUT}} \chi_{\mathbf{k}}^{\text{OUT}}(\eta) + a_{-\mathbf{k}}^{\text{OUT}\dagger} \chi_{\mathbf{k}}^{\text{OUT}*}(\eta) \right) e^{i\mathbf{k}\cdot\mathbf{x}}. \end{aligned} \quad (16)$$

The equivalence of these expressions and the freedom to move between them is captured by the Bogolubov transformations.

Bogolubov transformations. In general, pairs of orthonormal basis functions are related to one another by linear transformations that leave the field operator unchanged. Consider the matrix

$$\begin{pmatrix} \alpha_{\mathbf{k}} & \beta_{\mathbf{k}} \\ \beta_{\mathbf{k}}^* & \alpha_{\mathbf{k}}^* \end{pmatrix} \in \text{SU}(1, 1) \quad (17)$$

where the complex constant entries $\alpha_{\mathbf{k}}$ and $\beta_{\mathbf{k}}$ satisfy $|\alpha_{\mathbf{k}}|^2 - |\beta_{\mathbf{k}}|^2 = 1$. Each Fourier mode of the field operator can be written as

$$\begin{aligned} a_{\mathbf{k}} \chi_{\mathbf{k}}(\eta) + a_{-\mathbf{k}}^{\dagger} \chi_{\mathbf{k}}^*(\eta) &= \begin{pmatrix} a_{\mathbf{k}} & a_{-\mathbf{k}}^{\dagger} \end{pmatrix} \begin{pmatrix} \chi_{\mathbf{k}}(\eta) \\ \chi_{\mathbf{k}}^*(\eta) \end{pmatrix} \\ &= \begin{pmatrix} a_{\mathbf{k}} & a_{-\mathbf{k}}^{\dagger} \end{pmatrix} \begin{pmatrix} \alpha_{\mathbf{k}}^* & -\beta_{\mathbf{k}} \\ -\beta_{\mathbf{k}}^* & \alpha_{\mathbf{k}} \end{pmatrix} \begin{pmatrix} \alpha_{\mathbf{k}} & \beta_{\mathbf{k}} \\ \beta_{\mathbf{k}}^* & \alpha_{\mathbf{k}}^* \end{pmatrix} \begin{pmatrix} \chi_{\mathbf{k}}(\eta) \\ \chi_{\mathbf{k}}^*(\eta) \end{pmatrix} \\ &= \underbrace{\left[\begin{pmatrix} \alpha_{\mathbf{k}}^* & -\beta_{\mathbf{k}}^* \\ -\beta_{\mathbf{k}} & \alpha_{\mathbf{k}} \end{pmatrix} \begin{pmatrix} a_{\mathbf{k}} \\ a_{-\mathbf{k}}^{\dagger} \end{pmatrix} \right]^T}_{\equiv (\tilde{a}_{\mathbf{k}} \quad \tilde{a}_{-\mathbf{k}}^{\dagger})} \underbrace{\begin{pmatrix} \alpha_{\mathbf{k}} & \beta_{\mathbf{k}} \\ \beta_{\mathbf{k}}^* & \alpha_{\mathbf{k}}^* \end{pmatrix} \begin{pmatrix} \chi_{\mathbf{k}}(\eta) \\ \chi_{\mathbf{k}}^*(\eta) \end{pmatrix}}_{\equiv \begin{pmatrix} \tilde{\chi}_{\mathbf{k}}(\eta) \\ \tilde{\chi}_{\mathbf{k}}^*(\eta) \end{pmatrix}} \\ &= \tilde{a}_{\mathbf{k}} \tilde{\chi}_{\mathbf{k}}(\eta) + \tilde{a}_{-\mathbf{k}}^{\dagger} \tilde{\chi}_{\mathbf{k}}^*(\eta) \end{aligned}$$

where the last line defines a new basis of ladder operators and mode functions, denoted by a tilde. One can verify that the tilde'd ladder operators obey the commutation relations (9) and the tilde'd mode functions obey the Wronskian condition (10) and mode equations (11). It follows that the field operator admits a family of equivalent representations that are related to one another by $\text{SU}(1, 1)$ matrices, called Bogolubov transformations. Note that for fermionic fields, the commutation relations are replaced by anticommutation relations, and the Bogolubov transformations are implemented through $\text{SU}(2)$ matrices with $|\alpha_{\mathbf{k}}|^2 + |\beta_{\mathbf{k}}|^2 = 1$.

Since the IN and OUT mode functions and their complex conjugates both form complete bases of solutions of the same linear differential equation, it must be possible to write them as linear combinations of one another. This is accomplished by a Bogolubov transformation with

$$\begin{aligned}\chi_k^{\text{IN}}(\eta) &= \alpha_k \chi_k^{\text{OUT}}(\eta) + \beta_k \chi_k^{\text{OUT}*}(\eta) \\ a_{\mathbf{k}}^{\text{IN}} &= \alpha_k^* a_{\mathbf{k}}^{\text{OUT}} - \beta_k^* a_{-\mathbf{k}}^{\text{OUT}\dagger},\end{aligned}\quad (18)$$

where now α_k and β_k denote the set of Bogolubov coefficients linking specifically the IN and OUT mode functions. Inverting these relations and using the Wronskian condition allow the Bogolubov coefficients to be calculated from the IN and OUT mode functions

$$\begin{aligned}\alpha_k &= i(\chi_k^{\text{OUT}*} \chi_k^{\text{IN}'} - \chi_k^{\text{OUT}'} \chi_k^{\text{IN}}) \\ \beta_k &= i(\chi_k^{\text{OUT}'} \chi_k^{\text{IN}} - \chi_k^{\text{OUT}} \chi_k^{\text{IN}'}).\end{aligned}\quad (19)$$

Note that the individual factors and terms on the right sides may carry time dependence, but that this dependence must cancel when constructing the static Bogolubov coefficients.

Bunch-Davies vacuum. The set of ladder operators $a_{\mathbf{k}}^{\text{IN}}$ may be used to define a vacuum state and construct a Fock space of multi-particle states. The vacuum state, denoted by $|0^{\text{IN}}\rangle$, is defined by

$$a_{\mathbf{k}}^{\text{IN}}|0^{\text{IN}}\rangle = 0 \quad \text{for all } \mathbf{k}; \quad (20)$$

i.e., it is the state annihilated by all of the IN lowering operators. The vacuum state is normalized as $\langle 0^{\text{IN}}|0^{\text{IN}}\rangle = 1$. Despite the potentially confusing notation, one should not interpret $|0^{\text{IN}}\rangle$ as an initial vacuum state, which evolves into another state at late times. It is worth remembering that we are working in the Heisenberg picture in which states are static; a system prepared in the state $|0^{\text{IN}}\rangle$ remains in this state at all time. Anticipating the application of this discussion to inflationary cosmology, we refer to $|0^{\text{IN}}\rangle$ as the Bunch-Davies vacuum (Bunch and Davies, 1978). In studies of inflationary perturbations, it is customary to assume that the universe is prepared in the Bunch-Davies vacuum state.

Particle number. A system prepared in the IN vacuum state may contain particles with respect to the OUT ladder operators. The OUT number operator is defined by

$$N^{\text{OUT}} = \int \frac{d^3\mathbf{k}}{(2\pi)^3} a_{\mathbf{k}}^{\text{OUT}\dagger} a_{\mathbf{k}}^{\text{OUT}}. \quad (21)$$

If the IN and OUT operators are related by a Bogolubov transformation (18) with parameters α_k and β_k , then the expected number of particles measured by the OUT number operator in the IN vacuum state is given by

$$\langle 0^{\text{IN}}|N^{\text{OUT}}|0^{\text{IN}}\rangle = V \int \frac{d^3\mathbf{k}}{(2\pi)^3} |\beta_k|^2. \quad (22)$$

This calculation has an expected IR divergence, $V = (2\pi)^3 \delta(\mathbf{k} - \mathbf{k})$, associated with the homogeneous nature of particle production and the system's infinite volume.

Number density spectrum. The comoving number density of particles that the OUT number operator measures in the IN vacuum is given by

$$a^3 n = \int \frac{d^3\mathbf{k}}{(2\pi)^3} |\beta_k|^2, \quad (23)$$

and n is the physical number density. One can interpret $|\beta_k|^2$ as the occupation number of the Fourier mode with comoving wavevector \mathbf{k} . For bosons $0 \leq |\beta_k|^2$ whereas for fermions $0 \leq |\beta_k|^2 \leq 1$. Since β_k is independent of the wavevector's orientation in the isotropic FLRW spacetime, the angular integration is trivial. One finds

$$a^3 n = \int \frac{dk}{k} a^3 n_k \quad \text{with} \quad a^3 n_k = \frac{k^3}{2\pi^2} |\beta_k^2|, \quad (24)$$

where $a^3 n_k$ is the comoving number density spectrum; *i.e.*, the comoving number density of particles per logarithmic wavenumber interval.

Pair production. CGPP results from the behavior of quantum fields on a time-dependent background. Since the background breaks time-translation invariance, the field's energy need not be conserved, but since the background maintains spatial-translation invariance, the field's momentum must be conserved. Consequently, CGPP cannot induce single particle production; at leading order it corresponds to back-to-back pair production.

CGPP discussion. Let us briefly summarize the essential ingredients thus far. In a curved spacetime that is asymptotically flat, there is a natural notion of positive- and negative-frequency modes at early and late times since the spacetime in those regions is approximately Minkowski. However, the temporary departure from Minkowski at intermediate time leads to a mixing of positive- and negative-frequency modes: the solution $\chi_k^{\text{IN}}(\eta)$ that is asymptotic to the positive-frequency mode at early time can be written as a linear combination of the function $\chi_k^{\text{OUT}}(\eta)$ that is asymptotic to the *positive-frequency* mode at late time and the function $\chi_k^{\text{OUT}*}(\eta)$ that is asymptotic to the *negative-frequency* mode at late time. This mixing of the mode functions is captured by a Bogolubov transformation, which implies also a linear map between the associated sets of ladder operators. As such, a vacuum state with respect to the IN ladder operators may be an excited state with respect the OUT ladder operators, which is to say that it contains particles. This is the basis of the phenomenon of cosmological gravitational particle production. Of course the mathematical formalism has broader applicability to theories with a time-dependent Hamiltonian; the defining feature

of CGPP is that the time dependence is induced by the cosmological expansion.

Asymptotically adiabatic spacetimes. Ultimately we are interested in calculating CGPP for cosmological spacetimes that describe an early epoch of inflation followed by reheating and a subsequent hot Big Bang cosmology. For such spacetimes (at least the ones that we consider) the FLRW scale factor $a(\eta)$ is always growing, the spacetime is not asymptotically flat, and it becomes ambiguous how to identify the positive- and negative-frequency modes and how to define particles. For a general spacetime this ambiguity may be insurmountable, but typical cosmological spacetimes have the appealing property that the comoving angular frequency $\omega_k(\eta)$ is slowly varying (adiabatic) at both early and late time. In particular, one may define a dimensionless parameter to measure the departure from adiabaticity,

$$A_k(\eta) = \omega'_k(\eta)/\omega_k^2(\eta), \quad (25)$$

and verify that $A_k \rightarrow 0$ sufficiently quickly as $\eta \rightarrow \pm\infty$.

For asymptotically adiabatic spacetimes, a possible definition of the IN and OUT mode functions is given by

$$\begin{aligned} \chi_k^{\text{IN}}(\eta) &\sim \frac{e^{-i \int^\eta d\eta' \omega_k(\eta')}}{\sqrt{2\omega_k(\eta)}} \quad \text{as } \eta \rightarrow -\infty \\ \chi_k^{\text{OUT}}(\eta) &\sim \frac{e^{-i \int^\eta d\eta' \omega_k(\eta')}}{\sqrt{2\omega_k(\eta)}} \quad \text{as } \eta \rightarrow +\infty. \end{aligned} \quad (26)$$

In fact, these relations define the positive-frequency mode functions of 0th adiabatic order, and the corresponding ladder operators a_k^{IN} define an adiabatic IN vacuum $|0^{\text{IN}}\rangle$ of 0th adiabatic order. However, provided that $\omega_k(\eta)$ is sufficiently slowly varying at early and late times, the corrections from keeping terms of higher adiabatic order are vanishing as $\eta \rightarrow \pm\infty$, implying that $|0^{\text{IN}}\rangle$ is an IN vacuum of infinite adiabatic order. See Appendix D for a discussion of the JWKB method and adiabatic series.

Reparametrization. To find the solution $\chi_k^{\text{IN}}(\eta)$ it is useful to adopt the parametrization (Kofman *et al.*, 1997)

$$\chi_k^{\text{IN}}(\eta) = \tilde{\alpha}_k(\eta) \frac{e^{-i\Phi_k(\eta)}}{\sqrt{2\omega_k(\eta)}} + \tilde{\beta}_k(\eta) \frac{e^{i\Phi_k(\eta)}}{\sqrt{2\omega_k(\eta)}} \quad (27)$$

$$\text{where } \Phi_k(\eta) = \int^\eta d\eta' \omega_k(\eta'),$$

which introduces the new mode functions $\tilde{\alpha}_k(\eta)$ and $\tilde{\beta}_k(\eta)$. The condition in Eq. (26) requires $\tilde{\alpha}_k(\eta) \rightarrow 1$ and $\tilde{\beta}_k(\eta) \rightarrow 0$ as $\eta \rightarrow -\infty$, and $|\tilde{\alpha}_k(\eta)|^2 - |\tilde{\beta}_k(\eta)|^2 = 1$ is maintained by the equations of motion. This function $\chi_k^{\text{IN}}(\eta)$ will solve the mode equation provided that the new mode functions obey

$$\begin{aligned} \partial_\eta \tilde{\alpha}_k(\eta) &= \frac{1}{2} A_k(\eta) \omega_k(\eta) \tilde{\beta}_k(\eta) e^{2i \int^\eta d\eta' \omega_k(\eta')} \\ \partial_\eta \tilde{\beta}_k(\eta) &= \frac{1}{2} A_k(\eta) \omega_k(\eta) \tilde{\alpha}_k(\eta) e^{-2i \int^\eta d\eta' \omega_k(\eta')}, \end{aligned} \quad (28)$$

where $A_k(\eta)$ is the adiabaticity parameter from Eq. (25).

This parametrization is especially useful, because the late time behavior of $\tilde{\beta}_k(\eta)$ gives the Bogolubov coefficient β_k without needing to evaluate $\chi_k^{\text{OUT}}(\eta)$. This can be understood as follows. The Bogolubov coefficient β_k may be calculated from Eq. (19) if the the mode functions $\chi_k^{\text{IN}}(\eta)$ and $\chi_k^{\text{OUT}}(\eta)$ are known. Since the left- and right-hand sides of Eq. (19) are independent of time, we are free to evaluate the equation as $\eta \rightarrow +\infty$. Although $\chi_k^{\text{OUT}}(\eta)$ is unknown, its asymptotic behavior at late times is known by the defining relation (26). After a bit of algebra and also making use of Eqs. (27) and (28) one finds

$$\begin{aligned} \beta_k &= \lim_{\eta \rightarrow \infty} i(\chi_k^{\text{OUT}'} \chi_k^{\text{IN}} - \chi_k^{\text{OUT}} \chi_k^{\text{IN}'}) \\ &= \lim_{\eta \rightarrow \infty} \left[\tilde{\beta}_k - \frac{i}{4} A_k \left(\tilde{\alpha}_k e^{-2i \int^\eta d\eta' \omega_k(\eta')} + \tilde{\beta}_k \right) \right] \\ &= \lim_{\eta \rightarrow \infty} \tilde{\beta}_k(\eta). \end{aligned}$$

In the last equality it is assumed that $A_k(\eta)$ vanishes sufficiently quickly at late time to neglect the second term. This calculation reveals that the late-time limit of the mode function $\tilde{\beta}_k(\eta)$ coincides with the Bogolubov coefficient β_k linking the IN and OUT mode functions, and which is related to the amount of CGPP through Eq. (24). One can also invert Eq. (27) to find

$$\tilde{\alpha}_k(\eta) = \frac{\omega_k \chi_k^{\text{IN}} + i \partial_\eta \chi_k^{\text{IN}}}{\sqrt{2\omega_k}} e^{i \int^\eta d\eta' \omega_k(\eta')} \quad (29a)$$

$$\tilde{\beta}_k(\eta) = \frac{\omega_k \chi_k^{\text{IN}} - i \partial_\eta \chi_k^{\text{IN}}}{\sqrt{2\omega_k}} e^{-i \int^\eta d\eta' \omega_k(\eta')} \quad (29b)$$

$$|\tilde{\beta}_k(\eta)|^2 = \frac{\omega_k}{2} |\chi_k^{\text{IN}}|^2 + \frac{|\partial_\eta \chi_k^{\text{IN}}|^2}{2\omega_k} - \frac{1}{2}. \quad (29c)$$

The last expression assumes $\omega_k(\eta) \in \mathbb{R}$ and uses the Wronskian condition (10).

Correlation function & power spectrum. The field operator's equal-time two-point correlation is given by

$$\begin{aligned} \langle 0^{\text{IN}} | \Phi(\eta, \mathbf{x}) \Phi(\eta, \mathbf{y}) | 0^{\text{IN}} \rangle \\ = \frac{1}{a^2(\eta)} \int \frac{d^3 \mathbf{k}}{(2\pi)^3} |\chi_k^{\text{IN}}(\eta)|^2 e^{i\mathbf{k} \cdot (\mathbf{x} - \mathbf{y})} \end{aligned} \quad (30)$$

for $\mathbf{x} \neq \mathbf{y}$. The corresponding power spectrum is

$$\begin{aligned} \Delta_\Phi^2(\eta, k) &= \frac{k^3}{2\pi^2} \int d^3 \mathbf{r} \langle 0^{\text{IN}} | \Phi(\eta, \mathbf{x}) \Phi(\eta, \mathbf{y}) | 0^{\text{IN}} \rangle e^{-i\mathbf{k} \cdot \mathbf{r}} \\ &= \frac{1}{a^2(\eta)} \frac{k^3}{2\pi^2} |\chi_k^{\text{IN}}(\eta)|^2 \end{aligned} \quad (31)$$

where $\mathbf{y} = \mathbf{x} + \mathbf{r}$. Note that

$$\begin{aligned} |\chi_k^{\text{IN}}(\eta)|^2 &= \frac{1}{2\omega_k(\eta)} \left(|\tilde{\alpha}_k(\eta)|^2 + |\tilde{\beta}_k(\eta)|^2 \right. \\ &\quad \left. + 2\text{Re} \left[\tilde{\alpha}_k^*(\eta) \tilde{\beta}_k(\eta) e^{2i\Phi_k(\eta)} \right] \right). \end{aligned} \quad (32)$$

Typically the very small-scale modes ($k \rightarrow \infty$) remain adiabatic, corresponding to $\omega_k(\eta) \approx k$, $\tilde{a}_k(\eta) \approx 1$, and $\tilde{\beta}_k(\eta) \approx 0$, which leads to an asymptotically blue-tilted power spectrum $\Delta_\Phi^2(\eta, k) \sim k^2/4\pi^2 a^2$ as $k \rightarrow \infty$.

When is a particle a particle?. To close this subsection, let us address several common points of confusion. The phrase “cosmological gravitational particle production” uses the word “particle” and elicits the image of particle pair creation. On the other hand, when we talk about the inflationary quantum fluctuations of the inflaton field and metric, we do not usually speak of particle creation. However, both calculations use the Bogolubov formalism to study the evolution of quantum fields in an expanding universe. Is there some sense in which CGPP creates particles whereas inflationary quantum fluctuations creates something else (*e.g.*, field fluctuations)? In other words, when can we say that the excitations of a quantum field correspond to a collection of particles? Several conditions are required in order to talk about the number density of particles interpreted in a Minkowskian context.

1. Our background cosmological model assumes at sufficiently early times in the qdS phase, say $\eta < \eta_i$, that $\omega_k(\eta)$ is approximately constant and the evolution of the mode is approximately adiabatic, and at sufficiently late times, say $\eta > \eta_f$ the evolution is again approximately adiabatic. But for intermediate times $\eta_i < \eta < \eta_f$ the particle interpretation is ambiguous because positive and negative frequency solutions are mixing. The evolution is adiabatic when $|A_k| = |\omega'_k/\omega_k^2| \ll 1$: This condition is also necessary for the identification of $\tilde{\beta}_k$ with the Bogolubov coefficient β_k (see Eq. (29)) and for the decomposition onto positive- and negative-frequency modes to be performed unambiguously (Birrell and Davies, 1984). In the calculations above, we assumed that $A_k(\eta) \rightarrow 0$ sufficiently quickly as $\eta \rightarrow \pm\infty$, which allowed for an unambiguous identification of particles associated with the IN and OUT positive-frequency mode functions (Birrell and Davies, 1984).
2. The spacetime curvature must not vary across the spatial size of the wavepacket of momentum k/a (Mukhanov and Winitzki, 2007). In the FLRW cosmology this requires $k/a > H$: If this condition is not satisfied, the curvature of spacetime (of order H) will vary across the size of the wavepacket.
3. The mode must be oscillatory, which implies $\omega_k^2 > 0$. If this condition is not satisfied the mode equation does not have oscillatory solutions.

C. Energy, renormalization, and observables

The previous section reviewed how to calculate the number of gravitationally produced particles. If we’re interested in physics such as baryogenesis, *i.e.*, explaining the origin of the matter-antimatter asymmetry, then this number density is the observable quantity of interest. If we’re instead interested in relic particles that survive today as dark matter or dark radiation, which are probed through their gravitational interactions on cosmological scales, then an energy density is the quantity of interest. In this section we define the energy carried by gravitationally produced particles and discuss how to calculate it while handling ultraviolet (UV) divergences. We’re interested in both the average energy density as well as energy inhomogeneities, since the latter are probed by CMB isocurvature.

Semiclassical gravity. In the framework of semiclassical gravity the gravitational field is treated as classical and the radiation/matter fields are treated as quantum; it is expected to be a good approximation for systems with small fluctuations (Kuo and Ford, 1993). Gravity’s response to radiation/matter is governed by a variant of Einstein’s equation:

$$R_{\mu\nu} - \frac{1}{2}Rg_{\mu\nu} = M_{\text{Pl}}^{-2}\langle 0^{\text{IN}}|T_{\mu\nu}|0^{\text{IN}}\rangle. \quad (33)$$

On the left-side is the Einstein tensor $G_{\mu\nu}(x)$ for the classical gravitational field, and on the right-side is an expectation value of the stress-energy tensor $T_{\mu\nu}(x)$ for the theory’s various quantum fields. Assuming that the system is in the Bunch-Davies vacuum, the expectation value is evaluated with the IN vacuum state $|0^{\text{IN}}\rangle$. For the scalar field theory whose action appears in Eq. (1), its stress-energy tensor is

$$\begin{aligned} T_{\mu\nu}(x) = & (1 - 2\xi) (\partial_\mu \Phi \partial_\nu \Phi) \\ & + (2\xi - \frac{1}{2}) (g_{\mu\nu} g^{\alpha\beta} \partial_\alpha \Phi \partial_\beta \Phi) \\ & + 2\xi (g_{\mu\nu} \Phi \square \Phi) - 2\xi (\Phi \nabla_\mu \partial_\nu \Phi) \\ & + \xi (G_{\mu\nu} \Phi^2) + \frac{1}{2} (g_{\mu\nu} m^2 \Phi^2). \end{aligned} \quad (34)$$

Since this is a composite operator, constructed from products of field operators, one encounters UV divergences upon calculating its expectation value, which need to be regulated and renormalized.

Energy density. The energy density measured by an observer with 4-velocity U^μ is

$$\rho(x) = \langle 0^{\text{IN}}|T_{\mu\nu}U^\mu U^\nu|0^{\text{IN}}\rangle. \quad (35)$$

In the observer’s rest frame $U^\mu = (\sqrt{1/g_{00}}, 0, 0, 0)$ since $g_{\mu\nu}U^\mu U^\nu = 1$ normalizes the 4-velocity. Decomposing the field operator onto the IN basis of ladder operators

and mode functions leads to the expression

$$\begin{aligned} \rho(\eta) = a^{-4} \int \frac{d^3 \mathbf{k}}{(2\pi)^3} & \left[\frac{1}{2} |\chi_k^{\text{IN}*}|^2 + \frac{1}{2} \omega_k^2 |\chi_k^{\text{IN}}|^2 \right. \\ & + \frac{1}{2} (1 - 6\xi) (a^2 H^2 - \frac{1}{6} a^2 R) |\chi_k^{\text{IN}}|^2 \\ & \left. - (1 - 6\xi) aH \text{Re}[\chi_k^{\text{IN}} \chi_k^{\text{IN}*}] \right]. \end{aligned} \quad (36)$$

Further using the reparametrization in Eq. (27) and assuming $\omega_k(\eta) \in \mathbb{R}$ leads to

$$\begin{aligned} \rho(\eta) = a^{-4} \int \frac{d^3 \mathbf{k}}{(2\pi)^3} & \left[\frac{\omega_k}{2} (|\tilde{\alpha}_k|^2 + |\tilde{\beta}_k|^2) \right. \\ & + \frac{1}{4\omega_k} (1 - 6\xi) (a^2 H^2 - \frac{1}{6} a^2 R) (|\tilde{\alpha}_k|^2 + |\tilde{\beta}_k|^2) \\ & + \frac{1}{2\omega_k} (1 - 6\xi) (a^2 H^2 - \frac{1}{6} a^2 R) \text{Re}[\tilde{\alpha}_k^* \tilde{\beta}_k e^{2i\Phi_k}] \\ & \left. + (1 - 6\xi) aH \text{Im}[\tilde{\alpha}_k^* \tilde{\beta}_k e^{2i\Phi_k}] \right]. \end{aligned} \quad (37)$$

Notice that several terms vanish if the scalar is conformally coupled to gravity ($\xi = 1/6$). The value of this energy density toward late time $\eta \rightarrow \infty$ is a measure of the amount of particle production.

UV divergence. The integral in Eq. (36) has a UV divergence associated with the large $k = |\mathbf{k}|$ part of the integration domain. To identify the divergent behavior, it suffices to consider the $\eta \rightarrow -\infty$ limit, since the IN mode functions are given by Eq. (26). One finds that the various terms in Eq. (36) have either quadratic or quartic divergences as $k \rightarrow \infty$.

The appearance of this UV divergence should not be surprising. After all, a similar divergence arises when calculating a free field's energy density in Minkowski spacetime: each Fourier mode is a free harmonic oscillator with ground-state energy $\bar{\omega}_k/2$, and the number of modes grows like k^3 leading to a quartic divergence $k^3 \bar{\omega}_k \sim k^4$ as $k \rightarrow \infty$. To handle this divergence in Minkowski QFT, the standard approach is to introduce a counterterm that renormalizes the cosmological constant (*i.e.*, the vacuum energy). However, the situation is more subtle in a curved spacetime where $\omega_k(\eta)$ is not static, and the divergent part of the integral varies in time.

Adiabatic regularization. We briefly discuss two strate-

gies for defining and calculating a renormalized energy density. Adiabatic Regularization (AR) is a prescription for removing UV divergences that arise in the study of quantum field theory in curved spacetime (Fulling and Parker, 1974; Fulling *et al.*, 1974; Parker and Fulling, 1974). See the textbook Parker and Toms (2009) for an excellent introduction and Appendix D for supplemental details. To employ AR, it is first necessary to solve the equation of motion using the JWKB method, which allows the mode functions to be expressed as a series, $\chi_k(\eta) = \exp[i \sum_{n=-1}^{\infty} \varepsilon^n s_n(\eta)]$, known as an adiabatic series. Observables constructed from the mode functions, such as the energy density, are therefore naturally decomposed into a series. AR calls for the removal of any order in the series that contains a UV divergence. For instance, the quartic divergence mentioned previously arises at leading order in the adiabatic series, and once the order containing a divergence has been identified, AR requires all terms at that order to be dropped, whether or not they contain a UV divergence. In this way, one is able to define renormalized observables that are free of divergences. Although the machinery of adiabatic regularization is general and powerful, it is also cumbersome to construct the adiabatic series, and for these reasons we adopt a different prescription for renormalization.

Renormalization via normal ordering. When one encounters a quartic divergence in the Minkowski spacetime energy density, a simple renormalization procedure is to define the physical energy density using the normal-ordered energy operator. One may adopt a similar procedure in the FLRW spacetime (Chung *et al.*, 2005). Define the renormalized energy density as

$$\rho_{\text{ren}}(x) = \langle 0^{\text{IN}} | :T_{\mu\nu} U^\mu U^\nu : | 0^{\text{IN}} \rangle \quad (38)$$

where the normal ordering is performed with respect to the OUT basis of ladder operators. Normal-ordered products of IN-basis ladder operators are given by

$$:a_{\mathbf{k}}^{\text{IN}} a_{\mathbf{q}}^{\text{IN}}: = a_{\mathbf{k}}^{\text{IN}} a_{\mathbf{q}}^{\text{IN}} + (2\pi)^3 \delta(\mathbf{k} + \mathbf{q}) \alpha_k^* \beta_k^* \quad (39a)$$

$$:a_{\mathbf{k}}^{\text{IN}} a_{\mathbf{q}}^{\text{IN}\dagger}: = a_{\mathbf{k}}^{\text{IN}\dagger} a_{\mathbf{q}}^{\text{IN}} - (2\pi)^3 \delta(\mathbf{k} - \mathbf{q}) |\beta_k|^2 \quad (39b)$$

$$:a_{\mathbf{k}}^{\text{IN}\dagger} a_{\mathbf{q}}^{\text{IN}}: = a_{\mathbf{k}}^{\text{IN}\dagger} a_{\mathbf{q}}^{\text{IN}} - (2\pi)^3 \delta(\mathbf{k} - \mathbf{q}) |\beta_k|^2 \quad (39c)$$

$$:a_{\mathbf{k}}^{\text{IN}\dagger} a_{\mathbf{q}}^{\text{IN}\dagger}: = a_{\mathbf{k}}^{\text{IN}\dagger} a_{\mathbf{q}}^{\text{IN}\dagger} + (2\pi)^3 \delta(\mathbf{k} + \mathbf{q}) \alpha_k \beta_k. \quad (39d)$$

Using these relations, one can show that the renormalized energy density is

$$\begin{aligned} \rho_{\text{ren}}(\eta) = a^{-4} \int \frac{d^3 \mathbf{k}}{(2\pi)^3} & \left\{ \text{Re} \left[\alpha_k^* \beta_k^* \left((\partial_\eta \chi_k^{\text{IN}})^2 + \omega_k^2 (\chi_k^{\text{IN}})^2 - 2(1 - 6\xi) aH \chi_k^{\text{IN}} \partial_\eta \chi_k^{\text{IN}} \right. \right. \right. \\ & + (1 - 6\xi) (a^2 H^2 - \frac{1}{6} a^2 R) (\chi_k^{\text{IN}})^2 \left. \right] - |\beta_k|^2 \left[|\partial_\eta \chi_k^{\text{IN}}|^2 + \omega_k^2 |\chi_k^{\text{IN}}|^2 \right. \\ & \left. \left. - (1 - 6\xi) aH (\chi_k^{\text{IN}} \partial_\eta \chi_k^{\text{IN}*} + \chi_k^{\text{IN}*} \partial_\eta \chi_k^{\text{IN}}) + (1 - 6\xi) (a^2 H^2 - \frac{1}{6} a^2 R) |\chi_k^{\text{IN}}|^2 \right] \right\}, \end{aligned} \quad (40)$$

and upon using Eq. (27), it becomes

$$\begin{aligned} \rho_{\text{ren}}(\eta) = a^{-4} \int \frac{d^3 \mathbf{k}}{(2\pi)^3} \left\{ \omega_k \left(2 \operatorname{Re} [\alpha_k^* \tilde{\alpha}_k \beta_k^* \tilde{\beta}_k] - |\tilde{\alpha}_k|^2 |\beta_k|^2 - |\tilde{\beta}_k|^2 |\beta_k|^2 \right) \right. \\ - \frac{1}{2\omega_k} (1 - 6\xi) (a^2 H^2 - \frac{1}{6} a^2 R) (|\tilde{\alpha}_k|^2 + |\tilde{\beta}_k|^2) |\beta_k|^2 \\ + \frac{1}{2\omega_k} (1 - 6\xi) (a^2 H^2 - \frac{1}{6} a^2 R) \operatorname{Re} [2\alpha_k^* \tilde{\alpha}_k \beta_k^* \tilde{\beta}_k + (\alpha_k \tilde{\alpha}_k^{*2} \beta_k - 2\tilde{\alpha}_k^* \tilde{\beta}_k |\beta_k|^2 + \alpha_k^* \tilde{\beta}_k^2 \beta_k^*) e^{2i\Phi_k}] \\ \left. + (1 - 6\xi) aH \operatorname{Im} [(\alpha_k \tilde{\alpha}_k^{*2} \beta_k - 2\tilde{\alpha}_k^* \tilde{\beta}_k |\beta_k|^2 + \alpha_k^* \tilde{\beta}_k^2 \beta_k^*) e^{2i\Phi_k}] \right\}. \end{aligned} \quad (41)$$

The UV divergences are regulated by the factors of β_k that appear in each term. Modes with large k remain approximately adiabatic at all times, $A_k(\eta) \ll 1$, and do not experience appreciable CGPP so $|\beta_k| \ll 1$. Provided that β_k vanishes sufficiently quickly as $k \rightarrow \infty$, the UV divergence is avoided. Moreover, since ρ_{ren} vanishes in the absence of CGPP ($\beta_k = 0$), one can interpret this renormalized energy density as a measure of the energy carried by the gravitationally produced particles.

Cosmological energy density. For practical application, a simplified expression for the renormalized energy density is available. At late time the mode functions asymptote to the Bogolubov coefficients, $\tilde{\alpha}_k(\eta) \rightarrow \alpha_k$ and $\tilde{\beta}_k(\eta) \rightarrow \beta_k$. Additionally, it's typically the case that CGPP is inefficient in the sense that $|\beta_k| \ll |\alpha_k| \approx 1$, which allows terms suppressed by three or four powers of β_k to be neglected. Finally, in a cosmological FLRW spacetime, the Hubble parameter $H(\eta)$ and Ricci scalar $R(\eta)$ are monotonically decreasing. At sufficiently late time, terms suppressed by these factors can be neglected from the energy density, and the dispersion relation may be approximated as $\omega_k^2 \approx k^2 + a^2 m^2$. Using these simplifications, the energy density is approximately

$$\rho_{\text{ren}}(\eta) \approx a^{-4} \int \frac{d^3 \mathbf{k}}{(2\pi)^3} \sqrt{k^2 + a^2(\eta)m^2} |\beta_k|^2. \quad (42)$$

Since the angular integration is trivial, one can write the energy density spectrum $\rho_k(\eta)$ as

$$\rho_{\text{ren}} = \int \frac{dk}{k} \rho_k \quad \text{with} \quad \rho_k = \sqrt{(k/a)^2 + m^2} n_k, \quad (43)$$

where $E_k(\eta) = \sqrt{(k/a)^2 + m^2}$ is the energy carried per Fourier mode and $n_k(\eta) = (k^3/2\pi^2 a^3) |\beta_k|^2$ is the number density spectrum from Eq. (24). For the non-relativistic modes, which are expected to carry most of the energy at late time, we further have $\rho_k \approx m n_k$ and $\rho_{\text{ren}} \approx m n$ where n is the number density from Eq. (23).

Energy density inhomogeneities. Since CGPP is fundamentally a quantum phenomenon, one should anticipate the distribution of gravitationally produced particles to be spatially inhomogeneous even if the underlying FLRW spacetime were perfectly homogeneous and isotropic. Moreover, these energy inhomogeneities are a potential signal of CGPP, since the spatial distribution of dark matter is probed by measurements of the cosmic microwave background radiation and large-scale structure. In other words, CGPP leads to an isocurvature component, which is constrained by current cosmological observations, and can be searched for in the future.

For this discussion it is useful to identify operators with a hat. The energy density operator $\hat{\rho}(\eta, \mathbf{x})$ may be decomposed as

$$\hat{\rho}(\eta, \mathbf{x}) = :\hat{T}_{\mu\nu} U^\mu U^\nu: = \bar{\rho}(\eta) \hat{1} + \delta\hat{\rho}(\eta, \mathbf{x}). \quad (44)$$

The homogeneous component $\bar{\rho}(\eta) = \rho_{\text{ren}}(\eta)$ is simply the renormalized energy density from the preceding discussion. The inhomogeneous component $\delta\hat{\rho}(\eta, \mathbf{x})$ has vanishing expectation value in the IN vacuum, but contributes to the energy two-point function. The quantity of interest is the dimensionless power spectrum of the energy density contrast:

$$\begin{aligned} \Delta_\delta^2(\eta, k) = \frac{1}{\bar{\rho}^2(\eta)} \frac{k^3}{2\pi^2} \int d^3 \mathbf{r} e^{-i\mathbf{k} \cdot \mathbf{r}} \\ \times \langle 0^{\text{IN}} | \delta\hat{\rho}(\eta, \mathbf{x}) \delta\hat{\rho}(\eta, \mathbf{x} + \mathbf{r}) | 0^{\text{IN}} \rangle. \end{aligned} \quad (45)$$

The correlation function is independent of \mathbf{x} and the orientation of \mathbf{k} due to the homogeneity and isotropy of the IN vacuum state. The calculation of this quantity simplifies by focusing on nonrelativistic modes with $k \ll am$ at late times such that $H \ll m$. Under those assumptions, the leading terms are given by

$$\Delta_\delta^2(\eta, k) \approx \frac{a^{-8}(\eta)}{2\bar{\rho}^2(\eta)} \frac{k^3}{2\pi^2} \int \frac{d^3\mathbf{k}'}{(2\pi)^3} \left\{ |\partial_\eta \chi_{k'}^{\text{IN}}|^2 |\partial_\eta \chi_{|\mathbf{k}'-\mathbf{k}|}^{\text{IN}}|^2 + a^4 m^4 |\chi_{k'}^{\text{IN}}|^2 |\chi_{|\mathbf{k}'-\mathbf{k}|}^{\text{IN}}|^2 \right. \\ \left. + a^2 m^2 \left[(\chi_{k'}^{\text{IN}} \partial_\eta \chi_{k'}^{\text{IN}*}) (\chi_{|\mathbf{k}'-\mathbf{k}|}^{\text{IN}} \partial_\eta \chi_{|\mathbf{k}'-\mathbf{k}|}^{\text{IN}*}) + (\chi_{k'}^{\text{IN}*} \partial_\eta \chi_{k'}^{\text{IN}}) (\chi_{|\mathbf{k}'-\mathbf{k}|}^{\text{IN}*} \partial_\eta \chi_{|\mathbf{k}'-\mathbf{k}|}^{\text{IN}}) \right] \right\}, \quad (46)$$

and upon using Eq. (27), it becomes

$$\Delta_\delta^2(\eta, k) \approx \frac{a^{-6}(\eta) m^2}{\bar{\rho}^2(\eta)} \frac{k^3}{2\pi^2} \int \frac{d^3\mathbf{k}'}{(2\pi)^3} \left\{ |\tilde{\beta}_{k'}|^2 |\tilde{\alpha}_{|\mathbf{k}'-\mathbf{k}|}|^2 + \text{Re} [\tilde{\alpha}_{k'}^* \tilde{\beta}_{k'} \tilde{\alpha}_{|\mathbf{k}'-\mathbf{k}|} \tilde{\beta}_{|\mathbf{k}'-\mathbf{k}|}^* e^{2i\Phi_{k'} - 2i\Phi_{|\mathbf{k}'-\mathbf{k}|}}] \right\}. \quad (47)$$

The \mathbf{k}' integral is free of UV divergences provided that $\tilde{\beta}_{k'}$ drops off sufficiently quickly toward large $k' = |\mathbf{k}'|$.

If the integrand is sufficiently strongly peaked at some $k' = k_*$ then for $k \ll k_*$ the integrand is dominated by $k' \approx k_*$ and the integral becomes insensitive to k . Evaluating the integral, one finds $\Delta_\delta^2(\eta, k \ll k_*) \approx (2/a^3 n)(k^3/2\pi^2)$ where $\bar{\rho}(\eta) = mn(\eta)$. Intuitively, a causal generation mechanism implies a finite spatial correlation length and a characteristic k^3 power for the energy contrast; this point has been emphasized recently by [Amin and Mirbabayi \(2022\)](#) and [Hook et al. \(2021\)](#) in other contexts. Since CGPP leads to a blue-tilted field amplitude power spectrum for many models (the notable exception being the minimally coupled scalar field with $m \lesssim H_{\text{inf}}$), then a generic prediction of CGPP is a k^3 density contrast. When the inflaton and metric perturbations are also taken into account, this implies a negligible isocurvature on cosmological scales.

The term multiplying m^4 in Eq. (46) can also be written as ([Chung et al., 2005](#); [Liddle and Mazumdar, 2000](#))

$$\Delta_\delta^2(\eta, k) \supset \frac{m^4}{\bar{\rho}^2(\eta)} \frac{k^3}{8\pi} \int d^3\mathbf{k}' \frac{\Delta_\Phi^2(\eta, k') \Delta_\Phi^2(\eta, |\mathbf{k}' - \mathbf{k}|)}{k'^3 |\mathbf{k}' - \mathbf{k}|^3}, \quad (48)$$

where we have used $\Delta_\Phi^2(\eta, k)$ from Eq. (31). This expression reveals that the density contrast's power spectrum is related to a convolution over the field amplitude's power spectrum. However, one should take care in using Eq. (48), since the m^4 term in insolation contains a UV divergence that cancels against the other terms. If one replaces Δ_Φ^2 in this formula with $\widehat{\Delta}_\Phi^2 = \Delta_\Phi^2 - k^2/4\pi^2 a^2$ then the integral is convergent, and Δ_δ^2 is typically well approximated by Eq. (48) after including an additional factor of 2 to account for the derivative terms in Eq. (46).

IV. CGPP FOR SPIN-0 PARTICLES

Since CGPP is a consequence of the cosmological expansion, it is reasonable to expect that this phenomenon would be most efficient at the earliest moments in our cosmic history when the expansion rate H was largest. For this reason, CGPP is usually discussed in the context of inflation and reheating. In this section we provide

a brief overview of inflationary cosmology, followed by a summary of key results for scalar CGPP including a discussion of the implications for dark matter. We focus on spin-0 particles in this section, and studies of CGPP for fields with nonzero spin are discussed in the next section.

A. Inflationary cosmology

We use the phrase ‘inflationary cosmology’ to denote a cosmic history in which the Universe experienced an early qdS phase of inflation, followed by an approximately matter-dominated phase after the end of inflation during the epoch known as reheating, followed by the decay of the inflaton condensate into the primordial plasma that signaled the onset of a radiation-dominated phase and the start of hot Big Bang cosmology.

Scalar inflaton field. In this article we focus on single-field slow-roll inflation driven by a real scalar inflaton field, which we denote by $\varphi(x)$. However the phenomenon of CGPP is generic and expected to occur for the various known models of inflation ([Martin et al., 2014](#)). For the sake of concreteness, suppose that the inflaton field is minimally coupled to gravity with the action

$$S = \int d^4x \sqrt{-g} \left[\frac{1}{2} g^{\mu\nu} \nabla_\mu \varphi \nabla_\nu \varphi - V(\varphi) \right]. \quad (49)$$

The remaining model dependence lies in the specification of the inflaton potential $V(\varphi)$. Typically $V(\varphi)$ is assumed to have a sufficiently wide and flat region in φ that supports a few dozen e -foldings of inflation and that connects smoothly into a local minimum at $\varphi = v_\varphi$ where the potential is locally quadratic $V(\varphi) \approx m_\varphi^2 (\varphi - v_\varphi)^2/2$. In other models the minimum is locally quartic or there is no local minimum at all and that the inflaton instead rolls off to infinity during a kination-dominated phase. Precision observations of the CMB probe the flatness of the inflaton potential ([Akrami et al., 2020b](#)), but only away from the minimum, whereas CGPP probes a wider range of the potential, particularly near the minimum.

During inflation the inflaton field is assumed to dominate the stress-energy tensor $T_{\mu\nu}$ that appears in Einstein's equation. Focusing on the evolution of the homogeneous and isotropic background, *i.e.*, neglecting

perturbations, the field is uniform in space $\varphi(t, \mathbf{x}) = \varphi(t)$ and the metric is an FLRW spacetime $(ds)^2 = (dt)^2 - a^2(t)|d\mathbf{x}|^2$, where t is coordinate time. The homogeneous background field's equation of motion is $\ddot{\varphi} + 3H\dot{\varphi} + dV(\varphi)/d\varphi = 0$ where dots denote $\partial_t = a^{-1}\partial_\eta$. The field's homogeneous energy density and pressure,

$$\rho_\varphi(t) = \frac{1}{2}\dot{\varphi}^2 + V(\varphi) ; \quad p_\varphi(t) = \frac{1}{2}\dot{\varphi}^2 - V(\varphi) , \quad (50)$$

appear in Einstein's equation and source the FLRW spacetime. The equation of state is $w_\varphi(t) = p_\varphi/\rho_\varphi$.

Quasi-de Sitter phase of inflation. Inflation is defined as an epoch during which the comoving Hubble scale is decreasing, and the spacetime expansion is accelerating:

$$\dot{d}_H(t) < 0 , \quad \ddot{a}(t) > 0 , \quad \text{or} \quad \epsilon(t) < 1 . \quad (51)$$

In these relations $d_H(t) = 2\pi/aH$ is the comoving Hubble length scale, $\ddot{a}(t)$ is the expansion's acceleration in terms of coordinate time t , and $\epsilon(t) = -\dot{H}/H^2$ is the first slow-roll parameter. The spacetime is said to be *quasi-de Sitter* because the Hubble parameter $H(t)$ is slowly decreasing, rather than constant, throughout inflation.

Modes of fixed comoving wavenumber k are said to 'leave the horizon' if there's a time at which $(aH)^{-1}$ drops below k^{-1} . Modes of the inflaton field that eventually imprint themselves onto the CMB must leave the horizon several dozen e -foldings before the end of inflation (typically 30 to 60), but modes on much smaller length scales (much larger k) will never leave the horizon. For studies of CGPP we are often interested in modes of a spectator field that are just about leaving the horizon at the end of inflation and have comoving wavenumber $k \approx k_e \equiv a_e H_e$.

Inflationary observables. Cosmological inflation leaves its imprint on the temperature and polarization anisotropies of the cosmic microwave background radiation. Precision observations of the CMB by the *Planck* satellite telescope furnish measurements of the scalar power spectrum amplitude $\ln(10^{10}A_s) = 3.044 \pm 0.014$ and spectral tilt $n_s = 0.9649 \pm 0.0042$ (Akrami *et al.*, 2020b). Combining with data from BICEP2, *Keck Array*, and BICEP3 leads to a limit on the tensor-to-scalar ratio $r < 0.036$ at 95% CL (Ade *et al.*, 2021). The values of A_s and n_s imply a slightly red tilted dimensionless power spectrum for the primordial (scalar) curvature perturbations that has an amplitude of $\Delta_\zeta^2(k) \approx 2.099 \times 10^{-9}$ for $k \approx k_{\text{CMB}} = 0.05 a_0 \text{ Mpc}^{-1}$. Single-field slow-roll inflation predicts the tensor-to-scalar ratio to be

$$r = \frac{A_t}{A_s} = \frac{2H_{\text{inf}}^2}{\pi^2 M_{\text{Pl}}^2 A_s} \approx 0.16 \left(\frac{H_{\text{inf}}}{10^{14} \text{ GeV}} \right)^2 \quad (52)$$

where H_{inf} is the value of the Hubble parameter while the CMB-scale modes are leaving the horizon. Thus the observational constraint on r implies

$$H_{\text{inf}} < 0.5 \times 10^{14} \text{ GeV} . \quad (53)$$

The abundance of gravitationally produced particles typically goes as H_{inf}^2 , and Eq. (53) restricts the amount of CGPP. If inflationary gravitational waves are detected with next-generation telescopes, the value of H_{inf} may lie close to the current limit (Kamionkowski and Kovetz, 2016), which is particularly favorable for CGPP.

The end of inflation. The qdS phase of inflation must end in order for the hot Big Bang cosmology to commence. In most models of single-field slow-roll inflation, the end of inflation occurs when the inflaton field reaches a sufficiently steep region of the inflaton potential. We define the end of inflation to be the earliest time at which the conditions in Eq. (51) fail. For instance, at the end of inflation $\epsilon(t_e) = 1$. We denote the end of inflation with an e subscript: t_e for coordinate time, η_e for conformal time, a_e for scale factor, H_e for Hubble parameter, and φ_e for the inflaton field amplitude. It is convenient to use the end of inflation as a reference point for measuring time; for example, $N(t) = \ln a(t)/a_e$ gives the signed number of e -foldings that elapse between the time t and the time t_e at the end of inflation.

Hubble-scale modes. Modes that are on the Hubble scale at the end of inflation have a comoving wavenumber of $k \approx k_e \equiv a_e H_e$. Today this corresponds to a wavelength of $\lambda_{\text{phys}} = 2\pi a_0/k_e$ and a momentum of $p_{\text{phys}} = k_e/a_0$ where a_0 is the scale factor today. Assuming the cosmological expansion described below (with $w_{\text{RH}} = 0$), one finds $\lambda_{\text{phys}} \approx (4 \times 10^{-20} \text{ Mpc}) H_{12}^{-1/3} T_9^{-1/3}$ and $p_{\text{phys}} \approx (1 \times 10^{-18} \text{ GeV}) H_{12}^{1/3} T_9^{1/3}$ where $H_{12} = H_e/10^{12} \text{ GeV}$ and $T_9 = T_{\text{RH}}/10^9 \text{ GeV}$. Note that $10^{-20} \text{ Mpc} \approx 0.3 \text{ km}$! For reference, cosmological observables (CMB and large scale structure), probe much larger length scales with $k \approx (1-10^4)k_0$ where modes that are on the Hubble scale today have $k \approx k_0 \equiv a_0 H_0 \approx 3.33 \times 10^{-4} a_0 h \text{ Mpc}^{-1}$.

Coherent oscillations. After inflation has ended, it is customary to assume that the inflaton field finds a local quadratic minimum of its potential and begins a phase of spatially coherent oscillations. At this time the equation of motion for the homogeneous inflaton field is approximately $\ddot{\varphi} + 3H\dot{\varphi} + m_\varphi^2 \varphi = 0$ and the first Friedmann equation is approximately $3M_{\text{Pl}}^2 H^2 = \dot{\varphi}^2/2 + m_\varphi^2 \varphi^2/2$. These equations are solved by $\varphi(t) \approx \varphi_e (a/a_e)^{-3/2} \cos(m_\varphi t)$ up to corrections that are suppressed by additional factors of H^2/m_φ^2 or R/m_φ^2 . The field oscillates quasi-harmonically while the amplitude decreases monotonically due to the cosmological expansion. The time-averaged pressure is close to zero, since the system spends roughly equal time being potential and kinetic dominated, implying a vanishing equation of state $w_\varphi \approx 0$. During the epoch of oscillations the universe is effectively matter-dominated by a population of nonrelativistic inflaton particles.

Numerical examples. The end of inflation and the inflaton's coherent oscillations play an important role in many models of CGPP. At the end of inflation, the dominant energy component in the universe changes from the inflaton's potential energy (with equation of state $w_\varphi \approx -1$) to a balance between its potential and kinetic energies (with time-average equation of state $w_\varphi \approx 0$). As a result of this shift in dominant energy component, there is a corresponding change in the cosmological expansion rate, parameterized by a , $H = a'/a^2$, and $R = -6a''/a^3$. Additionally, as the inflaton field oscillates around the minimum of its potential, the scale factor and its derivatives develop oscillatory components. Besides the inflaton field and gravity, the various matter-sector fields of the theory 'feel' this change in the cosmological expansion rate, leading to non-adiabatic evolution and CGPP.

This behavior is illustrated in Fig. 2 for two models of inflation: Quadratic (Chaotic) Inflation with $V(\varphi) = m_\varphi^2 \varphi^2/2$ (Linde, 1983) and (a particular implementation of) Hilltop Inflation with $V(\varphi) = m_\varphi^2 v^2(1 - \varphi^6/v^6)^2/72$ and $v = M_{\text{Pl}}/2$. The evolution of the scale factor a , Hubble parameter H , Ricci scalar R , and inflaton field φ are shown as functions of conformal time η . Note that the relationships between $\eta/a_e H_e$ and $m_\varphi(t - t_e)$ are different in the two models, because Quadratic Inflation has $m_\varphi \approx 2H_e$ and Hilltop Inflation has $m_\varphi \approx 30H_e$.

During inflation H , R , and the inflaton field φ are approximately constant while the growth of the scale factor a accelerates. If the spacetime were exactly de Sitter, one would find $a(\eta) = a_e/(1 - a_e H_e \eta)$, $H(\eta) = H_e$, and $R(\eta) = -12H_e^2$. The end of inflation is normalized to $\eta_e = 0$. After the qdS phase the Hubble parameter begins to decrease quickly and the growth of the scale factor decelerates. At this time the inflaton oscillates around the minimum of its potential with an effective equation of state $w_\varphi \approx 0$, corresponding to a matter-dominated phase. If the equation of state were identically zero then Friedmann's equations would give $a(\eta) = a_e(1 + a_e H_e \eta/2)^2$, $H(\eta) = H_e/(1 + a_e H_e \eta/2)^3$, and $R(\eta) = -3H_e^2/(1 + a_e H_e \eta/2)^6$ implying $H(\eta) = H_e[a(\eta)/a_e]^{-3/2}$. Notice how the expansion changes 'abruptly' around the end of inflation. This is one source of non-adiabaticity that particularly impacts the evolution of modes with comoving wavenumber $k \approx a_e H_e$ and contributes to CGPP.

Epoch of reheating. During the epoch of coherent oscillations, the inflaton field gradually transfers its energy into relativistic particles, and so this period is also known as the epoch of reheating. The inflaton's energy transfer is typically accomplished by a combination of perturbative decay channels, *e.g.*, $\varphi \rightarrow \text{SM} + \text{SM}$, and non-perturbative channels such as tachyonic instability and parametric resonance; see Amin *et al.* (2014) for a review of nonlinear inflaton dynamics and preheating. The inflaton's decay products scatter and thermalize to form the primordial

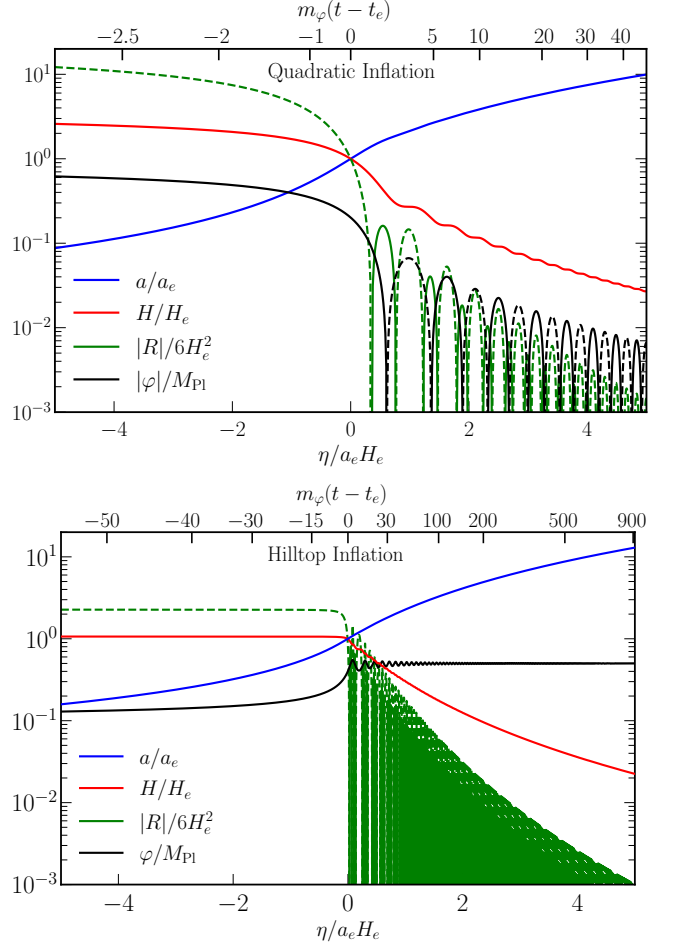


FIG. 2 Evolution of the FLRW scale factor $a(\eta)$, Hubble parameter $H(\eta)$, Ricci $R(\eta)$, and inflaton field amplitude $\varphi(\eta)$ near the end of inflation. Conformal time is normalized to vanish at the end of inflation, $\eta_e = 0$ when the scale factor and Hubble parameter take values a_e and H_e . The curves were calculated by numerically solving the homogeneous inflaton equation of motion assuming a quadratic inflaton potential (upper figure) and a hilltop inflaton potential with $v = M_{\text{Pl}}/2$ (lower figure). Since R (and φ for the quadratic model) oscillate around zero after inflation, positive (negative) values are indicated with solid (dashed) curves.

plasma, and we denote the plasma's temperature by T . Although T tends to grow due to energy injection from the inflaton decay, it also tends to decrease due to the cosmological expansion with the net effect typically going as $T \propto a^{-3/8}$ (Giudice *et al.*, 2001). When the energy stored in the growing plasma first exceeds the energy stored in the decaying inflaton condensate, the point of reheating is said to be reached. This typically occurs when the age of the universe H^{-1} rises to meet the inflaton's lifetime Γ_φ^{-1} . We denote the point of reheating with an RH subscript: t_{RH} for coordinate time, η_{RH} for conformal time, a_{RH} for scale factor, H_{RH} for Hubble parameter, and T_{RH} for plasma temperature. However, notice that "reheat"

is somewhat of a misnomer since T_{RH} is not the maximum temperature reached after inflation (Giudice *et al.*, 2001); rather, it is the maximum temperature of the radiation-dominated universe. Moreover, the universe may have never been “heated” before it was “reheated.”

Reheating temperature. The value of T_{RH} is empirically undetermined. The smallest viable reheating temperature $T_{\text{RH}}^{(\text{min})} \approx 5 \text{ MeV}$ is required for successful nucleosynthesis and neutrino thermalization (de Salas *et al.*, 2015). The largest possible reheating temperature follows from energy conservation: if the inflaton’s energy were immediately converted into a thermal bath of radiation at the end of inflation (*i.e.*, instantaneous reheating and thermalization) then the plasma temperature would be

$$T_{\text{RH}}^{(\text{max})} = \left(\frac{\rho_\varphi(t_e)}{\pi^2 g_{*\text{RH}}/30} \right)^{1/4} = \left(\frac{90 H_e^2 M_{\text{Pl}}^2}{\pi^2 g_{*\text{RH}}} \right)^{1/4} \quad (54)$$

$$\approx 8 \times 10^{14} \text{ GeV} \left(\frac{H_e}{10^{12} \text{ GeV}} \right)^{1/2} \left(\frac{g_{*\text{RH}}}{106.75} \right)^{-1/4}.$$

Here $g_{*\text{RH}}$ counts the effective number of degrees of freedom in the plasma at a temperature of T_{RH} . For a given H_e , lowering T_{RH} corresponds to extending the duration of the reheating epoch. Assuming that the universe is matter-dominated during reheating ($w_{\text{RH}} = 0$), such that $H \propto a^{-3/2}$ for $a_e < a < a_{\text{RH}}$, one finds

$$\frac{a_{\text{RH}}}{a_e} \approx (8 \times 10^7) \left(\frac{H_e}{10^{12} \text{ GeV}} \right)^{2/3} \times \left(\frac{T_{\text{RH}}}{10^9 \text{ GeV}} \right)^{-4/3} \left(\frac{g_{*\text{RH}}}{106.75} \right)^{-1/3}. \quad (55)$$

A different relation is obtained for other choices of w_{RH} . Since the universe is radiation-dominated at the point of reheating, the first Friedmann equation implies $\pi^2 g_{*\text{RH}} T_{\text{RH}}^4/30 = 3 H_{\text{RH}}^2 M_{\text{Pl}}^2$, which gives

$$H_{\text{RH}} \approx (1.4 \text{ GeV}) \left(\frac{T_{\text{RH}}}{10^9 \text{ GeV}} \right)^2 \left(\frac{g_{*\text{RH}}}{106.75} \right)^{1/2}. \quad (56)$$

This formula will prove useful, since one can compare m with H_{RH} to determine if a field of mass m is released from Hubble drag during the reheating epoch ($H_{\text{RH}} < m$, ‘early reheating’) or during the radiation epoch ($m < H_{\text{RH}}$, ‘late reheating’).

Comoving entropy conservation. After reheating is completed ($a > a_{\text{RH}}$) it is customary to assume that the comoving entropy density of the primordial plasma remains constant. The entropy density at time t is written as $s(t) = (2\pi^2/45) g_{*S}(t) T^3(t)$ where $g_{*S}(t)$ is the effective number of relativistic species. Entropy conservation after reheating implies $a_{\text{RH}}^3 s_{\text{RH}} = a^3(t) s(t) = a_0^3 s_0$, and thus

$$\frac{a_0}{a_{\text{RH}}} \approx (1 \times 10^{22}) \left(\frac{T_{\text{RH}}}{10^9 \text{ GeV}} \right) \left(\frac{g_{*\text{RH}}}{106.75} \right)^{1/3}, \quad (57)$$

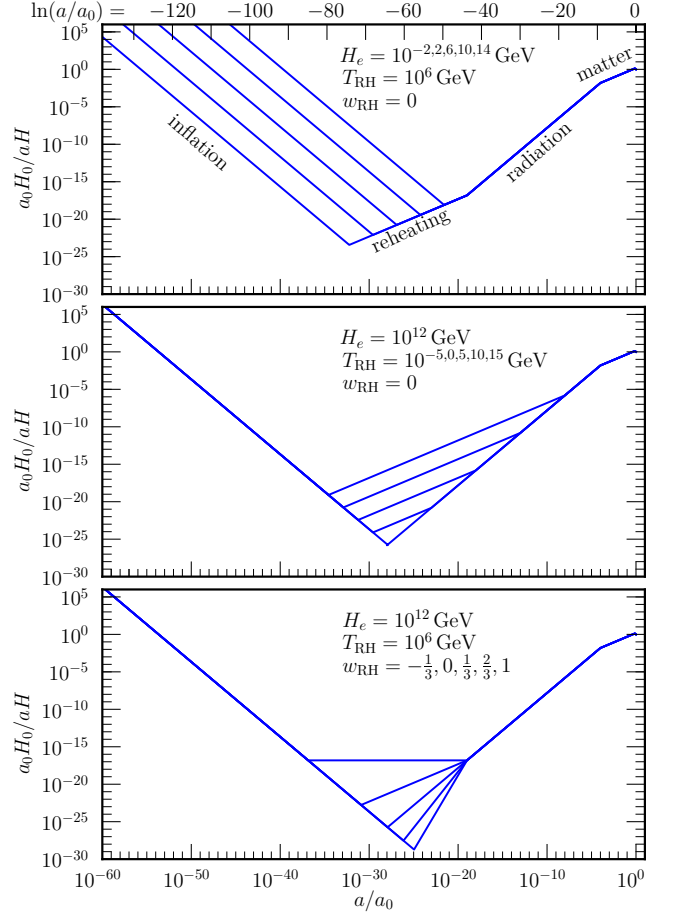


FIG. 3 Cosmological expansion history. The comoving Hubble length $d_H(a) = 1/aH(a)$ is shown as a function of the FLRW scale factor a . The three panels show the impact of varying the Hubble parameter at end of inflation H_e (top), the reheating temperature T_{RH} (middle), and the equation of state during reheating w_{RH} (bottom). From top to bottom, the curves show $\log_{10} H_e/\text{GeV} = -2, 2, 6, 10, 14$, $\log_{10} T_{\text{RH}}/\text{GeV} = -5, 0, 5, 10, 15$, and $w_{\text{RH}} = -\frac{1}{3}, 0, \frac{1}{3}, \frac{2}{3}, 1$.

where $T_0 \approx 0.234 \text{ meV}$ and $g_{*S,0} \approx 3.91$.

Λ CDM Cosmology. After reheating has occurred, the hot primordial plasma is formed and the subsequent cosmological evolution is described by the Λ CDM Cosmological Concordance Model. See Kolb and Turner (1990) for an introduction to Big-Bang nucleosynthesis (BBN), radiation-matter equality, recombination, the cosmic microwave background (CMB), large scale structure (LSS), and dark energy. The full cosmological expansion history is illustrated in Fig. 3. This figure shows the evolution of the comoving Hubble length scale $d_H(a) = 1/aH(a)$ as a function of the FLRW scale factor a in terms of its present value. Reading from the left, the first segment corresponds to the epoch of inflation during which time $H(a) = H_e$ is approximately constant and $d_H(a)$ de-

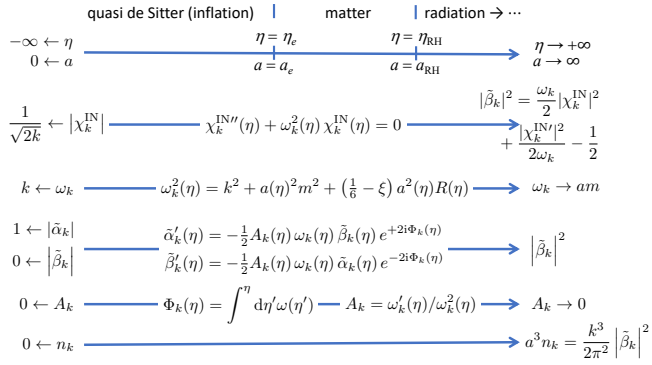


FIG. 4 A graphical summary of the CGPP calculation for inflationary cosmology. One seeks to calculate the comoving number density spectrum $a^3 n_k$, which requires the Bogolubov coefficient $\tilde{\beta}_k$, which is related to the mode function χ_k^{IN} , which solves the oscillator equation with time-dependent frequency $\omega_k(\eta)$ subject to a Bunch-Davies initial condition as $\eta \rightarrow -\infty$.

creases; the second segment corresponds to the epoch of reheating during which time $H(a) \propto a^{-3(1+w_{RH})/2}$; the third segment corresponds to the radiation-dominated era during which time $H(a) \propto a^{-2}$; the fourth segment corresponds to the matter-dominated era during which time $H(a) \propto a^{-3/2}$; and the final segment (hard to see at $a/a_0 \approx 1$) corresponds to the Λ -dominated era during which time $H(a) = H_0$ is approximately constant. Note that this figure does not capture the slow evolution of $H(a)$ during inflation and the smooth transition at the end of inflation, which are shown in Fig. 2.

B. Mode evolution and spectrum

This section discusses the evolution of the mode functions $\chi_k(\eta)$ and the resultant comoving number density spectrum $a^3 n_k$. We consider CGPP for massive spin-0 particles that correspond to the quantum excitations of either conformally-coupled or minimally-coupled scalar fields. Our approach is to present an example of numerical results, discuss the salient features, and provide an analytical understanding. A detailed derivation of the analytical results will be provided in Jenks *et al.* (2024). We first discuss conformally-coupled scalars and afterward minimally-coupled scalars. In this section we employ the dimensionless variables

$$\begin{aligned} \tilde{a} &= a/a_e, \quad \tilde{m} = m/H_e, \quad \tilde{H} = H/H_e, \\ \tilde{k} &= k/a_e H_e, \quad \text{and} \quad \tilde{\eta} = a_e H_e (\eta - \eta_e), \end{aligned} \quad (58)$$

where a_e , H_e , and η_e are the values of the FLRW scale factor, Hubble parameter, and conformal time at the end of inflation. Recall that Hubble-scale modes at the end of inflation have $k \approx k_e \equiv a_e H_e$ corresponding to $\tilde{k} \approx 1$.

Procedure. Figure 4 illustrates the key formulas in the

CGPP calculation. First a model of inflation is selected. Then the Friedmann equation is solved along with the inflaton's (homogeneous) equation of motion to find the FLRW scale factor $a(\eta)$. If solving numerically, it's necessary to select a wide enough range of η such that the modes of interest are initially inside the horizon ($a < k/H_{\text{inf}}$) and eventually they either reenter the horizon or the field is released from Hubble drag ($H < m$). Next the equation of motion for the spectator field (12) is solved along with the initial condition (26) that $\chi_k^{IN}(\eta) \rightarrow e^{-ik\eta}/\sqrt{2k}$ as $\eta \rightarrow -\infty$. If solving numerically, one can impose $\chi_k^{IN}(\eta_i) = 1/\sqrt{2\omega_k(\eta_i)}$ and $\partial_\eta \chi_k^{IN}(\eta_i) = -i\omega_k(\eta_i)\chi_k^{IN}(\eta_i)$ at an early time η_i when the modes with comoving wavenumber k are inside the horizon. The mode functions $\tilde{\beta}_k(\eta)$ are calculated using Eq. (29) and CGPP is completed when $|\tilde{\beta}_k(\eta)|^2$ reaches a constant, which coincides with the Bogolubov coefficient $|\beta_k|^2$ linking the IN and OUT ladder operators. Alternatively, one can solve Eq. (28) to obtain $\tilde{\alpha}_k(\eta)$ and $\tilde{\beta}_k(\eta)$ directly, which is most useful when ω_k^2 remains positive. Either way, Eq. (24) gives the comoving number density spectrum $a^3 n_k = (k^3/2\pi^2)|\beta_k|^2$ and Eq. (43) gives the energy density spectrum $\rho_k = E_k n_k$.

Numerical results: comoving number density spectrum.

Figure 5 shows a selection of numerical results for CGPP of massive scalars that are conformally-coupled to gravity ($\xi = 1/6$). Several notable features can be observed: (1) For small wavenumber, the spectrum scales as $n_k \propto k^2$ for low mass and more steeply for high mass. (2) For intermediate wavenumber, the spectrum reaches a peak at a value of k that depends on m . (3) Beyond the peak, the spectrum decreases exponentially with increasing k . (4) For yet larger k , the spectrum develops a power law tail that goes as $\tilde{k}^{-3/2}$ or $\tilde{k}^{-15/2}$. (5) The amplitude of the spectrum grows as $n_k \propto m$ as \tilde{m} approaches ≈ 1 from below, and it decreases as $n_k \propto e^{-c\tilde{m}}$, where c is a constant, as \tilde{m} increases beyond ≈ 1 . In what follows we discuss each of these features.

Low- k power law. The behavior of the spectrum toward small \tilde{k} is a simple power law. Modes with small wavenumber ($\tilde{k} < 1$) leave the horizon during inflation and re-enter later during the reheating or radiation era. Consequently the evolution of the mode functions $\chi_k(\eta)$ is insensitive to the dynamics of the inflaton field at the end of inflation, but instead can be studied by treating the spacetime as de Sitter with a constant Hubble parameter during inflation. It is well known that the mode equations for a scalar spectator field in de Sitter spacetime are Hankel functions; see Appendix C. Using the de Sitter solution leads to

$$\frac{a^3 n_k}{a_e^3 H_e^3} \simeq \frac{1}{8\pi^2} \tilde{k}^{3-2\text{Re}[\nu]} \tilde{m}^{1/3} \quad \text{for } \tilde{k} < \tilde{m}^{1/3} < 1 \quad (59)$$

where the index $\nu = \sqrt{1/4 - \tilde{m}^2}$ is given by Eq. (C5)

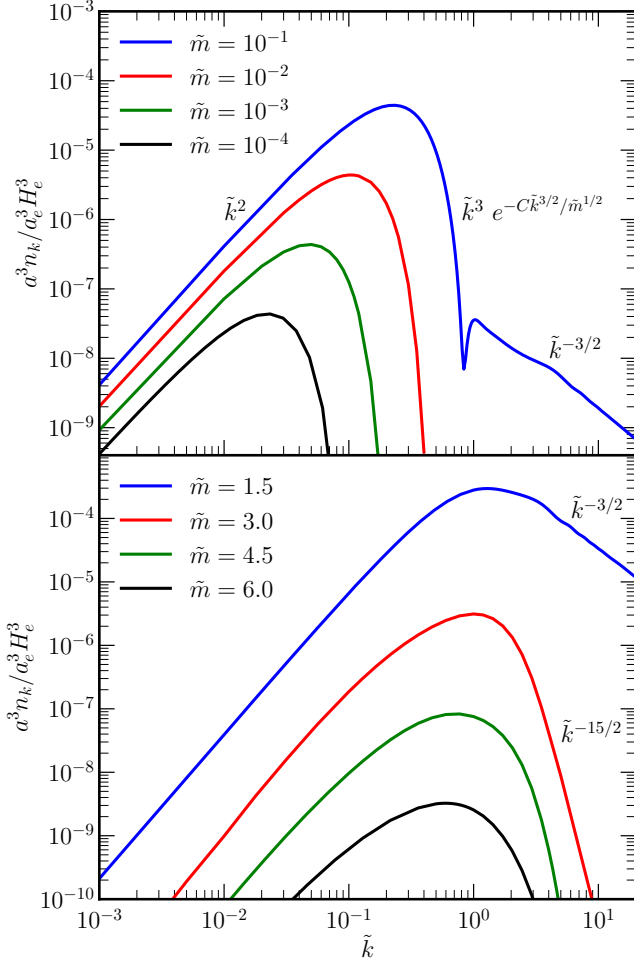


FIG. 5 The comoving number density spectrum $a^3 n_k$ resulting from CGPP for a conformally-coupled scalar field in Quadratic Inflation assuming late reheating ($H_{\text{RH}} < m$). On the horizontal axis the comoving wavenumber is expressed as $\tilde{k} = k/a_e H_e$ such that $\tilde{k} \approx 1$ correspond to Hubble-scale modes at the end of inflation. The various curves show different values of the scalar field's mass with $\tilde{m} = m/H_e$.

with $\xi = 1/6$. For $\tilde{m} < 1/2$ the spectrum scales like \tilde{k}^2 , which agrees with the scaling seen in the figure. For larger mass $\tilde{m} > 1/2$ the index ν is imaginary, and the spectrum is expected to scale as \tilde{k}^3 . The figure displays a redder spectrum, closer to \tilde{k}^2 , since the Hubble parameter decreases by a factor of almost 10 during Quadratic Inflation, rather than remaining constant as in de Sitter; see Fig. 2.

Dominant modes: k_* . For models with $\tilde{m} < 1$, the spectrum is largest for values of the comoving wavenumber around $\tilde{k} \approx \tilde{k}_*^{(\text{late})} \equiv \tilde{m}^{1/3}$. These correspond to modes that leave the horizon during inflation and reenter the horizon at the same time when the Hubble parameter $H(\eta)$ drops below the mass m and the field is released

from Hubble drag. In brief:

$$H(\eta_*) = m \quad \text{and} \quad k_* = a(\eta_*)H(\eta_*) = a(\eta_*)m. \quad (60)$$

The meaning of the superscript “late” is discussed below.

A blue-tilted spectrum. It is straightforward to calculate the spectrum analytically for small \tilde{k} where the de Sitter approximation is applicable. However, it is important to draw attention to the fact that the spectrum rises with increasing \tilde{k} , corresponding to a blue spectral tilt. The modes that carry most of the energy have $\tilde{k} \approx \tilde{m}^{1/3}$, which is possibly ≈ 1 , corresponding to modes that are on the Hubble scale at the end of inflation. Therefore, in order to calculate the total number of produced particles, it is necessary to more accurately model the dynamics of the inflaton field at the end of inflation as the Universe transitions from a quasi-de Sitter phase of inflation into an effectively matter-dominated phase of reheating. For example, [Chung *et al.* \(1998b\)](#) noted that assuming an instantaneous transition from de Sitter into matter domination can lead to a spurious overestimate of CGPP; see also [Li *et al.* \(2019\)](#).

Exponential drop. For models with $\tilde{m} < 1$, the spectrum begins to drop exponentially for the modes with $\tilde{k} > \tilde{m}^{1/3}$ that are past the peak. This behavior can be derived analytically by several related approximations including steepest descent method ([Chung, 2003](#)) and Stokes phenomenon ([Hashiba and Yamada, 2021](#); [Li *et al.*, 2019](#)); see also [Birrell and Davies \(1984\)](#); [Chung *et al.* \(2019, 1998b\)](#) for supplementary discussions. The result is found to be

$$\frac{a^3 n_k}{a_e^3 H_e^3} \approx \frac{\tilde{k}^3}{2\pi^2} e^{-C \tilde{k}^{3/2}/\tilde{m}^{1/2}} \quad \text{for} \quad \tilde{m}^{1/3} < \tilde{k} < \frac{m_\varphi \kappa}{H_e}, \quad (61)$$

where $C \sim 2\pi$ agrees well with the numerical results and $\kappa = (1 - m^2/m_\varphi^2)^{1/2}$. The upper boundary $m_\varphi \kappa/H_e$ is discussed in the following paragraphs.

To develop intuition, consider the mode equations in terms of $\tilde{\alpha}_k(\eta)$ and $\tilde{\beta}_k(\eta)$ from Eq. (28). Anticipating that CGPP will be inefficient for $\tilde{m} > 1$, the solution will have $|\tilde{\beta}_k| \ll 1$ and $|\tilde{\alpha}_k| \approx 1$. Setting $\tilde{\alpha}_k(\eta) \approx 1$ yields

$$\tilde{\beta}_k(\eta) \approx \int^\eta d\eta' \frac{1}{2} A_k(\eta') \omega_k(\eta') e^{-2i \int^{\eta'} d\eta'' \omega_k(\eta'')} . \quad (62)$$

Moreover, for models with $\tilde{m} > 1$, the nonrelativistic modes have $\omega_k \approx am$. At late time $\tilde{\beta}_k \rightarrow \beta_k$ leading to

$$\beta_k \approx \int_{-\infty}^{\infty} dt' \frac{1}{2} \frac{\dot{\omega}_k(t')}{\omega_k(t')} e^{-2imt'} \quad (63)$$

where $ad\eta = dt$. This expression reveals that β_k is the Fourier transform of $\dot{\omega}_k/2\omega_k$ evaluated at an angular frequency of $2m$. Since the time dependence is induced

by the cosmological expansion, which varies on the time scale $1/H$, one doesn't expect $\dot{\omega}_k/\omega_k$ to include a mode that varies on the much shorter time scale of $1/m$, which is the origin of the exponential suppression.

High- k power law tail. For the highest wavenumber modes shown on the figure, the spectrum develops a power law tail that falls off like $\tilde{k}^{-3/2}$ or $\tilde{k}^{-15/2}$ depending on \tilde{m} . This behavior is discussed at length in Sec. VI.D, and here we briefly summarize. At the end of inflation, the inflaton field oscillates around the minimum of its potential. If $m_\varphi > H_e$ then these oscillations are rapid, which evades the argument at the end of the preceding paragraph by providing support for the Fourier transform of $\dot{\omega}_k/\omega_k$ at frequency of $2m \approx 2m_\varphi$. Moreover, the system can be understood to consist of a collection of cold inflaton particles. These particles interact gravitationally with one another and with the scalar spectator. In particular, they can annihilate as $\varphi\varphi \rightarrow \chi\chi$ through an s -channel graviton exchange provided that $m \equiv m_\chi < m_\varphi$. The χ particles produced in this way carry a momentum of $p_\chi \approx m_\varphi$, which begins to decrease due to cosmological redshift. The earliest particles to be produced have an comoving wavenumber (*i.e.*, comoving momentum) of approximately $k \approx a_e m_\varphi$ and the last particles to be produced just before reheating is completed have $k \approx a_{\text{RH}} m_\varphi$. By considering the scattering rate, one can show that the spectrum decreases as a power law across this range of wavenumbers. If $m < m_\varphi$ then the 2-to-2 channel is kinematically accessible and it dominates giving

$$\frac{a^3 n_k}{a_e^3 H_e^3} \approx C \tilde{m}^4 \tilde{k}^{-3/2} \quad \text{for} \quad \frac{m_\varphi \kappa}{H_e} < \tilde{k} < \tilde{a}_{\text{RH}} \frac{m_\varphi \kappa}{H_e}, \quad (64)$$

where $C = (9/1024\pi)(m_\varphi/H_e)^{-5/2}\kappa^{5/2}$ Chung *et al.* (2019) is applicable for Quadratic Inflation. However, if $m_\varphi < m < 2m_\varphi$ then the 2-to-2 channel is kinematically forbidden and the 4-to-2 channel dominates giving $n_k \propto \tilde{k}^{-15/2}$ instead. To understand the change in this power law behavior in Fig. 5 recall that Quadratic Inflation has $m_\varphi \approx 2H_e$, so the break from $\tilde{k}^{-3/2}$ to $\tilde{k}^{-15/2}$ happens at around $\tilde{m} = 2$.

Although not pronounced in Fig. 5, there are oscillations in $a^3 n_k$ in the region of $\tilde{k}^{-3/2}$ scaling. These oscillations are the result of quantum interference between the $2\varphi \rightarrow \chi\chi$ and $4\varphi \rightarrow \chi\chi$ channels (Basso *et al.*, 2022). The interference is more pronounced in models with a φ^3 term at the bottom of the inflaton potential, such as Hilltop Inflation, where there will be interference between $2\varphi \rightarrow \chi\chi$ and $3\varphi \rightarrow \chi\chi$.

Conformally-coupled scalar: summary. To summarize, the numerical results in Fig. 5 for CGPP of a massive scalar field that is conformally coupled to gravity are well de-

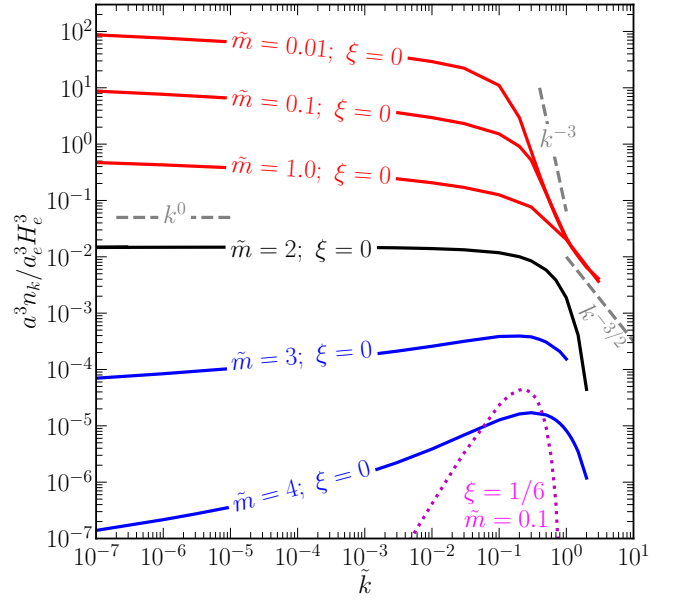


FIG. 6 Same as Fig. 5, but here we show spectra for a minimally-coupled scalar (solid curves). For comparison, the dotted curve shows a conformally-coupled scalar.

scribed by the following analytical approximations:

$$\frac{a^3 n_k}{a_e^3 H_e^3} \approx \begin{cases} \frac{1}{8\pi^2} \tilde{k}^2 \tilde{m}^{1/3} & 0 < \tilde{k} < \tilde{m}^{1/3} \\ \frac{1}{2\pi^2} \tilde{k}^3 e^{-C\tilde{k}^{3/2}/\tilde{m}^{1/2}} & \tilde{m}^{1/3} < \tilde{k} < \frac{m_\varphi \kappa}{H_e} \\ C \tilde{m}^4 \tilde{k}^{-3/2} & \frac{m_\varphi \kappa}{H_e} < \tilde{k} < \tilde{a}_{\text{RH}} \frac{m_\varphi \kappa}{H_e} \end{cases}, \quad (65)$$

provided that $m < m_\varphi$.

Numerical results: comoving number density spectrum.

Figure 6 shows a selection of numerical results for CGPP of massive scalars that are minimally-coupled to gravity ($\xi = 0$). Several notable features can be observed: (1) For the same mass (see $m/H_e = 0.1$) the spectrum for a minimally-coupled scalar is much larger than a conformally-coupled scalar. (2) For small wavenumber, the spectrum is nearly flat but slightly red-tilted for low masses $m/H_e \lesssim 1$, but it becomes increasingly blue-tilted for large masses $m/H_e \gtrsim 1$. (3) For larger wavenumber, the spectrum decreases as either a power law or an exponential. In what follows we discuss each of these features.

Contrasting conformal and minimal. The distinct behavior between the gravitational production of conformally- and minimally-coupled scalars (that are light during inflation) can be understood by inspecting their respective equations of motion. Both mode equations take the form $\chi_k''(\eta) + \omega_k^2(\eta)\chi_k(\eta) = 0$ where the angular frequency is given by Eq. (12): $\omega_k^2 = k^2 + a^2 m^2 + (1/6 - \xi)a^2 R$. For the conformally coupled scalar, $\xi = 1/6$ and the $a^2 R$

term is absent; however, for the minimally coupled scalar, $\xi = 0$ and the $a^2 R$ term appears with a positive coefficient. During inflation, the Hubble parameter is approximately constant ($H' \approx 0$) and the Ricci scalar is negative ($R \approx -12H^2$). Therefore, whereas $\omega_k^2(\eta)$ remains always positive for the conformally-coupled scalar, it may become negative for the minimally-coupled scalar; specifically, for a light scalar ($m < H_{\text{inf}}$) and for modes outside the horizon ($k < aH$). For the tachyonic modes with $\omega_k^2 < 0$, the mode functions grow like $\chi_k(\eta) \propto a(\eta)$. This correspond to a frozen amplitude ($\Phi \propto a^0$) for the original field variable before canonically normalizing its kinetic term; see above Eq. (3). This growth of $\chi_k(\eta)$ for modes outside the horizon is primarily responsible for the enhanced CGPP for minimally-coupled scalars relative to conformally-coupled scalars.

Low- k behavior. As per the discussion above in regard to the conformally-coupled scalar, the evolution of modes with $\tilde{k} < 1$ is captured by the de Sitter approximation, and a simple analytic form for the spectrum can be derived. Using the expressions from Appendix C gives

$$\frac{a^3 n_k}{a_e^3 H_e^3} \simeq \frac{1}{8\pi^2} \tilde{m}^{-1} \tilde{k}^{3-2\text{Re}[\nu]} \quad \text{for } \tilde{k} < \tilde{m}^{1/3} < 1 \quad (66)$$

where the index $\nu = \sqrt{9/4 - \tilde{m}^2}$ is given by Eq. (C5) with $\xi = 0$. For $\tilde{m} \ll 9/4$ the exponent approaches a zero, and the scaling approaches \tilde{k}^0 , corresponding to a flat spectrum. The predicted flatness is linked with the assumption of a constant Hubble parameter throughout inflation. For a model in which the Hubble parameter decreases significantly, such as Quadratic Inflation used to derive the numerical results in Fig. 6, the spectrum is red-tilted instead.

Intermediate- k behavior. For models in which the minimally-coupled scalar is light ($\tilde{m} < 1$), the spectrum has a break at $\tilde{k} \approx \tilde{k}_*^{(\text{late})} \equiv \tilde{m}^{1/3}$. These modes are entering the horizon at the same time when the field is released from Hubble drag; see Eq. (60). Modes with larger values of \tilde{k} enter the horizon earlier during the epoch of reheating, which is assumed to be effectively matter-dominated, while they are still relativistic. By tracking the evolution of these modes, one finds

$$\frac{a^3 n_k}{a_e^3 H_e^3} \approx \frac{1}{8\pi^2} \tilde{k}^{-3} \quad \text{for } \tilde{m}^{1/3} < \tilde{k} < \frac{m_\varphi \kappa}{H_e}. \quad (67)$$

On the other hand, in models with a heavy scalar ($\tilde{m} > 1$) the modes with $\tilde{m}^{1/3} < \tilde{k}$ are already nonrelativistic. Consequently the power law becomes an exponential.

High- k behavior. The range of modes with $a_e m_\varphi \kappa < k < a_{\text{RH}} m_\varphi \kappa$ are populated by the inflaton's coherent oscillations between the end of inflation and the end of reheating. The calculation is similar to the conformally-coupled

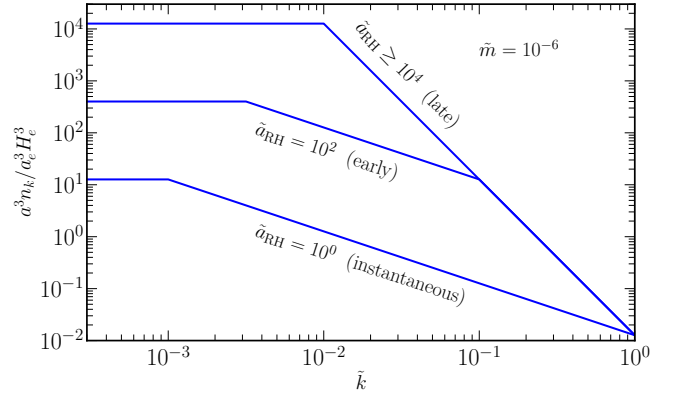


FIG. 7 An illustration of the reheating temperature's effect on the comoving number density spectrum $a^3 n_k$ for massive scalars that are light ($\tilde{m} < 1$) and minimally-coupled to gravity ($\xi = 0$). In the “late reheating” regime, corresponding to $\tilde{a}_{\text{RH}} > \tilde{m}^{-2/3} = 10^4$, the spectrum is insensitive to the reheating temperature. In the “early reheating regime” $\tilde{a}_{\text{RH}} < \tilde{m}^{-2/3} = 10^4$, the spectrum is suppressed by raising the reheating temperature (reducing a_{RH}).

scalar, discussed above. One notable difference is that the cross section for gravitational production via inflaton annihilations $\varphi\varphi \rightarrow \chi\chi$ is enhanced relative to the conformally-coupled calculation by a factor of m_φ^4/m^4 . Consequently the spectrum is insensitive to the mass:

$$\frac{a^3 n_k}{a_e^3 H_e^3} \approx C \tilde{k}^{-3/2} \quad \text{for } \frac{m_\varphi \kappa}{H_e} < \tilde{k} < \tilde{a}_{\text{RH}} \frac{m_\varphi \kappa}{H_e}, \quad (68)$$

where $C \approx (9/256\pi)(m_\varphi/H_e)^{3/2}\kappa^{5/2}$ for Quadratic Inflation. This mass insensitivity can be observed on Fig. 6 as the three red curves appear to converge at large \tilde{k} .

Minimally-coupled scalar: summary. To summarize, the numerical results in Fig. 6 for CGPP of a massive scalar field that is minimally coupled to gravity are well described by the following analytical approximations:

$$\frac{a^3 n_k}{a_e^3 H_e^3} \approx \begin{cases} \frac{1}{8\pi^2} \tilde{m}^{-1} \tilde{k}^0 & 0 < \tilde{k} < \tilde{m}^{1/3} \\ \frac{1}{8\pi^2} \tilde{k}^{-3} & \tilde{m}^{1/3} < \tilde{k} < \frac{m_\varphi \kappa}{H_e} \\ C \tilde{k}^{-3/2} & \frac{m_\varphi \kappa}{H_e} < \tilde{k} < \tilde{a}_{\text{RH}} \frac{m_\varphi \kappa}{H_e} \end{cases}, \quad (69)$$

provided that $m \ll H_e < m_\varphi$. As m rises to approach $3H_e/2$, the low- k power law begins tilting blue-ward as $\tilde{k}^{3-2\text{Re}[\nu]}$, and the peak at $\tilde{k}_*^{(\text{late})} = \tilde{m}^{1/3}$ moves toward $\tilde{k} = 1$, which pinches off the intermediate \tilde{k}^{-3} behavior revealing an exponential suppression. As m grows to exceed m_φ the $\tilde{k}^{-3/2}$ power-law tail gives way to a $\tilde{k}^{-15/2}$ power law tail associated with $4\varphi \rightarrow \chi\chi$ scattering.

Dependence on reheating. Finally let us address how the comoving number density spectrum $a^3 n_k$ depends on the

reheating temperature T_{RH} . For the numerical results in Fig. 5 and Fig. 6, the spacetime background corresponds to a quasi-de Sitter phase of inflation followed by an effectively matter-dominated phase of reheating. We have not implemented an inflaton decay rate, and the system remains matter dominated for an arbitrarily long time. This is a reasonable approximation when T_{RH} is low and reheating completes at later times, but the calculation should be modified when T_{RH} is high and reheating completes at earlier times.

To understand the dependence on reheating, it is useful to compare the particle mass m with the Hubble parameter at reheating H_{RH} ; see Eq. (56). If the reheating temperature is low such that $H_{\text{RH}} < m$ then the field is released from Hubble drag (H drops below m) during the epoch of reheating. Modes entering the horizon at this time correspond to the special wavenumber k_* defined by Eq. (60), and we have already seen that $\tilde{k}_*^{(\text{late})} = \tilde{m}^{1/3}$. On the other hand, if the reheating temperature is high such that $H_{\text{RH}} > m$ then the field is not released from Hubble drag until the radiation era. Then Eq. (60) gives $\tilde{k}_*^{(\text{early})} = \tilde{a}_{\text{RH}}^{1/4} \tilde{m}^{1/2}$, which has a different scaling with the mass $\tilde{m} = m/H_e$, and which depends on the reheating temperature through the ratio $\tilde{a}_{\text{RH}} = a_{\text{RH}}/a_e$; see Eq. (55). In summary, the two regimes are

$$\begin{aligned} \text{late-RH: } H_{\text{RH}} < m, \quad \tilde{k}_*^{(\text{late})} &= \tilde{m}^{1/3} \\ \text{early-RH: } H_{\text{RH}} > m, \quad \tilde{k}_*^{(\text{early})} &= \tilde{a}_{\text{RH}}^{1/4} \tilde{m}^{1/2}, \end{aligned} \quad (70)$$

where $H_{\text{RH}} \lesssim m$ is equivalent to $\tilde{a}_{\text{RH}}^{-3/2} \lesssim \tilde{m}$.

We have already provided spectra for the late reheating regime, and we now address how the spectra are modified for the early reheating regime. For the sake of illustration we focus on a massive scalar that is light ($\tilde{m} < 1$) and minimally-coupled to gravity ($\xi = 0$). For such a model, the spectrum in the late reheating regime is given by Eq. (69); in particular, it is flat for $\tilde{k} < \tilde{k}_*^{(\text{late})} = \tilde{m}^{1/3}$ and falls like \tilde{k}^{-3} for $\tilde{k} > \tilde{m}^{1/3}$. Here we focus on just the low- k modes ($\tilde{k} < 1$) that leave the horizon during inflation. For larger T_{RH} the spectrum develops a second break point corresponding to the modes that reenter the horizon at the end of reheating; these modes have wavenumbers around $k \approx k_{\text{RH}} \equiv a_{\text{RH}} H_{\text{RH}}$ corresponding to $\tilde{k}_{\text{RH}} = a_{\text{RH}}^{-1/2}$. The spectrum is modified to

$$\frac{a^3 n_k}{a_e^3 H_e^3} = \begin{cases} \frac{1}{8\pi^2} \tilde{a}_{\text{RH}}^{3/4} \tilde{m}^{-1/2} & \tilde{k} < \tilde{a}_{\text{RH}}^{1/4} \tilde{m}^{1/2} \\ \frac{1}{8\pi^2} \tilde{a}_{\text{RH}} \tilde{k}^{-1} & \tilde{a}_{\text{RH}}^{1/4} \tilde{m}^{1/2} < \tilde{k} < \tilde{a}_{\text{RH}}^{-1/2} \\ \frac{1}{8\pi^2} \tilde{k}^{-3} & \tilde{a}_{\text{RH}}^{-1/2} < \tilde{k} < 1 \end{cases} \quad (71)$$

which is also illustrated in Fig. 7. The highest- k modes enter the horizon during the reheating era; the

intermediate- k modes enter the horizon during the radiation era but before the field is released from Hubble drag ($H > m$); and the lowest- k modes enter the horizon during the radiation era and after the field is released from Hubble drag ($H < m$). For instantaneous reheating (54), $\tilde{a}_{\text{RH}} = 1$ and the \tilde{k}^{-3} branch is absent.

C. Resultant particle abundance

Depending on the application, the total amount of particles arising from CGPP is typically quantified using either the comoving number density $a^3 n$ or the cosmological energy fraction today Ω . See Sec. VI for a discussion of applications including baryogenesis and dark matter.

Comoving number density. The comoving number density $a^3 n$ is calculated by integrating the spectrum n_k (or n_p) over comoving wavenumber (or momentum):

$$a^3 n = \int_0^\infty \frac{dk}{k} a^3 n_k. \quad (72)$$

By performing this calculation for two models discussed in the previous subsection, the conformally-coupled scalar and the minimally-coupled scalar, one finds

$$a^3 n \approx \begin{cases} \frac{a_e^3 H_e^2 m}{16\pi^2} & , \xi = 1/6, \text{ late-RH} \\ \frac{a_e^3 H_e^4}{8\pi^2 m} \log \frac{k_*^{(\text{late})}}{k_{\text{min}}} & , \xi = 0, \text{ late-RH} \\ \frac{a_e^{9/4} a_{\text{RH}}^{3/4} H_e^{7/2}}{8\pi^2 m^{1/2}} \log \frac{k_*^{(\text{early})}}{k_{\text{min}}} & , \xi = 0, \text{ early-RH} \end{cases} \quad (73)$$

For these estimate we have assumed $m < H_e$. For the conformally-coupled scalar, lowering the mass m reduces the total number of particles, but for the minimally-coupled scalar it raises the number. For the minimally-coupled model, the spectrum n_k is independent of the comoving wavenumber for $k < k_*$ where $k_*^{(\text{late})} = a_e H_e^{2/3} m^{1/3}$ and $k_*^{(\text{early})} = a_e^{3/4} a_{\text{RH}}^{1/4} H_e^{1/2} m^{1/2}$. We regulate the integral by imposing an IR cutoff $k \geq k_{\text{min}}$. A physically-motivated choice for the cutoff is $k_{\text{min}} = a_0 H_0$ since all the modes that are outside the horizon today ($k < a_0 H_0$) appear homogeneous on our Hubble patch. Since they all oscillate with the same frequency $\omega_k \approx am$, they are indistinguishable from the $k = 0$ mode.

Comoving number conservation. After CGPP has completed, if particle-number-changing reactions are inactive, then the comoving number density is conserved:

$$a^3 n = a^3(t) n(t) = a_0^3 n_0. \quad (74)$$

Specifically $a^3 n$ gives the value today when the FLRW scale factor is a_0 and the cosmological number density is

n_0 . For example, Eq. (74) would not hold if the particles were unstable (or at least not cosmologically long-lived). Similarly it would be violated if the particles had large nongravitational interactions that allowed them to thermalize with the primordial plasma or be produced via thermal freeze-in; see Sec. VI.C.

Cosmological energy fraction. The cosmological energy fraction Ω is calculated by evaluating the ratio

$$\Omega = \frac{\rho_0}{\rho_c} \quad \text{or} \quad \Omega h^2 = \frac{\rho_0}{3M_{\text{Pl}}^2 H_{100}^2}. \quad (75)$$

The denominator ρ_c is the cosmological critical density today, given by $\rho_c \equiv 3M_{\text{Pl}}^2 H_0^2$ where $H_0 = H_{100}h$ is the Hubble constant, $H_{100} \equiv 100 \text{ km/sec/Mpc}$, and $h = 0.674 \pm 0.005$ (Aghanim *et al.*, 2020). The numerator ρ_0 is the spatially-averaged energy density today carried by a particular species of radiation/matter. For a spatially flat FLRW cosmology, the values of Ω for all the cosmological components must sum to 1, and therefore $0 < \Omega \leq 1$ gives the fractional energy carried by a particular species. For dark matter in the Universe today, observations of the CMB yield a measurement of $\Omega_{\text{dm}} h^2 = 0.120 \pm 0.001$ (Aghanim *et al.*, 2020). See also

Kolb and Turner (1990).

Relating Ωh^2 with $a_0^3 n_0$. For particles that are non-relativistic today, the energy density ρ_0 and number density n_0 are related by a factor of mass $\rho_0 \approx m n_0$, neglecting kinetic energy. Then writing $n = (a_0^3 n_0 / a_e^3 H_e^3) (a_e^3 H_e^3 / a_0^3)$, the redshift factors can be evaluated with the help of Eqs. (55) and (57) to obtain

$$\frac{\Omega h^2}{0.12} \approx \left(\frac{m}{H_e} \right) \left(\frac{H_e}{10^{12} \text{ GeV}} \right)^2 \times \left(\frac{T_{\text{RH}}}{10^9 \text{ GeV}} \right) \left(\frac{1}{10^{-5}} \frac{a_0^3 n_0}{a_e^3 H_e^3} \right). \quad (76)$$

Note that n_0 may bring an additional mass dependence. It is worth emphasizing that Eq. (76) holds for any cosmological relic with mass m and number density n_0 , not just for gravitationally produced particles; however, it does assume $w_{\text{RH}} = 0$ and $a_{\text{RH}}^3 s_{\text{RH}} = a_0^3 s_0$.

Cosmological energy fraction from CGPP. Using the analytical results derived for the two models discussed in the previous subsection, the conformally-coupled scalar and the minimally-coupled scalar, the cosmological energy fraction is found to be

$$\frac{\Omega h^2}{0.1} \approx \begin{cases} 7 \left(\frac{m}{10^{11} \text{ GeV}} \right)^2 \left(\frac{T_{\text{RH}}}{10^9 \text{ GeV}} \right) & , \quad \xi = 1/6 \\ \left(\frac{H_e}{10^{14} \text{ GeV}} \right)^2 \left(\frac{T_{\text{RH}}}{10^2 \text{ GeV}} \right) \log \left(\frac{k_{\star}^{(\text{late})}}{k_{\text{min}}} \right) & , \quad \xi = 0, \text{ late-RH} \\ \left(\frac{H_e}{10^{14} \text{ GeV}} \right)^2 \left(\frac{m}{10^{-5} \text{ eV}} \right)^{1/2} \left(\frac{g_{\star \text{RH}}}{106.75} \right)^{-1/4} \log \left(\frac{k_{\star}^{(\text{early})}}{k_{\text{min}}} \right) & , \quad \xi = 0, \text{ early-RH} \end{cases} \quad (77)$$

for $m < H_e$. The logarithmic factors depend on H_e , m , and T_{RH} ; for $k_{\text{min}} = a_0 H_0$, these factors are on the order of $\text{few} \times 10$. For the conformally-coupled scalar, note that the cosmological energy fraction decreases for small mass like $\Omega h^2 \propto m^2$. On the other hand, for the minimally-coupled scalar, the energy fraction is insensitive to the mass m in the late-reheating regime, and it varies like $\Omega h^2 \propto m^{1/2}$ in the early-reheating regime. One can see from Eq. (77) that there is generally a two-parameter family of models for which the predicted Ωh^2 matches the observed dark matter energy fraction $\Omega_{\text{dm}} h^2 \approx 0.12$.

D. Inhomogeneity

Here, we address the spatial inhomogeneity of the gravitationally produced particles, and in Sec. VI.M we discuss the observational probes of the dark matter spatial inhomogeneities (dark-matter/radiation isocurvature

perturbations), which are probed in the CMB.

Density contrast power spectrum. To quantify inhomogeneity in the gravitationally produced particles, it is useful to employ the dimensionless energy density contrast power spectrum $\Delta_\delta^2(k)$, which can be calculated using Eq. (47). If these particles are intended to provide a dark matter candidate, then the behavior of $\Delta_\delta^2(k)$ toward small values of k is especially important, since cosmological observables probe the dark matter inhomogeneity on length scales corresponding to $k \approx 10^{-4}$ to $1 a_0 \text{ Mpc}^{-1}$, which is generally much smaller than $k_e = a_e H_e$.

Conformally-coupled scalar field. Consider a scalar spectator field that is light during inflation ($m < H_e$) and conformally coupled to gravity ($\xi = 1/6$). As remarked already below Eq. (47), if the spectrum n_k is sufficiently strongly peaked at some nonzero $k \approx k_{\star}$ then the dimensionless power spectrum has a universal scaling

$\Delta_\delta^2(\eta, k \ll k_\star) \propto k^3$. This is the case for a conformally-coupled scalar, which has $n_k \propto k^2$ for small k and a peak at $k \approx k_\star^{(\text{late})} = a_e H_e (m/H_e)^{1/3}$. The resulting power spectrum is evaluated to be

$$\Delta_\delta^2(k \ll k_\star) \approx 24 \frac{k^3}{a_e^3 H_e^2 m} \quad \xi = 1/6, \quad (78)$$

which is also $24(k/k_\star^{(\text{late})})^3$. For the small-scale modes with k approaching $k_\star^{(\text{late})}$ from below, the power spectrum approaches $O(1)$, whereas for the large-scale modes with smaller k the power decreases as k^3 .

The scaling $\Delta_\delta^2(k) \propto k^3$ is especially significant if the conformally-coupled scalar is intended to provide a candidate for dark matter. Notice that $\Delta_\delta^2 \approx (8 \times 10^{-71})(k/a_0 H_0)^3 (m/10^{12} \text{ GeV})^{-1} (T_{\text{RH}}/10^9 \text{ GeV})^{-1}$ is tiny for cosmological-scale modes today (this estimate assumes $w_{\text{RH}} = 0$). As $\Delta_\delta^2 \rightarrow 0$ the dark matter inhomogeneities correspond to adiabatic perturbations, and CMB constraints on dark matter isocurvature are easily evaded. For additional details, see Sec. VI.M.

Minimally-coupled scalar field. Next consider a scalar spectator field that is light during inflation ($m < H_e$) and minimally coupled to gravity ($\xi = 0$). The spectrum is approximately scale invariant on large scales, corresponding to $n_k \propto k^0$ or $\beta_k \propto k^{-3}$ for $k < k_\star$. As a result, the power spectrum integral in Eq. (47) is dominated by the small $|\mathbf{k}'|$ region of the integration domain. To estimate the power spectrum, one can neglect the second term in Eq. (47) and divide the integration domain into two regions: $k_{\text{min}} < |\mathbf{k}'| < k$ and $k < |\mathbf{k}'| < k_\star$, approximating $\tilde{\alpha}_{|\mathbf{k}'-\mathbf{k}|}$ as $\tilde{\alpha}_k$ in the first region and $\tilde{\alpha}_{k'}$ in the second. The resulting power spectrum is evaluated to be

$$\Delta_\delta^2(k \ll k_\star) \sim \frac{\log(k/k_{\text{min}})}{\log^2(k_\star/k_{\text{min}})} \quad \xi = 0, \quad (79)$$

up to $O(1)$ factors and additional terms that are subleading for small k . For the minimally-coupled scalar spectator the dimensionless power spectrum is nearly scale invariant, varying only logarithmically with wavenumber.

Dark matter isocurvature. If the gravitationally produced particles are to provide a viable candidate for dark matter, their spatial inhomogeneities are constrained by observations of the CMB anisotropies. In particular, it is necessary to avoid an unacceptably large value of dark matter isocurvature on CMB scales. The connections with isocurvature are discussed further in Sec. VI. In short, the conformally-coupled scalar evades isocurvature constraints since $\Delta_\delta^2 \propto k^3$ is tiny on cosmological scales, whereas the minimally-coupled scalar that's light during inflation is strongly constrained by isocurvature since $\Delta_\delta^2(k) \propto \log k$ is nearly scale invariant. More generally, whenever the spectrum is sufficiently blue-tilted,

i.e. $n_k \propto k^n$ with $n > 0$, the power spectrum is strongly blue-tilted $\Delta_\delta^2 \propto k^3$, evading isocurvature constraints.

V. EXTENSION TO FIELDS WITH SPIN

The preceding discussion of CGPP in scalar field theories may be extended to fields with spin. One appealing aspect of invoking CGPP to explain the origin of cosmological relics, such as dark matter, is that the exercise of model building is limited to specifying only the particle's mass and spin if a minimal coupling to gravity is assumed. Therefore it is worthwhile to survey this limited parameter space by considering a range of spins.

In this section we first provide a general argument that CGPP requires conformal symmetry breaking. We then discuss several representations of the Lorentz group with nonzero spin. For each representation we illustrate how the cosmological expansion leads to time-dependent equations of motion. We highlight how the phenomenon of CGPP differs for each of these theories as compared with the scalar theories discussed previously.

A. CGPP requires conformal symmetry breaking

General argument. The phenomenon of CGPP derives from the mixing of positive- and negative-frequency modes due to a time-dependent dispersion relation in an expanding universe. Clearly no particle production would occur in Minkowski spacetime. Since the (homogeneous, isotropic, and expanding) FLRW spacetime is related to the (homogeneous, isotropic, and static) Minkowski spacetime by a time-dependent conformal transformation, any fields that exhibit a conformal symmetry in their coupling to gravity do not experience CGPP. For such fields, the trace of the stress-energy tensor is the order parameter for conformal symmetry breaking, and it can be used as a diagnostic tool to assess whether CGPP will occur in a given theory.

Trace of the stress-energy tensor. One can show that T_μ^μ is the order parameter for conformal symmetry breaking as follows. Consider a conformal transformation

$$g_{\mu\nu}(x) \mapsto e^{2\Omega(x)} g_{\mu\nu}(x), \quad (80)$$

where $\Omega(x)$ is a real scalar field. These are also known as Weyl or scale transformations, since they locally stretch or shrink spacetime. For example, a conformal transformation with $e^{2\Omega} = a^{-2}(\eta)$ maps the FLRW metric $g_{\mu\nu}^{\text{FLRW}} = a^2(\eta)\eta_{\mu\nu}$ to the Minkowski metric $g_{\mu\nu}^{\text{Mink}} = \eta_{\mu\nu}$. Under an arbitrary infinitesimal variation of the metric $\delta g_{\mu\nu}(\eta, \mathbf{x})$ the variation in the radiation/matter action is

$$\delta S_M = -\frac{1}{2} \int d^4x \sqrt{-g} T^{\mu\nu} \delta g_{\mu\nu}, \quad (81)$$

which defines the stress-energy tensor $T^{\mu\nu}$. Specializing to a conformal transformation, $\delta g_{\mu\nu} = 2\delta\Omega g_{\mu\nu}$, gives

$$\delta S_M = - \int d^4x \sqrt{-g} T^\mu_\mu \delta\Omega. \quad (82)$$

If the trace of the stress-energy tensor vanishes, then the matter action is invariant under conformal transformations, and the previous argument implies that no CGPP will take place. When quantum effects are taken into account, even conformally flat spacetimes may admit CGPP via the trace anomaly $\langle T^\mu_\mu \rangle \neq 0$ (Dolgov, 1981). In general, conformal invariance must be broken for particle creation to occur.

Example: massless conformal scalar. For the scalar field theory that was discussed in detail above, the trace of the stress-energy tensor (34) is

$$T^\mu_\mu = (6\xi - 1)(g^{\mu\nu}\partial_\mu\Phi\partial_\nu\Phi + \Phi\Box\Phi) + m^2\Phi^2. \quad (83)$$

Notice that the trace vanishes for the model with $m^2 = 0$ and $\xi = 1/6$, and by the preceding argument, there should be no gravitational particle production for a massless scalar that is conformally coupled to gravity. This conclusion can also be drawn from the scalar's mode equation (11), which becomes $\chi''_k + k^2\chi_k = 0$ through the static squared angular frequency $\omega_k^2 = k^2$. In the absence of a time-dependent frequency, positive- and negative-frequency modes do not mix, and no CGPP occurs. In the broader parameter space, observables must connect continuously to the absence of CGPP at $m^2 = 0$ and $\xi = 1/6$. This behavior is reflected in the analytical and numerical results that appear in the previous section, which show a suppression of the cosmological energy fraction Ωh^2 as m^2 and ξ approach the enhanced conformal symmetry point; see also Sec. VI.A.

Example: massless vector (photon). The covariant action for a massless real vector field $A_\mu(x)$ with a minimal coupling to gravity is written as

$$S = \int d^4x \sqrt{-g} \left[-\frac{1}{4} g^{\mu\rho} g^{\nu\sigma} F_{\mu\nu} F_{\rho\sigma} \right], \quad (84)$$

where $F_{\mu\nu} = \nabla_\mu A_\nu - \nabla_\nu A_\mu$. For example, $A_\mu(x)$ could be the electromagnetic field with the photon as its quantum excitation. The corresponding stress-energy tensor is

$$T_{\mu\nu} = \left(\frac{1}{4} g_{\mu\nu} g^{\rho\sigma} - \delta^\rho_\mu \delta^\sigma_\nu \right) g^{\alpha\beta} F_{\rho\alpha} F_{\sigma\beta}. \quad (85)$$

Note that the parenthetical factor vanishes when contracted with $g^{\mu\nu}$. It follows that the stress-energy tensor is traceless $T^\mu_\mu = 0$, and no CGPP occurs. In other words, a massless vector boson that's minimally coupled to gravity is also conformally coupled to gravity. If the conformal symmetry were broken, for example by introducing a mass $m^2 A_\mu A^\mu$ or a nonminimal coupling to gravity like $R A_\mu A^\mu$ or $R^{\mu\nu} A_\mu A_\nu$, then CGPP may occur (see below).

B. Massive spin-1/2 field

The analysis of CGPP for spin-1/2 particles runs parallel to the procedure discussed previously for spin-0 particles. Excellent introductions to spinor fields in curved spacetime are available in Parker and Toms (2009) and Freedman and Van Proeyen (2012), and their applications to CGPP are discussed in various references, including Boyle *et al.* (2022); Chung *et al.* (2012); and Kuzmin and Tkachev (1999). In this subsection, we present the key formulas and briefly summarize the main results.

Action in FLRW spacetime. Massive spin-1/2 particles interacting with gravity are described by a spinor field $\Psi(x)$ with the action

$$S = \int d^4x e \left[\frac{i}{4} \bar{\Psi} \gamma^\mu \nabla_\mu \Psi - \frac{i}{4} \bar{\Psi} \overleftarrow{\nabla}_\mu \gamma^\mu \Psi - \frac{1}{2} m \bar{\Psi} \Psi \right], \quad (86)$$

which generalizes the Dirac action (Dirac, 1928; Weyl, 1929) to curved spacetime. See Appendix A for a brief refresher on spinors in curved spacetime and the frame-field formalism. We require $\Psi = \Psi^C \equiv -i\gamma^2 \Psi^*$ such that $\Psi(x)$ is a self-conjugate Majorana spinor. Restricting attention to an FLRW spacetime, the field equation is

$$(i\gamma^a \delta^\mu_a \partial_\mu - a(\eta)m) [a^{3/2}(\eta)\Psi(\eta, \mathbf{x})] = 0. \quad (87)$$

This equation of motion for $\psi = a^{3/2}\Psi$ takes the same form as the Dirac equation in Minkowski spacetime, with the exception that the mass m is replaced by a time-dependent effective mass $a(\eta)m$. For a massless spin-1/2 particle ($m = 0$) there is no explicit time dependence in the equation of motion, no mixing of positive- and negative-frequency modes, and no particle production. One also arrives at this conclusion by inspecting the trace of this theory's stress-energy tensor, $T^\mu_\mu = a^3 m \bar{\Psi} \Psi$, which vanishes at $m = 0$, so the spin-1/2 particle is conformally coupled to gravity; see Sec. V.A. More generally, one expects to find a suppression of CGPP as $m \rightarrow 0$.

Mode equations. Solutions of the field's equation of motion take the form

$$\begin{aligned} \Psi(\eta, \mathbf{x}) &= [a(\eta)]^{-3/2} \int \frac{d^3\mathbf{k}}{(2\pi)^3} \sum_{\lambda=\pm 1/2} \quad (88) \\ &\quad \times \left[a_{\mathbf{k},\lambda} U_{\mathbf{k},\lambda}(\eta, \mathbf{x}) + a_{\mathbf{k},\lambda}^\dagger V_{\mathbf{k},\lambda}(\eta, \mathbf{x}) \right] \\ U_{\mathbf{k},\pm 1/2}(\eta, \mathbf{x}) &= \begin{pmatrix} u_{A,k}(\eta) \\ \pm u_{B,k}(\eta) \end{pmatrix} \otimes h_{\mathbf{k},\pm} e^{i\mathbf{k}\cdot\mathbf{x}} \end{aligned}$$

where $V_{\mathbf{k},\lambda} = -i\gamma^2 U_{\mathbf{k},\lambda}^*$. The ladder operators $a_{\mathbf{k},\lambda}$ and mode functions $U_{\mathbf{k},\lambda}(\eta, \mathbf{x})$ are labeled by a comoving wavevector \mathbf{k} and helicity λ . The two-component spinors $h_{\mathbf{k},\pm}$ are eigenspinors of the helicity operator $\frac{1}{2}\hat{\mathbf{k}}\cdot\boldsymbol{\sigma} h_{\mathbf{k},\pm} = \pm \frac{1}{2} h_{\mathbf{k},\pm}$ and are normalized such that $h_{\mathbf{k},2\lambda}^\dagger h_{\mathbf{k},2\lambda'} = \delta_{\lambda\lambda'}$.

We write $\mathbf{k} = (k \sin \theta \cos \phi, k \sin \theta \sin \phi, k \cos \theta)$ and

$$h_{\mathbf{k},+} = \begin{pmatrix} e^{-i\phi} \cos \frac{\theta}{2} \\ \sin \frac{\theta}{2} \end{pmatrix}, \quad h_{\mathbf{k},-} = \begin{pmatrix} e^{-i\phi} \sin \frac{\theta}{2} \\ -\cos \frac{\theta}{2} \end{pmatrix}, \quad (89)$$

up to irrelevant phases. The time-dependent components of the spinor wavefunction, $u_{A,k}(\eta)$ and $u_{B,k}(\eta)$, are required to obey

$$i\partial_\eta \begin{pmatrix} u_{A,k} \\ u_{B,k} \end{pmatrix} = \begin{pmatrix} am & k \\ k & -am \end{pmatrix} \begin{pmatrix} u_{A,k} \\ u_{B,k} \end{pmatrix}, \quad (90)$$

in the Dirac representation of the gamma matrices. This linear mode equation takes the same form as the time-dependent Schrödinger equation for a two-level system with the matrix on the right-hand side playing the role of the Hamiltonian; its time-dependent eigenvalues are $\omega_k(\eta) = \pm[k^2 + a^2(\eta)m^2]^{1/2}$.

Ansatz. In analogy with the scalar model discussed previously, one is looking for the mode functions $u_{A/B,k}^{\text{IN}}(\eta)$ and $u_{A/B,k}^{\text{OUT}}(\eta)$ that solve the mode equation, respect the orthonormality conditions, and have the desired asymptotic behavior toward early and late time. It is convenient to take the Ansatz

$$\begin{pmatrix} u_{A,k}^{\text{IN}} \\ u_{B,k}^{\text{IN}} \end{pmatrix} = \begin{pmatrix} \sqrt{\frac{\omega_k + am}{2\omega_k}} e^{-i\Phi_k} & -\sqrt{\frac{\omega_k - am}{2\omega_k}} e^{i\Phi_k} \\ \sqrt{\frac{\omega_k - am}{2\omega_k}} e^{-i\Phi_k} & \sqrt{\frac{\omega_k + am}{2\omega_k}} e^{i\Phi_k} \end{pmatrix} \begin{pmatrix} \tilde{\alpha}_k \\ \tilde{\beta}_k \end{pmatrix} \quad (91)$$

where $\Phi_k(\eta) = \int^\eta d\eta' \omega_k(\eta')$. The analogous relation for the scalar model appears in Eq. (27). This introduces the new mode functions $\tilde{\alpha}_k(\eta)$ and $\tilde{\beta}_k(\eta)$, which are normalized to obey $|\tilde{\alpha}_k|^2 + |\tilde{\beta}_k|^2 = 1$ at all time. The IN mode functions are asymptotic to the leading-order WKB approximation at early time, which corresponds to $\tilde{\alpha}_k(\eta) \rightarrow 1$ and $\tilde{\beta}_k(\eta) \rightarrow 0$ as $\eta \rightarrow -\infty$. In terms of the new mode functions, the mode equations are

$$\begin{aligned} \partial_\eta \tilde{\alpha}_k(\eta) &= -\frac{1}{2} A_k(\eta) \omega_k(\eta) \tilde{\beta}_k(\eta) e^{2i\Phi_k} \\ \partial_\eta \tilde{\beta}_k(\eta) &= +\frac{1}{2} A_k(\eta) \omega_k(\eta) \tilde{\alpha}_k(\eta) e^{-2i\Phi_k}, \end{aligned} \quad (92)$$

which has the same form as Eq. (28) for scalars. The dimensionless variable $A_k(\eta)$, which is defined by

$$A_k(\eta) = \frac{a^2 H m k}{(k^2 + a^2 m^2)^{3/2}}, \quad (93)$$

serves as the adiabaticity measure. Note that this is different from $\omega'_k/\omega_k^2 = a^3 H m^2/(k^2 + a^2 m^2)^{3/2}$.

CGPP intuition. By inspecting the adiabaticity measure (93), one can develop intuition for the CGPP of spin-1/2 particles. Since the equations of motion and adiabaticity parameter are the same for both $\lambda = \pm 1/2$, each of the two polarization modes will be produced

equally. Since $A_k(\eta)$ vanishes as $m \rightarrow 0$, we can anticipate a suppression of CGPP for low-mass spin-1/2 particles. Typically CGPP for spin-1/2 particles is most efficient for masses around the inflationary Hubble scale, perhaps $m \sim H_{\text{inf}} \sim 10^{14}$ GeV, corresponding to the superheavy regime. Similarly, since $A_k(\eta)$ vanishes as $k \rightarrow 0$, one expects CGPP to be suppressed for long-wavelength modes, implying a negligible power in the energy contrast on cosmological scales and if the particles survive as dark matter, predominantly adiabatic perturbations. Both of these behaviors mirror the results for conformally-coupled scalars.

Numerical example. Figure 9 shows the results of a numerical evaluation of CGPP for a massive spinor field in Quadratic Inflation; see the curves labeled $s_\lambda = 1/2_{\pm 1/2}$. As expected, the relic abundance of spin-1/2 fermions tracks closely the abundance of conformally-coupled scalars with the same mass. As the fermion mass is decreased below $m/H_e \approx 1$ the comoving number density decreases as $a^3 n \propto m^1$ and the cosmological energy fraction decreases as $\Omega h^2 \propto m^2$. CGPP leads to the largest relic abundance for $m/H_e \approx 1$, and reasonable choices of H_e and T_{RH} lead to $\Omega h^2 \approx 0.12$. Therefore if the fermions are stable, they provide a candidate for superheavy dark matter. Here we have considered CGPP for a Majorana spinor field, and the relic abundance would be doubled for a Dirac spinor field, which has both spin-1/2 particles and antiparticles as its quantum excitation. The number density spectrum $a^3 n_k$ (not shown) also tracks the conformally coupled scalar, being peaked for modes with $k \approx k_e = a_e H_e$ and suppressed for modes with $k \ll k_e$. Consequently, $\Delta_\delta^2(k) \propto k^3$ and isocurvature constraints are easily avoided.

C. Massive spin-1 field

Recent years have seen a renewed interest in the cosmological production of stable massive spin-1 particles (Ahmed *et al.*, 2020; Arvanitaki *et al.*, 2021; Cembranos *et al.*, 2023; Dimopoulos, 2006; Ema *et al.*, 2019; Garcia *et al.*, 2023a; Graham *et al.*, 2016; Gross *et al.*, 2021; Kolb and Long, 2021; Özsoy and Tasinato, 2023). This attention is partly motivated by studies of ultra-light dark photon dark matter (Caputo *et al.*, 2021), which is a candidate for wave-like dark matter with mass $m \ll 10$ eV. When applied to massive spin-1 particles, the phenomenon of CGPP can explain the origin of dark photon dark matter as well as its heavier cousins with $m \sim H_{\text{inf}}$.

Action in FLRW spacetime. Massive spin-1 particles interacting with gravity are described by a vector field $A_\mu(x)$

with the action

$$S = \int d^4x \sqrt{-g} \left[-\frac{1}{4} g^{\mu\rho} g^{\nu\sigma} F_{\mu\nu} F_{\rho\sigma} + \frac{1}{2} m^2 g^{\mu\nu} A_\mu A_\nu \right], \quad (94)$$

which generalizes the de Broglie-Proca action (de Broglie, 1922, 1934; Proca, 1936) to curved spacetime. The field strength tensor is $F_{\mu\nu} = \nabla_\mu A_\nu - \nabla_\nu A_\mu$. We require $A_\mu = A_\mu^C \equiv A_\mu^*$ such that $A_\mu(x)$ is a self-conjugate (real) vector. Here a minimal coupling to gravity is assumed; additional terms, such as $R^{\mu\nu} A_\mu A_\nu$ and $R g^{\mu\nu} A_\mu A_\nu$, may be introduced to allow for a nonminimal coupling (Golovnev *et al.*, 2008; Himmetoglu *et al.*, 2009), which impacts CGPP (Cembranos *et al.*, 2023; Kolb and Long, 2021; Özsoy and Tasinato, 2023). We assume $m \neq 0$ such that A_μ propagates three polarization modes (two transverse and one longitudinal) and CGPP may occur. The model with $m = 0$ has an enhanced gauge symmetry, which reduces the number of propagating degrees of freedom to simply two transverse polarization modes, and it has an enhanced conformal symmetry, which prohibits CGPP; see Sec. V.A.

Upon fixing $g_{\mu\nu}(x) = g_{\mu\nu}^{\text{FLRW}}(\eta, \mathbf{x})$ to be an FLRW metric with scale factor $a(\eta)$, the action becomes

$$S = \int d\eta d^3x \left[\frac{1}{2} A'_i A'_i - \frac{1}{2} a^2 m^2 A_i A_i - \frac{1}{2} \epsilon^{ijk} \epsilon^{lmk} \partial_i A_j \partial_l A_m + \frac{1}{2} m^2 a^2 A_0^2 + \frac{1}{2} \partial_i A_0 \partial_i A_0 - A'_i \partial_i A_0 \right] \quad (95)$$

where repeated Latin indices are summed from 1 to 3. Among the four components of A_μ , only three of them are propagating, and the fourth is restricted by an algebraic constraint that links it to the others.

Mode equations. Solutions of the field's equation of motion take the form

$$A_\mu(\eta, \mathbf{x}) = \int \frac{d^3\mathbf{k}}{(2\pi)^3} \sum_{\lambda=\pm 1,0} \times \left[a_{\mathbf{k},\lambda} U_{\mathbf{k},\lambda,\mu}(\eta, \mathbf{x}) + a_{\mathbf{k},\lambda}^\dagger V_{\mathbf{k},\lambda,\mu}(\eta, \mathbf{x}) \right] \quad (96)$$

$$U_{\mathbf{k},\lambda,0}(\eta, \mathbf{x}) = -i \frac{\mathbf{k}_i U'_{\mathbf{k},\lambda,i}}{k^2 + a^2 m^2}$$

$$U_{\mathbf{k},\lambda,i}(\eta, \mathbf{x}) = \chi_{\mathbf{k},\lambda}(\eta) \varepsilon_{\mathbf{k},\lambda,i} e^{i\mathbf{k}\cdot\mathbf{x}}$$

where $V_{\mathbf{k},\lambda,\mu} = U_{\mathbf{k},\lambda,\mu}^*$. The ladder operators $a_{\mathbf{k},\lambda}$ and mode functions $U_{\mathbf{k},\lambda,i}(\eta, \mathbf{x})$ are labeled by a comoving wavevector \mathbf{k} and helicity λ . The 3-vectors $\varepsilon_{\mathbf{k},\lambda,i}$ are eigenvectors of the helicity operator $i\hat{\mathbf{k}} \times \varepsilon_{\mathbf{k},\lambda} = \lambda \varepsilon_{\mathbf{k},\lambda}$ and are normalized such that $\varepsilon_{\mathbf{k},\lambda,i}^* \varepsilon_{\mathbf{k},\lambda',i} = \delta_{\lambda\lambda'}$. If

$\mathbf{k} = k(\sin\theta \cos\phi, \sin\theta \sin\phi, \cos\theta)$ then

$$\varepsilon_{\mathbf{k},\pm,i} = \frac{i}{\sqrt{2}} e^{\mp i\gamma} \begin{pmatrix} \mp \cos\theta \cos\phi + i \sin\phi \\ \mp \cos\theta \sin\phi - i \cos\phi \\ \pm \sin\theta \end{pmatrix} \quad (97)$$

$$\varepsilon_{\mathbf{k},0,i} = \begin{pmatrix} \sin\theta \cos\phi \\ \sin\theta \sin\phi \\ \cos\theta \end{pmatrix},$$

up to an irrelevant phase γ . Note that $\lambda = 0$ can be identified as the longitudinal polarization mode and $\lambda = \pm 1$ as the two transverse polarization modes. The mode functions are required to solve the equations of motion

$$(\partial_\eta^2 + \omega_T^2) \chi_{k,\pm} = 0$$

$$(\partial_\eta^2 + \omega_L^2) \left(\sqrt{\frac{a^2 m^2}{k^2 + a^2 m^2}} \chi_{k,0} \right) = 0. \quad (98)$$

where the time-dependent squared frequencies are

$$\omega_T^2 = k^2 + a^2 m^2 \quad (99)$$

$$\omega_L^2 = k^2 + a^2 m^2 + \frac{1}{6} \frac{k^2 R}{k^2 + a^2 m^2} + 3 \frac{k^2 a^4 H^2 m^2}{(k^2 + a^2 m^2)^2}.$$

CGPP intuition. Since the vector field's equations of motion (98) take the same form as a scalar field's equations of motion (11), the Bogolubov coefficients are calculated in the same way. Notice that the transverse modes obey the same equations of motion as the modes of a conformally coupled scalar field with $\xi = 1/6$; see Eq. (12). Thus, one should anticipate the same behavior in regard to CGPP, *e.g.*, a suppression of particle production as $m \rightarrow 0$. On the other hand, the longitudinal-polarization mode has a time-dependent equation of motion, even for $m = 0$, and one expects some amount of particle production. It is important to remember that sending $m \rightarrow 0$ in the de Broglie-Proca action yields the theory of a massless vector and a massless scalar with $\omega_k^2 = k^2 + R/6$.

Numerical example. Figures 8 and 9 show the numerical results of evaluating CGPP for a massive vector field in Quadratic Inflation. The comoving number density spectrum is shown in Fig. 8 for a vector field with mass $m = 0.1 H_e$. Both the transverse and longitudinal polarization modes display a blue-tilted spectrum that rises like \tilde{k}^2 for small values of $\tilde{k} = k/a_e H_e$. The spectrum reaches a peak at scales $\tilde{k} \approx \tilde{k}_*^{(\text{late})} \equiv \tilde{m}^{1/3}$, corresponding to modes that are entering the horizon at the same time when the field is released from Hubble drag; see Eq. (60). The suppression of n_k toward small k translates into a similar suppression in the dimensionless power spectrum $\Delta_\delta^2(k)$, and allows the model to evade constraints on dark matter isocurvature (Graham *et al.*, 2016); see Sec. IV.D.

The relic abundance of gravitationally produced vectors is shown in Fig. 9. The longitudinal polarization

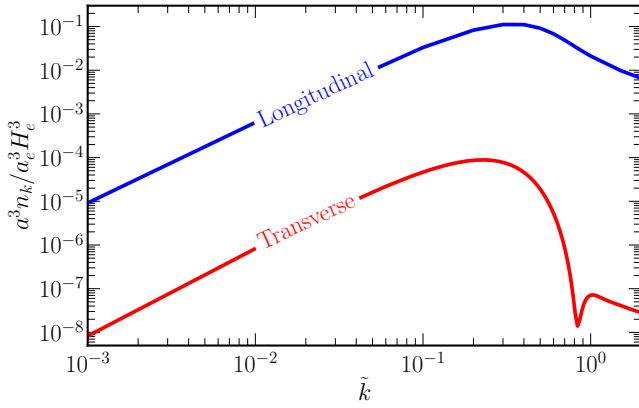


FIG. 8 The comoving number density spectrum $a^3 n_k$ as a function of $\tilde{k} = k/a_e H_e$ that results from CGPP for a massive vector field with $m = 0.1 H_e$ in Quadratic Inflation. The curves show the spectra for the single longitudinal polarization mode and the sum of the two transverse polarization modes.

modes are populated more efficiently than the transverse polarization modes, corresponding to a larger comoving number density $a^3 n$ and cosmological energy fraction Ωh^2 . For models with $m \ll H_e$, the production of transverse polarization modes goes as $a^3 n \propto m$, similar to a conformally-coupled scalar ($s_\xi = 0_{1/6}$; however, the production of longitudinal polarization modes goes as $a^3 n \propto m^{-1}$, similar to a minimally-coupled scalar ($s_\xi = 0_0$); see Eq. (73). These calculations assume late reheating (70), and for early reheating the scaling changes to $a^3 n \propto m^0$ for the longitudinal polarization modes (Ahmed *et al.*, 2020; Graham *et al.*, 2016; Kolb and Long, 2021). Both cases are captured by the relations in Eq. (77), and setting the logarithm factors equal to 1 gives a good estimate of the particle abundance.

D. Massive spin-3/2 field

A long-standing interest in massive spin-3/2 particles and their role in cosmology has largely derived from the spin-3/2 gravitino, superpartner to the graviton in theories of supergravity; for an introduction see the textbook Freedman and Van Proeyen (2012). The gravitino's weak coupling to ordinary matter allows these particles to be cosmologically long-lived, and thus their over-production in the early universe through thermal or non-thermal channels presents a serious constraint on theories of supergravity in the context of cosmology (Ellis *et al.*, 1984b; Kawasaki and Moroi, 1995; Krauss, 1983). The implications of CGPP for gravitinos and spin-3/2 particles more generally were explored in several landmark papers (Bastero-Gil and Mazumdar, 2000; Giudice *et al.*, 1999a,b; Kallosh *et al.*, 2000) and developed further in later studies (Antoniadis *et al.*, 2021; Casagrande *et al.*,

2023; Dudas *et al.*, 2021; Garcia *et al.*, 2020; Hasegawa *et al.*, 2017; Kaneta *et al.*, 2023; Kolb *et al.*, 2021a).

Action in FLRW spacetime. Massive spin-3/2 particles interacting with gravity are described by a vector-spinor field $\Psi_\mu(x)$ with the action

$$S = \int d^4x e \left[\frac{i}{4} \bar{\Psi}_\mu \gamma^{\mu\nu\rho} \nabla_\nu \Psi_\rho - \frac{i}{4} \bar{\Psi}_\mu \overleftarrow{\nabla}_\nu \gamma^{\mu\nu\rho} \Psi_\rho + \frac{1}{2} m \bar{\Psi}_\mu \gamma^{\mu\nu} \Psi_\nu \right], \quad (100)$$

which generalizes the Rarita-Schwinger action (Rarita and Schwinger, 1941) to curved spacetime. See Appendix A for a review of the frame-field formalism. We require $\Psi_\mu = \Psi_\mu^C \equiv -i\gamma^2 \Psi_\mu^*$ such that $\Psi_\mu(x)$ is a self-conjugate vector-spinor. Restricting attention to an FLRW spacetime, the field's equation of motion becomes

$$\left[i\gamma^{abc} \delta_b^\mu \partial_\mu - iaH(\gamma^a \eta^{c0} - \gamma^c \eta^{a0}) + am\gamma^{ac} \right] (a^{1/2} \Psi_c) = 0 \quad (101)$$

where $\Psi_c = \delta_c^\mu \Psi_\mu$. Latin-alphabet indices are raised and lowered with the Minkowski metric η_{ab} and inverse η^{ab} .

Mode equations. Solutions of the field's equation of motion take the form (see also Kaneta *et al.* (2023))

$$\begin{aligned} \Psi_a(\eta, \mathbf{x}) &= [a(\eta)]^{-1/2} \int \frac{d^3 \mathbf{k}}{(2\pi)^3} \sum_{\lambda=\pm 3/2, \pm 1/2} \quad (102) \\ &\times \left[a_{\mathbf{k},\lambda} U_{\mathbf{k},\lambda,a}(\eta, \mathbf{x}) + a_{\mathbf{k},\lambda}^\dagger V_{\mathbf{k},\lambda,a}(\eta, \mathbf{x}) \right] \\ U_{\mathbf{k},\lambda,0}(\eta, \mathbf{x}) &= \frac{R/3 + H^2 - 3m^2}{3(H^2 + m^2)} \gamma^0 \gamma^i U_{\mathbf{k},\lambda,i} \\ U_{\mathbf{k},\pm 3/2,i}(\eta, \mathbf{x}) &= \begin{pmatrix} u_{A,3/2,k}(\eta) \\ \pm u_{B,3/2,k}(\eta) \end{pmatrix} \otimes h_{\mathbf{k},\pm} \varepsilon_{\mathbf{k},\pm,i} e^{i\mathbf{k}\cdot\mathbf{x}} \\ U_{\mathbf{k},\pm 1/2,i}(\eta, \mathbf{x}) &= \left\{ \sqrt{\frac{1}{3}} \begin{pmatrix} u_{A,1/2,k}(\eta) \\ \mp u_{B,1/2,k}(\eta) \end{pmatrix} \otimes h_{\mathbf{k},\mp} \varepsilon_{\mathbf{k},\pm,i} \right. \\ &\quad \left. - i e^{\mp i\gamma} \sqrt{\frac{2}{3}} \begin{pmatrix} u_{A,1/2,k}(\eta) + \frac{k}{am - iaH} u_{B,1/2,k}(\eta) \\ \mp u_{B,1/2,k}(\eta) \pm \frac{k}{am + iaH} u_{A,1/2,k}(\eta) \end{pmatrix} \right. \\ &\quad \left. \otimes h_{\mathbf{k},\pm} \varepsilon_{\mathbf{k},0,i} \right\} e^{i\mathbf{k}\cdot\mathbf{x}} \end{aligned}$$

where $V_{\mathbf{k},\lambda,a} = -i\gamma^2 U_{\mathbf{k},\lambda,a}^*$. The ladder operators $a_{\mathbf{k},\lambda}$ and mode functions $U_{\mathbf{k},\lambda,a}(\eta, \mathbf{x})$ are labeled by the comoving wavenumber \mathbf{k} and helicity λ . The mode functions carry a spacetime index a and a (suppressed) spinor index. The temporal components are restricted by a constraint equation, and the spatial components are decomposed onto an orthonormal basis of helicity eigenspinors $h_{\mathbf{k},\pm}$ and 3-vectors $\varepsilon_{\lambda,\mathbf{k},i}$. In the Dirac representation of

the gamma matrices, the equations of motion are

$$\begin{aligned} i\partial_\eta \begin{pmatrix} u_{A,3/2,k} \\ u_{B,3/2,k} \end{pmatrix} &= \begin{pmatrix} am & k \\ k & -am \end{pmatrix} \begin{pmatrix} u_{A,3/2,k} \\ u_{B,3/2,k} \end{pmatrix} \\ i\partial_\eta \begin{pmatrix} u_{A,1/2,k} \\ u_{B,1/2,k} \end{pmatrix} &= \begin{pmatrix} am & c_s k \\ c_s^* k & -am \end{pmatrix} \begin{pmatrix} u_{A,1/2,k} \\ u_{B,1/2,k} \end{pmatrix}, \end{aligned} \quad (103)$$

where the time-dependent complex sound speed is

$$c_s(\eta) = \frac{m^2 - \frac{1}{3}H^2 - \frac{1}{9}R}{(m - iH)^2}. \quad (104)$$

Note that the helicity $\pm 3/2$ mode functions solve the same equation of motion as a spin- $1/2$ Dirac spinor field, and the analysis of CGPP is equivalent as well. On the other hand the helicity $\pm 1/2$ mode functions have a modified gradient term, which has arisen as a consequence of the constraint that eliminated Ψ_0 for Ψ_i .

CGPP intuition. A novel feature of the spin- $3/2$ field in the FLRW spacetime is that the helicity $\pm 1/2$ polarization modes develop an effective sound speed $c_s(\eta)$, which varies in time in response to the cosmological expansion (Giudice *et al.*, 1999b; Hasegawa *et al.*, 2017). If the FLRW expansion is driven by a perfect fluid with energy density $\rho(\eta)$ and pressure $p(\eta)$ then Friedmann's equations may be used to write the squared sound speed as

$$|c_s(\eta)|^2 = \frac{(3m^2 M_{\text{Pl}}^2 - p)^2}{(3m^2 M_{\text{Pl}}^2 + \rho)^2}. \quad (105)$$

Although this quantity cannot be negative, it may drop to zero if there exists a time η_* , or several such times, when $p(\eta_*) = 3m^2 M_{\text{Pl}}^2$. During inflation $p < 0$, since $w = p/\rho \approx -1$, and $|c_s|^2 > 0$ remains positive, but after inflation $p(\eta)$ oscillates around zero, and if these oscillations have sufficiently large amplitude the sound speed may momentarily vanish. Typically small-scale modes with large comoving wavenumber k have a nearly adiabatic evolution, since $\omega_k^2 \approx k^2$ is approximately static, and their CGPP is suppressed. However, a vanishing sound speed momentarily lifts the suppression for CGPP in high-wavenumber modes, allowing for ‘catastrophic’ particle production up to the cutoff of the theory (Hasegawa *et al.*, 2017; Kolb *et al.*, 2021a). These dynamics are similar to gradient instabilities in other systems where the squared sound speed is negative; for a few examples see Alexander *et al.* (2006); Comelli *et al.* (2015); Gumerkuoglu *et al.* (2015); and Lue *et al.* (1999). If the gradient instability is to be avoided, one requires the mass of the spin- $3/2$ particle to be larger than the Hubble parameter at the end of inflation $m > \sqrt{p_{\text{max}}/3M_{\text{Pl}}^2} \approx H_e$. Then unless the mass varies in time, one is typically considering superheavy CGPP in the context of spin- $3/2$ particles.

Numerical example. Figure 9 shows the results of a numerical evaluation of CGPP for a massive vector-spinor

field in Quadratic Inflation; see the curves labeled $s_\lambda = 3/2_{\pm 3/2}$ and $s_\lambda = 3/2_{\pm 1/2}$. The spectrum of the helicity $\pm 3/2$ polarization modes is identical to the spectrum of spin- $1/2$ particles, since their mode equations are identical. CGPP is more efficient for the helicity $\pm 1/2$ polarizations. Lowering the mass toward the threshold of the gradient instability $m \approx H_e$ enhances the abundance.

Connections with gravitinos. This discussion has focused on a spin- $3/2$ vector-spinor field with constant mass parameter m . In theories of supergravity with a spin- $3/2$ gravitino, the mass parameter may also vary in response to the evolving scale of supersymmetry breaking (Nilles *et al.*, 2001a,b). If $dm/d\eta \neq 0$ the squared sound speed (105) develops an additional contribution preventing $|c_s|^2 = 0$ (Kolb *et al.*, 2021a). Similarly the mixing of the goldstino and inflatino can modify the equations of motion so as to avoid the gradient instability for models with $m < H_e$ (Antoniadis *et al.*, 2021; Dudas *et al.*, 2021). For such models the CGPP spectrum is expected to differ significantly from the fixed-mass vector-spinor field. Possible connections between gravitino CGPP and supergravity's UV embedding have been discussed by Antoniadis *et al.* (2021); Castellano *et al.* (2021); Cribiori *et al.* (2021); Dudas *et al.* (2021); Kallosh and Linde (2004); Kolb *et al.* (2021b); and Terada (2021).

E. Massive spin-2 field

Finally we discuss the phenomenon of CGPP for a massive spin-2 tensor field, which is a spectator during inflation and not the graviton. Several recent studies have explored the idea that the dark matter might be a massive spin-2 particle (Aoki and Mukohyama, 2016; Babichev *et al.*, 2016a,b). The properties and interactions of such particles can be studied in the framework of ghost-free nonlinear bigravity (Hassan and Rosen, 2012). Here we first discuss the theory of a massive spin-2 field in an inflationary cosmology and the resultant CGPP, and afterward we discuss the connection with bigravity.

Action in FLRW spacetime. To study the gravitational production of massive spin-2 particles during and after inflation, one desires an effective field theory that describes a massive tensor field and a scalar inflaton field on a fixed curved spacetime background. A relativistically covariant action can be constructed using a symmetric two-index tensor field $v_{\mu\nu}(x)$. Among the 10 independent variables in $v_{\mu\nu}$ only 5 of them corresponds to the polarization modes of the massive spin-2 particle, and the remaining variables are eliminated by constraints or gauge symmetries. Care must be taken to construct an action that does not promote the extraneous variables into propagating degrees of freedom, which may be ghostly having a wrong-sign kinetic term (Hinterbich-

ler, 2012; de Rham, 2014). A free theory with the usual minimally-coupled matter sector can be obtained by expanding the Einstein-Hilbert action plus matter sector to quadratic order in perturbations around any background that satisfies the GR equations of motion and adding the Fierz-Pauli mass term (Fierz and Pauli, 1939). The resulting theory of a free massive spin-2 field on a fixed background is ghost-free, while non-linearities generically introduce a ghost.

The aforementioned procedure leads to an action of the form (Kolb *et al.*, 2023a)

$$S = \int d^4x \sqrt{-g} \left(\mathcal{L}_{vv}^{(2)} + \mathcal{L}_{\varphi_v \varphi_v}^{(2)} + \mathcal{L}_{v \varphi_v}^{(2)} + \mathcal{L}_{\text{int}} \right), \quad (106)$$

where $\mathcal{L}_{vv}^{(2)}$ are terms quadratic in the massive metric perturbation $v_{\mu\nu}(x)$ including a Fierz-Pauli mass term, $\mathcal{L}_{\varphi_v \varphi_v}^{(2)}$ are terms quadratic in the inflaton perturbations $\varphi_u(x)$, $\mathcal{L}_{v \varphi_v}^{(2)}$ are terms that mix the scalar metric perturbations with the inflaton perturbations, and \mathcal{L}_{int} are cubic and higher-order terms corresponding to interactions. It is important to retain the time-dependent mixing, since dropping it would lead to an expression that violates gauge symmetry and introduces a ghost.

Mode equations. The massive spin-2 field $v_{\mu\nu}(x)$ may be decomposed onto components that transform as 3-scalars, 3-vectors, and 3-tensors under the $\text{SO}(3)$ symmetry group of spatial rotations; this is the usual SVT decomposition (Baumann, 2022). Upon eliminated components that are restricted by constraints, one obtains the equations of motion for the 5 polarization modes with helicity ± 2 , ± 1 , and 0 (Kolb *et al.*, 2023a). The Fourier components of the helicity ± 2 modes obey

$$\begin{aligned} \chi''_{k,s} + \omega_k^2 \chi_{k,s} &= 0 \quad \text{for } \lambda = \pm 2 \\ \omega_k^2(\eta) &= k^2 + a^2 m^2 + \frac{1}{6} a^2 R. \end{aligned} \quad (107)$$

These are equivalent to the equations of motion for a minimally coupled scalar field, which appear in Eq. (11), and the analysis of CGPP is identical. Moreover, setting $m = 0$ yields the familiar equations of motion that arise in the study of primordial gravitational wave generation during inflation. The helicity ± 1 modes obey

$$\begin{aligned} \chi''_{k,s} + \omega_k^2 \chi_{k,s} &= 0 \quad \text{for } \lambda = \pm 1 \\ \omega_k^2(\eta) &= k^2 + a^2 m^2 - f''/f, \quad f = \frac{a^2}{\sqrt{k^2 + a^2 m^2}}. \end{aligned} \quad (108)$$

For nonrelativistic modes ($k < am$) both the tensor and vector polarizations have $\omega_k^2 \approx a^2 m^2 + a^2 R/6$, and one can anticipate similar solutions and implications for CGPP. The helicity 0 modes have a much more complicated equation of motion, since the scalar metric perturbations mix with the inflaton perturbation, and the system of two degrees of freedom must be solved simultaneously. Expressions for the quadratic action can be found in Kolb *et al.* (2023a); see also Gorji (2023).

CGPP intuition. It is worth emphasizing that the helicity-0 mode of a massive spin-2 field in curved spacetime threatens to acquire a wrong-sign kinetic term and develop a ghost instability (Fasiello and Tolley, 2012, 2013). In an FLRW spacetime this pathology is avoided if the field's mass respects the lower limit (Kolb *et al.*, 2023a)

$$m^2 > 2H^2(\eta)[1 - \epsilon(\eta)], \quad (109)$$

where $\epsilon = -H'/aH^2$ is the first slow-roll parameter; this relation is not an expansion in small ϵ . During the qdS phase of inflation, the right-hand side is approximately static $2H_{\text{inf}}^2$, and the Higuchi bound (Higuchi, 1987) is regained. After inflation $1 - \epsilon < 0$ is negative, and the ghost instability is avoided for any nonnegative choice of the squared mass parameter. Models with $m > \sqrt{2}H_{\text{inf}}$ that evade the ghost during inflation, typically have superheavy spin-2 particles, particularly if the energy scale of inflation is high, say $H_{\text{inf}} \approx 10^{14}$ GeV. Conversely, models of ultralight spin-2 dark matter require additional assumptions (such as a time-dependent mass or low cut-off) to evade a ghost instability during inflation.

Numerical example. Figure 9 shows the results of a numerical evaluation of CGPP for a massive spin-2 tensor field in Quadratic Inflation; see the curves labeled $s_\lambda = 2_{\pm 2}$. The helicity ± 2 mode functions obey the same equation of motion as a conformally-coupled scalar field with the same mass, and the predictions for CGPP are identical. We do not show results for the other polarization modes $\lambda = \pm 1$ and $\lambda = 0$.

Connection with ghost-free nonlinear bigravity. One may ask whether the quadratic action presented here can be extended into a fully nonlinear theory of massive spin-2 particles interacting with gravity without introducing ghosts. This may be accomplished in the framework of ghost-free nonlinear bigravity (Hassan and Rosen, 2012); see also the review article de Rham (2014). Theories of bigravity are formulated in terms of two dynamical metrics, typically denoted by $g_{\mu\nu}$ and $f_{\mu\nu}$, that interact with one another and may interact with matter. When both metrics are expressed as background plus perturbation, the quadratic action for the perturbations describes a massless spin-2 field, which corresponds to the usual gravitational field, and an additional massive spin-2 field, which corresponds to our $v_{\mu\nu}$. Additional model dependence enters in how the metrics couple to matter. Different couplings to matter, see for example de Rham *et al.* (2015), may lead to strikingly different results for CGPP (Kolb *et al.*, 2023a).

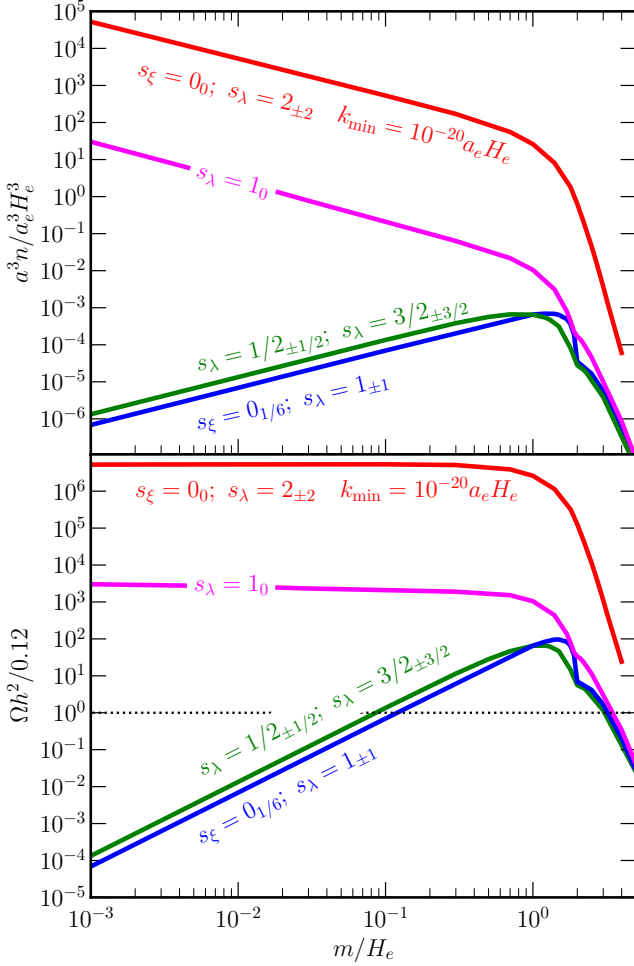


FIG. 9 The predicted abundance of gravitationally produced particles *per polarization state* assuming Quadratic Inflation. Each curve corresponds to different model labeled by the particle’s spin s , helicity λ , and (for scalar fields) its coupling to gravity ξ . For instance the curve labeled by “ $s_\lambda = 1_0$ ” corresponds to the longitudinal polarization mode of a massive vector field. Assuming the particles are stable, the figure gives the abundances today. *Top panel*: The comoving number density $a^3 n$ of produced particles in units of $a_e^3 H_e^3$ as a function of the particle’s mass m . *Lower panel*: The cosmological energy fraction Ωh^2 assuming a reheating temperature of $T_{\text{RH}} = 10^9 \text{ GeV}$ and $H_e = 10^{12} \text{ GeV}$ (see Eq. (76) for the scaling with T_{RH} and H_e). The calculation assumes late reheating.

F. Numerical comparison

Assumptions. In this section we present the results of several numerical calculations of CGPP for particles of different spin. For the examples presented here, we model the cosmological expansion using Quadratic Inflation (see Fig. 2); the inflaton drives a phase of quasi-de Sitter inflation and afterward oscillates around the minimum

of its quadratic potential during an effectively matter-dominated epoch of reheating. We do not explicitly model the inflaton decay, which corresponds to an assumption of late reheating (70). For the particle species that experiences gravitational production, we vary its mass m , its spin s , and (in the case of scalars) its coupling to gravity ξ . For particles with spin ($s \neq 0$) we further distinguish the various polarization modes (labeled by λ), which experience different levels of gravitational production. We neglect nongravitational interactions, and assume that the particles are long-lived; see Sec. VI for a few remarks about how relaxing these assumptions could modify the results.

Relic abundance. Figure 9 shows the total abundance of gravitationally produced particles. The top panel shows the comoving number density $a^3 n$ and the lower panel shows the cosmological energy fraction today Ωh^2 . These quantities are related by Eq. (76) and we take $T_{\text{RH}} = 10^9 \text{ GeV}$, but more generally $\Omega h^2 \propto T_{\text{RH}}$ in late reheating.

Superheavy and ultralight dark matter. For $\Omega h^2 \approx \Omega_{\text{dm}} h^2 \approx 0.12$, the gravitationally-produced particles can make up all of the dark matter. For the spin-0 conformally-coupled scalar field ($s_\xi = 0_{1/6}$), the spin-1/2 spinor field ($s_\lambda = 1/2_{\pm 1/2}$), the spin-3/2 vector-spinor field ($s_\lambda = 3/2_{\pm 3/2}$), and the spin-2 tensor field ($s_\lambda = 2_{\pm 2}$) the cosmological energy fraction decreases toward small mass like $\Omega h^2 \propto m^2$. Consequently, reaching $\Omega h^2 \approx 0.12$ is easier for a larger mass $m \approx H_e$, corresponding to ‘superheavy’ dark matter. On the other hand, for the spin-0 minimally-coupled scalar field ($s_\xi = 0_0$) and the longitudinal polarization of the spin-1 vector field ($s_\lambda = 1_0$), the energy fraction is insensitive to the mass $\Omega h^2 \propto m^0$. However, keep in mind that this scaling only holds while $m > H_{\text{RH}}$ and the system is in the late reheating regime (70); for small m the system is in the early reheating regime and Ωh^2 decreases with decreasing m (77). For these models all of the dark matter can be produced gravitationally for masses as low as $m \sim 10^{-5} \text{ eV}$. However, the minimally-coupled scalar is constrained by dark matter isocurvature; see Sec. VI.M.

G. Higher-spin particles

One may ask how the analysis of CGPP is extended to particle species with spin $s > 2$, here called higher-spin particles, that transform under larger representations of the Lorentz group. Although no-go theorems forbid higher-spin particles that are massless (Aragone and Deser, 1979; Coleman and Mandula, 1967; Weinberg, 1964; Weinberg and Witten, 1980), particles that are massive may evade these theorems (Bellazzini *et al.*, 2019). Moreover such particles naturally arise in nuclear physics, in condensed matter physics as compos-

ite fermions (Golkar *et al.*, 2016), and play a starring role in string theory (see *e.g.*, Sagnotti (2013)) where the higher-spin fields, originating from massive string excitations, are responsible for curing the UV divergences of gravity. Further motivation is provided by recent interest in higher-spin particles as candidates for the dark matter (Alexander *et al.*, 2021; Capanelli *et al.*, 2023; Criado *et al.*, 2020; Falkowski *et al.*, 2021; Jenks *et al.*, 2023).

Higher spin fields in de Sitter spacetime. While CGPP in higher-spin theories remains largely unexplored, the results of a few ground-breaking studies have indicated that CGPP may provide an explanation for the origin of higher-spin dark matter. The work of Alexander *et al.* (2021) focuses on bosonic fields of spin $s > 2$ that are minimally coupled to gravity, and approximates the inflationary spacetime as de Sitter with constant Hubble parameter H . On this background the components $\sigma_{\mu_1 \dots \mu_s}(\eta, \mathbf{x})$ of the higher-spin field solve the equation of motion $[\square - m^2 + (s^2 - 2s - 2)H^2]\sigma_{\mu_1 \dots \mu_s}$ (Lee *et al.*, 2016). A ghost instability develops for small masses, and the avoidance of this ghost requires $m^2 \geq s(s-1)H^2$, which is a higher-spin generalization of the Higuchi bound for massive spin-2 particles (Higuchi, 1987). This wave equation takes the same form as the equation of motion for a minimally coupled scalar field in de Sitter, and the analytical results derived previously for scalar CGPP during inflation can be carried over with the appropriate replacements. One may conclude that CGPP provides a viable explanation for the origin of higher-spin dark matter for a wide range of superheavy masses $m > H$ and spins.

Limitations and possible extensions. Treating the spacetime as de Sitter is a reasonable approach for studying CGPP in modes whose nonadiabaticity occurs during inflation as they leave the horizon, *i.e.*, $k \ll a_e H_e$. For modes on the Hubble scale at the end of inflation $k \approx a_e H_e$, which tend to carry most of the particle number, their evolution probes the transition from inflation to reheating and requires a modeling of the inflationary cosmology beyond the de Sitter approximation. This distinction may be especially important for the helicity-0 mode of the higher spin field, which can mix with the scalar inflaton perturbation, leading to an enhancement of CGPP, similar to the behavior observed in spin-2 fields.

VI. RECENT AND ONGOING ACTIVITY

In this section we summarize some of the exciting recent and ongoing activity in the study of CGPP.

A. Modeling: nonminimal gravitational interaction

There is some degree of model building freedom with regard to a particle's gravitational interaction. A field is said to be minimally coupled to gravity if its covariant action can be obtained from the flat spacetime action by promoting the Minkowski metric to a curved spacetime metric. If the covariant action contains additional interaction terms, then the field is said to couple non-minimally to gravity. Some examples of nonminimal interactions include $\mathcal{L} \supset \Phi R$, $\Phi^2 R$, $\bar{\Psi}\Psi R$, and $A_\mu A_\nu R^{\mu\nu}$.

The presence of a nonminimal interaction can greatly enhance or diminish the efficiency of CGPP. For example, a conformally-coupled scalar field with $\mathcal{L}_{\text{int}} = \frac{1}{2}\xi\Phi^2 R$ and $\xi = 1/6$ experiences less CGPP than a minimally-coupled scalar with $\xi = 0$; see Sec. III. On the other hand, a nonminimally coupled scalar with $\xi \gtrsim 1$ can experience significantly more CGPP (Cembranos *et al.*, 2020; Clery *et al.*, 2022a; Fairbairn *et al.*, 2019; Garcia *et al.*, 2023b; Markkanen and Nurmi, 2017; Markkanen and Rajantie, 2017; Yu *et al.*, 2023). This is because the Fourier mode amplitude $\chi_k(\eta)$ evolves in response to the time-dependent oscillator equation (11) with frequency $\omega_k^2 = k^2 + a^2 m^2 + (1/6 - \xi)a^2 R$, which is dominated by the $a^2 R$ term for large ξ . During inflation the Ricci scalar is approximately constant, $R \approx -12H^2$, but after inflation while the inflaton field oscillates during the epoch of reheating, the Ricci scalar R also oscillates from positive to negative values; see Fig. 2. Consequently the frequency develops an oscillatory component that increases in amplitude for larger ξ and enhances CGPP.

A global picture on the parameter space of the nonminimally coupled scalar field is shown in Fig. 10. Within the white region, it is possible to find a reheating temperature $T_{\text{reh}} \equiv T_{\text{RH}}$ such that the predicted relic abundance equals the observed dark matter relic abundance $\Omega h^2 \propto T_{\text{RH}}$; see Eq. (76). In the blue region, which contains the conformally-coupled point $\xi = 1/6$ at low mass, CGPP is less efficient and the required reheating temperature $T_{\text{reh}} > T_{\text{max}}$ would exceed the maximum possible temperature (54). In the green region where $\xi \gg 1$ CGPP is more efficient and the needed reheating temperature $T_{\text{reh}} < T_{\text{BBN}}$ would fall below the BBN temperature.

B. Modeling: scale and shape of inflaton potential

One appealing aspect of CGPP as the origin of cosmological relics is that the assumed gravitational interaction implies a limited degree of model dependence. For the particle being produced, one need only to specify its spin, its mass, and the nature of its coupling to gravity. The discussion in Secs. IV and V illustrates how CGPP depends on these parameters. Any additional model dependence enters through the physics of inflation and reheating, which controls the time dependent FLRW back-

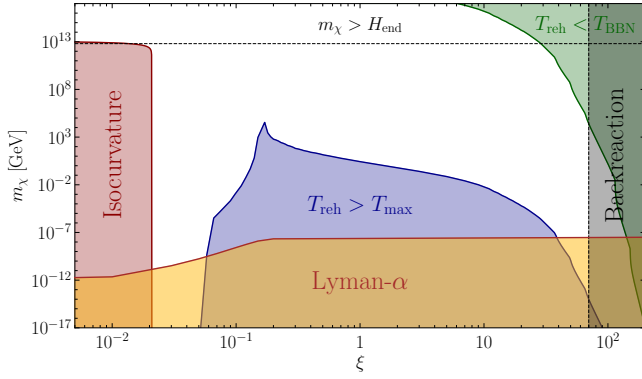


FIG. 10 CGPP predictions and constraints across the parameter space of a nonminimally coupled real scalar field. Cosmological inflation is assumed to arise from the T-Model α -Attractor (Kallosh and Linde, 2013) with $\alpha = 1$ and $V(\varphi) \approx 3m_\varphi^2 M_{\text{Pl}}^2 \tanh^2(\varphi/\sqrt{6}M_{\text{Pl}})$. This figure is published in Garcia *et al.* (2023b) and reproduced here with permission from the authors.

ground $a(\eta)$. The energy scale of inflation (parametrized by H_e) and the duration of reheating (parametrized by T_{RH}) directly impact the efficiency of CGPP, and the dependence of observables on these parameters is easy to assess; for instance, see Sec. IV.C. On the other hand, the shape of the inflaton potential typically has a weaker impact on the CGPP observables.

To assess the dependence of CGPP on the model of inflation, we consider three models that were discussed in Sec. IV.A: Quadratic Inflation, Hilltop Inflation, and T-Model α -Attractor Inflation ($\alpha = 1$). For each model, we choose the parameters such that m/H_e takes the same value. In Fig. 11 we show the comoving number density spectrum $a^3 n_k$ for a massive scalar ($m/H_e = 0.1$) with a conformal coupling to gravity ($\xi = 1/6$). For Quadratic Inflation and T-Model α -Attractor Inflation with $\alpha = 1$, the spectra are indistinguishable to the eye, and Hilltop Inflation differs by an $O(1)$ factor at the maximum. Recall that Hilltop Inflation is not symmetric about the minimum of the potential, whereas sending $\alpha \rightarrow \infty$ in α -Attractor Inflation yields the parabolic potential of Quadratic Inflation. This numerical example illustrates the insensitivity of CGPP to the shape of the inflaton potential. For studies of CGPP in models of inflation with a plateau, see also Karam *et al.* (2021).

C. Modeling: gravity-mediated thermal freeze-in

During the epoch of reheating, the decay of the inflaton condensate produces the hot primordial plasma. It is interesting to consider a scenario in which the theory contains a hidden sector that couples very weakly to the inflaton and is not populated via inflaton decays. Nevertheless, if the mass scale of hidden-sector particles

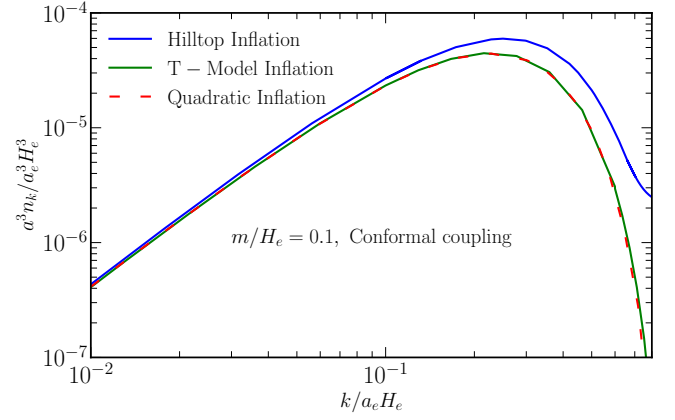


FIG. 11 An illustration of the insensitivity of CGPP to the shape of the inflaton potential. The three curves correspond to different models: Hilltop Inflation, T-Model α -Attractor Inflation ($\alpha = 1$), and Quadratic Inflation. The comoving number density spectrum is shown as a function of $k/a_e H_e$.

is not much larger than the temperature of the visible-sector radiation, then one can expect the hidden sector to be populated via annihilations of visible-sector particles through gravitational interactions alone. This is a form of UV-dominated thermal freeze-in (Hall *et al.*, 2010), similar to gravitino production (Ellis *et al.*, 1984a; Khlopov and Linde, 1984; Nanopoulos *et al.*, 1983; Olive *et al.*, 1985). If the hidden sector contains stable massive particles, they are candidates for dark matter, and the freeze-in provides a viable mechanism for their creation.

To illustrate the parametric dependence of gravity-mediated thermal freeze-in, consider the following simplified example. Let the visible sector particles be represented by S and the hidden sector particles be represented by X . Suppose that S particles are in thermal equilibrium with temperature T , and that X particles are initially absent but gradually produced via $SS \rightarrow h_{\mu\nu} \rightarrow XX$ where the reaction could be mediated by an s -channel graviton exchange illustrated in Fig. 12. This reaction is assumed to arise from a gravitational strength coupling such that X population never becomes too large, and the reverse process can be neglected; *i.e.*, the X particles freeze-in.

The number density $n_X(t)$ of X particles is required to solve the Boltzmann equation (Kolb and Turner, 1990)

$$\frac{dn_X}{dt} + 3Hn_X = -\langle\sigma v\rangle_{SS\rightarrow XX} [(n_X)^2 - (n_X^{\text{eq}})^2]. \quad (110)$$

The reaction $SS \rightarrow XX$ has a temperature-dependent thermally-averaged cross section $\langle\sigma v\rangle_{SS\rightarrow XX}$ (Gondolo and Gelmini, 1991) that depends on the mass and spin of the particles involved (Garny *et al.*, 2018, 2019). We take $\langle\sigma v\rangle_{SS\rightarrow XX} \approx T^2/M_{\text{Pl}}^4$ for these estimates. The number density n_X of X particles is much smaller than

the number density n_X^{eq} that the X particles would have if they were in equilibrium at temperature T . If $m_X \ll T$ then $n_X^{\text{eq}} \approx \zeta(3)T^3/\pi^2$ up to an $O(1)$ factor that depends on the spin and number of internal degrees of freedom associated with the X particles.

To solve the equation, it is necessary to specify how the Hubble parameter $H(t)$ and temperature $T(t)$ depend on time. During the epoch of reheating, these variables depend on the cosmological equation of state and the inflaton's decay rate. To make a simple estimate, we suppose that the epoch of reheating is brief and can be ignored (*i.e.*, instantaneous reheating). When reheating is completed, the universe is radiation dominated at a temperature T_{RH} , and subsequently $H(t) \propto a^{-2}(t)$ and $T(t) \propto a^{-1}(t)$. Then the solution can be written as

$$n_X(t) = \frac{1}{a^3(t)} \int_{t_{\text{RH}}}^t dt' a^3(t') \langle \sigma v \rangle_{SS \rightarrow XX}(t') (n_X^{\text{eq}}(t'))^2 \\ \approx \frac{1}{a(t)^3} \frac{\sqrt{10}\zeta^2(3)}{\pi^5} \frac{a_{\text{RH}}^3 T_{\text{RH}}^6}{M_{\text{Pl}}^3}. \quad (111)$$

Notice that the number density has a power-law sensitivity to the maximum temperature T_{RH} , which is characteristic of UV-dominated freeze-in. Assuming that the X particles eventually become nonrelativistic, their cosmological energy fraction today is

$$\Omega_X h^2 \approx 0.6 \left(\frac{m_X}{10^{12} \text{ GeV}} \right) \left(\frac{T_{\text{RH}}}{10^{13} \text{ GeV}} \right)^3 \quad (112)$$

for $m_X \lesssim T_{\text{RH}}$. Note that this estimate is compatible with the dark matter energy fraction $\Omega_{\text{dm}} h^2 \approx 0.12$ for appropriate choices of m_X and T_{RH} .

The rough estimate here is only provided for illustrative purposes. Several studies (Barman and Bernal, 2021; Bernal *et al.*, 2018; Chianese *et al.*, 2020, 2021c; Chung *et al.*, 1999; Clery *et al.*, 2022a,b; Garcia *et al.*, 2022; Garny *et al.*, 2018, 2016; Kaneta *et al.*, 2019; Mambrini *et al.*, 2022; Redi *et al.*, 2021; Tang and Wu, 2016, 2017; Zhang *et al.*, 2023; Zhang and Zheng, 2023) have more accurately modeled various aspects of the calculation including: replacing S with the full Standard Model particle content, which affects $\langle \sigma v \rangle_{SS \rightarrow XX}$; modeling the plasma temperature evolution during the epoch of reheating, which affects the scaling $T(a)$ as well as the maximum temperature (Giudice *et al.*, 2001); and extending the analysis to models with $m_X > T$, which introduces a Boltzmann suppression. The conclusion is that gravity-mediated thermal freeze-in can explain the origin of dark matter and play a significant role in populating weakly-coupled sectors.

D. Modeling: gravity-mediated inflaton annihilation

During the epoch of reheating, it is often assumed that the inflaton field oscillates around a quadratic minimum

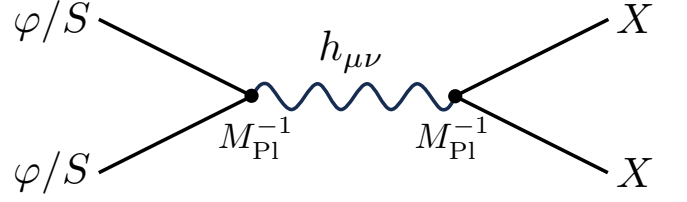


FIG. 12 Annihilation channels contributing to gravitational particle production.

of its effective potential $V(\varphi) \approx m_\varphi^2 \varphi^2/2$. This configuration describes a universe that is permeated by a non-relativistic condensate of inflaton particles. Each particle carries an energy of approximately m_φ (neglecting kinetic energy) and if the maximum field amplitude is φ_{max} then the number density of particles in the condensate is approximately $m_\varphi \varphi_{\text{max}}^2/2$. It is important to emphasize that this density can be very large. For instance, if the energy density that drives inflation $\rho_\varphi \approx 3M_{\text{Pl}}^2 H_e^2$ is transferred entirely to the condensate $\rho_\varphi \approx m_\varphi^2 \varphi_{\text{max}}^2/2$ then $\varphi_{\text{max}} \approx \sqrt{6} M_{\text{Pl}} H_e / m_\varphi$ and $n_\varphi \approx 3M_{\text{Pl}}^2 H_e^2 / m_\varphi$ at the end of inflation such that the number of inflaton particles per Hubble volume is $n_\varphi / H_e^3 \approx 3M_{\text{Pl}}^2 / m_\varphi H_e \gg 1$.

The high density of inflaton particles enhances the rate of inflaton annihilations. Suppose that the theory contains a particle species X in a hidden sector that only couples gravitationally to the inflaton. Such particles can be produced due to inflaton annihilations via an s -channel graviton $\varphi\varphi \rightarrow h_{\mu\nu} \rightarrow XX$ provided that the X particles are lighter than the inflaton particles $m_X < m_\varphi$ such that the 2-to-2 channel is not kinematically blocked. To calculate the relic density, one can solve a Boltzmann equation similar to the one in Eq. (110) but with the replacements $H \rightarrow H_e(a/a_e)^{-3/2}$, $\langle \sigma v \rangle_{SS \rightarrow XX} \rightarrow (\sigma v)_{\varphi\varphi \rightarrow XX} \approx m_\varphi^2 / M_{\text{Pl}}^4$, and $n_X^{\text{eq}} \rightarrow n_\varphi \approx (3M_{\text{Pl}}^2 H_e^2 / m_\varphi)(a/a_e)^{-3}$. Assuming the X particles are stable and nonrelativistic, their cosmological energy fraction today is

$$\Omega_X h^2 \approx 0.7 \left(\frac{H_e}{10^9 \text{ GeV}} \right) \left(\frac{m_X}{10^9 \text{ GeV}} \right) \left(\frac{T_{\text{RH}}}{10^{10} \text{ GeV}} \right) \\ \times \left(\frac{(\sigma v)_{\varphi\varphi \rightarrow XX}}{m_\varphi^2 / M_{\text{Pl}}^4} \right) \left(\frac{n_\varphi(a_e)}{3M_{\text{Pl}}^2 H_e^2 / m_\varphi} \right)^2, \quad (113)$$

where the dependence on T_{RH} enters through the redshift factor and not because particles are produced thermally from the plasma. This corresponds to a number density $n_X(t_e) \approx 6H_e^3$ at the end of inflation: a few particles per Hubble volume. This normalization of the cross section is appropriate if X is a minimally-coupled scalar, and for other particle species (such as a conformally-coupled scalar) an additional dependence on m_X may enter (Ema *et al.*, 2018). The predicted $\Omega_X h^2$ can be comparable to the observed dark matter energy fraction

today $\Omega_{\text{dm}} h^2 \approx 0.12$, indicating that gravity-mediated inflaton annihilations offer a viable explanation for the origin of dark matter.

Inflaton annihilations lead to a characteristic energy spectrum for the produced X particles. Since each inflaton particle carries an energy of $E_\varphi \approx m_\varphi$, and assuming $m_X < m_\varphi$, the 2-to-2 scattering leads to X particles with momentum $p_X \approx m_\varphi$ at the time of production. Consequently, the first particles to be produced at the end of inflation have a comoving momentum (wavenumber) of $k = a_e m_\varphi$, and the last particles to be produced at the end of reheating have a larger $k = a_{\text{RH}} m_\varphi$. Conversely, particles with comoving wavenumber k in the range $a_e m_\varphi < k < a_{\text{RH}} m_\varphi$ are produced at a time when the scale factor is $a = k/m_\varphi$. For a given k , integrating the Boltzmann equation over one Hubble time gives

$$a^3 n_{X,k} \approx a^3 (\sigma v)_{\varphi\varphi \rightarrow XX} n_\varphi^2(a) H^{-1}(a) \Big|_{a=k/m_\varphi} \quad (114)$$

$$\approx (9a_e^3 H_e^3) \left(\frac{H_e}{10^9 \text{ GeV}} \right)^{-3/2} \left(\frac{m_\varphi}{10^9 \text{ GeV}} \right)^{3/2} \left(\frac{k}{a_e H_e} \right)^{-3/2},$$

which is the comoving number density of X particles with comoving wavenumbers around k . Note that $n_{X,k} \propto k^{-3/2}$. If X particles were heavier such that $m_\varphi < m_X < 3m_\varphi/2$, then the 2-to-2 channel would be blocked and the $\varphi\varphi\varphi \rightarrow XX$ channel would be dominant. Since the production rate would go as n_φ^3 it would decrease more rapidly in time, leading to a steeper spectrum $n_{X,k} \propto k^{-9/2}$. Moreover, these exponents all assume $w_{\text{RH}} = 0$, and changing the equation of state during reheating will change the spectral indices.

Although the preceding discussion characterizes gravitational particle production from inflaton annihilations as a scattering process, the same phenomenon is also captured by the Bogolubov framework. While the inflaton field oscillates with decreasing amplitude during the epoch of reheating, the FLRW scale factor $a(\eta)$ develops an oscillatory component as well; see Fig. 2. The mode equations for a spectator field on this FLRW background take the form $\chi_k'' + \omega_k^2(\eta)\chi_k = 0$; for example, a minimally-coupled scalar field has $\omega_k^2(\eta) = k^2 + a^2(\eta)m^2 + a^2(\eta)R(\eta)/6$ as in Eq. (11). The Bogolubov coefficient β_k is calculated by solving Eq. (28) for $\tilde{\beta}_k(\eta)$ and then taking $\eta \rightarrow \infty$ as in Eq. (29). Provided that particle production is inefficient such that $|\beta_k|^2 \ll 1$ and $|\alpha_k|^2 \approx 1$, the solution is written as the integral

$$\beta_k = -\frac{1}{2} \int_{-\infty}^{\infty} d\eta \frac{\omega_k'(\eta)}{\omega_k(\eta)} e^{-2i \int_{-\infty}^{\eta} d\eta' \omega_k(\eta')} . \quad (115)$$

This integral resembles a Fourier transform, and similar to a Fourier transform it selects out the amplitude of oscillations in ω_k'/ω_k . This leads to $\beta_k \approx \beta_k^{(1 \rightarrow 2)} + \beta_k^{(2 \rightarrow 2)} + \beta_k^{(3 \rightarrow 2)} + \dots$ where $\beta_k^{(n \rightarrow 2)}$ corresponds to the contribution from applying the stationary phase approximation at a time η_* when $n^2 m_\varphi^2 = k^2/a^2(\eta_*) + m_X^2$. Each of

these terms corresponds to a scattering channel where n inflaton particles annihilate into two X particles.

CGPP from homogeneous metric oscillations at the end of inflation was first discussed by [Suen and Anderson \(1987\)](#) and [Vilenkin \(1985\)](#) and later by [Markkanen and Nurmi \(2017\)](#). The scattering description (gravitational annihilation) was developed by [Ema et al. \(2015, 2016, 2018\)](#), and its equivalence with the Bogolubov formalism was established by [Basso and Chung \(2021\)](#); [Chung et al. \(2019\)](#); and [Kaneta et al. \(2022\)](#). Phenomenological applications for the production of cosmological relics such as dark matter were explored in these studies as well as many others ([Barman and Bernal, 2021](#); [Clery et al., 2022a,b](#); [Ema et al., 2019](#); [Garcia et al., 2022](#); [Mambrini and Olive, 2021](#)). Of particular note is the relative importance of particle production via gravity-mediated thermal freeze-in from the plasma and gravity-mediated inflation annihilations. It is worth emphasizing that typically the latter dominates over the former, since more energy is available in the inflaton at the end of inflation than in the plasma ([Clery et al., 2022b](#)).

E. Modeling: interference effects

The discussion in the preceding subsection explains that while the inflaton field φ oscillates during the epoch of reheating, CGPP can be described as gravity-mediated inflaton annihilations. Particles of species X are produced via reactions such as $\varphi\varphi \rightarrow XX$ and $\varphi\varphi\varphi \rightarrow XX$ with an s -channel graviton exchange. In familiar calculations of S -matrix elements, interference effects can arise when various intermediate states (usually corresponding to distinct Feynman graphs) contribute to transitions between the same pair of initial and final states; in short, if $\mathcal{M} = \mathcal{M}_1 + \mathcal{M}_2$ then $|\mathcal{M}|^2 = |\mathcal{M}_1|^2 + |\mathcal{M}_2|^2 + 2\text{Re}[\mathcal{M}_1^* \mathcal{M}_2]$ where the last term is the interference. It would appear that reactions such as $\varphi\varphi \rightarrow XX$ and $\varphi\varphi\varphi \rightarrow XX$ cannot interfere since they have different initial states (2 versus 3 inflaton particles) as well as different final states ($E_X \approx m_\varphi$ versus $E_X \approx 3m_\varphi/2$). However this conclusion is premature.

[Basso et al. \(2022\)](#) argues that interference effects can arise in CGPP and leave their imprint on the spectrum of produced particles. This conclusion is most easily understood in the Bogolubov formalism since the stationary phase approximation gives $\beta_k \approx \beta_k^{(2 \rightarrow 2)} + \beta_k^{(3 \rightarrow 2)}$ leading to a comoving number density $a^3 n_k \propto |\beta_k|^2 = |\beta_k^{(2 \rightarrow 2)}|^2 + |\beta_k^{(3 \rightarrow 2)}|^2 + 2\text{Re}[\beta_k^{(2 \rightarrow 2)*} \beta_k^{(3 \rightarrow 2)}]$ where the last term is the interference. To understand the interference in the scattering formalism it is useful to recognize two important aspects of the calculation. First, while the inflaton field oscillates after inflation, the quantum mechanical description of this system is a coherent state ([Albrecht et al., 1994](#)), *i.e.*, a state of indefinite particle number that is constructed as a coherent superposi-

tion of n -particle states. The notation $\varphi\varphi \rightarrow XX$ and $\varphi\varphi\varphi \rightarrow XX$ is potentially misleading, since it suggests different initial states, whereas both reactions correspond to the same initial state, and they can interfere. Second, the cosmological expansion reduces the energy of the produced X particles. As a result, higher-energy X particles produced earlier can interfere with lower-energy X particles produced later, since they all have the same energy at late times. For instance, if production occurs via the 3-to-2 channel at a time when the redshift is $a_{3\rightarrow 2}$ then the comoving energy of the X particles is $a_{3\rightarrow 2}(3m_\varphi/2)$, and similarly the 2-to-2 channel gives $a_{2\rightarrow 2}m_\varphi$. These comoving energies are equal provided that $a_{2\rightarrow 2} = (3/2)a_{3\rightarrow 2}$, and the scatterings can interfere.

These interference effects lead to characteristic “fringes” in the spectrum n_k of gravitationally produced particles. A combination of constructive and destructive interference leads to a ‘wiggly’ spectra, which have been observed in several numerical studies of CGPP; see [Basso et al. \(2022\)](#) for references and additional details. Careful inspection of the curve marked $\tilde{k}^{-3/2}$ in [Fig. 5](#) shows such wiggles. They are not pronounced for Quadratic Inflation because the symmetry of the potential precludes the $3 \rightarrow 2$ process, so interference first appears in $\beta_k^{(2\rightarrow 2)} + \beta_k^{(4\rightarrow 2)}$. The $3 \rightarrow 2$ process is allowed for other models like Hilltop Inflation, and the interference fringes are much more pronounced.

F. Relics: dark matter

Gravitational particle production offers an elegant explanation for the origin of the cold dark matter. All of the evidence for the presence of dark matter in the Universe today and throughout the cosmic history derives from the dark matter’s gravitational influence on light, ordinary matter, and itself. Moreover, various observations constrain the dark matter’s nongravitational interactions with itself and ordinary matter. Therefore, it is natural to ask whether the gravitational force may have also governed the creation of dark matter particles.

Various studies by many groups have explored the idea of gravitationally-produced dark matter over the years. Among the earliest studies are [Chung \(2003\)](#); [Chung et al. \(2001, 1998a,b\)](#); [Kuzmin and Tkachev \(1998, 1999\)](#), which focused on superheavy dark matter dubbed WIMPZILLAS ([Kolb et al., 1999a,b](#)). The phrase WIMPZILLA was originally used to describe any superheavy and weakly coupled dark matter candidate regardless of its origin; different production scenarios were considered including thermal freeze-in, nonthermal production during preheating, direct production from inflaton decay, and gravitational production. The language was intended to contrast with the prevailing WIMP paradigm in which thermal freeze-out of heavier particles requires larger coupling to yield the same relic abundance ([Gri-](#)

[est and Kamionkowski, 1990](#)). Here we focus on WIMPZILLA dark matter created by CGPP. In the WIMPZILLA regime, the dark matter’s mass is assumed to reside close to the inflationary Hubble scale and the inflaton mass scale, $m_\chi \approx H_e \approx m_\varphi$. This is because CGPP is strongly suppressed for $m_\chi \gg H_e \approx m_\varphi$, making production of heavier particles ineffective – however see [Kanike et al. \(2017\)](#); [Kim et al. \(2021, 2023\)](#) – and because several considerations disfavored $m_\chi \ll H_e \approx m_\varphi$. For spin-1/2 particles and conformally-coupled spin-0 particles, CGPP is suppressed for small m_χ , making it difficult to accommodate all the dark matter for masses below the WIMPZILLA regime; see [Sec. V.B](#). On the other hand, for minimally-coupled spin-0 particles CGPP is effective even for $m_\chi \ll H_e \approx m_\varphi$, but such models were found to be in conflict with CMB limits on dark matter isocurvature ([Chung et al., 2005](#)), and these constraints were evaded by raising the dark matter’s mass up to the WIMPZILLA regime; see [Sec. VI.M](#). More recent work has explored models that allow for efficient CGPP of light dark matter away from the classic WIMPZILLA regime. For scalar dark matter, introducing a nonminimal gravitational coupling suppresses isocurvature on scales probed by the CMB ([Fairbairn et al., 2019](#); [Garcia et al., 2023b](#); [Kolb et al., 2023b](#)). Additionally, for spin-1 particles the isocurvature constraints are naturally evaded since the evolution of vector and scalar fields differ for nonrelativistic modes outside the horizon ([Graham et al., 2016](#)).

If the dark matter were to *only* interact gravitationally, this could be considered a “nightmare scenario” from the perspective of dark matter phenomenology. For instance, there would be no sign of dark matter at direct detection experiments searching for nuclear recoil, no detectable signals of dark matter annihilation in the galactic halo, and no significant production of dark matter at high-energy collider experiments. Instead one would need to search for dark matter’s gravitational influence in the laboratory or in cosmological observables; see the discussion in subsections below.

On the other hand, from the perspective of effective field theory one generally expects the dark matter to experience nongravitational interactions. Provided that these interactions are sufficiently weak, they would not play a significant role in dark matter production, leaving the dark matter’s relic abundance to be determined by CGPP. The relative importance of nongravitational production (*e.g.*, thermal freeze-in) and CGPP must be assessed on a model-by-model basis to identify the regions of parameter space where each process dominates ([Chianese et al., 2020](#); [Kolb and Long, 2017](#)).

The presence of nongravitational interactions also threatens to disrupt the dark matter’s stability. This issue is particularly relevant for superheavy dark matter, since a larger mass typically translates into a shorter lifetime for unstable particles. For the sake of illustration, consider a real scalar field χ , serving as the dark

matter candidate, that couples to the Standard Model Higgs doublet Φ via $\mathcal{L}_{\text{int}} = -c_n M_{\text{Pl}}^{3-2n} \chi (\phi^\dagger \Phi)^n$ where c_n is an $O(1)$ coefficient and $n \geq 1$ is an integer. Provided that the decay $\chi \rightarrow n\Phi + n\bar{\Phi}$ is kinematically accessible, the decay rate is parametrically $\Gamma_\chi \sim m_\chi^{4n-5} M_{\text{Pl}}^{6-4n}$. Comparing the lifetime $\tau_\chi \sim 1/\Gamma_\chi$ with the age of the Universe today $t_U \approx 13.7 \text{ Gyr}$ gives

$$\tau_\chi/t_U \sim \begin{cases} 10^{-67} m_{12} & , \quad n = 1 \\ 10^{-41} m_{12}^{-3} & , \quad n = 2 \\ 10^{-16} m_{12}^{-7} & , \quad n = 3 \\ 10^{10} m_{12}^{-11} & , \quad n = 4 \end{cases} \quad (116)$$

where $m_{12} = m_\chi/10^{12} \text{ GeV}$. In order for χ to be cosmologically long lived ($\tau_\chi/t_U \gg 1$) with a superheavy mass $m_\chi \approx 10^{12} \text{ GeV}$ it is necessary to forbid (or at least strongly suppress) the operators with $n = 1, 2, 3$. For example, one can argue that when constructing the effective field theory, we should impose a symmetry to forbid operators that would mediate χ decay; *e.g.*, a discrete \mathbb{Z}_2 symmetry that takes $\chi \rightarrow -\chi$ and leaves other fields unchanged. Although, this approach runs counter to the conjectured absence of global symmetries in theories of quantum gravity (Mambrini *et al.*, 2016). Alternatively if perturbative decay is forbidden and the decay must proceed through nonperturbative phenomena then the rate for instanton-like transitions can be estimated as $\Gamma_\chi \sim m_\chi e^{-4\pi/\alpha_\chi}$ where α_χ is the corresponding non-Abelian gauge coupling (Kuzmin and Rubakov, 1998); for $m_\chi = 10^{12} \text{ GeV}$ and $\alpha_\chi = 0.1$ the lifetime exceeds the age of the universe today.

G. Relics: gravitational reheating

It is often assumed that inflation ends when the inflaton field finds a local minimum of its potential and begins oscillating. During the ensuing epoch of reheating, energy is transferred from the inflaton condensate into a relativistic plasma through a combination of direct (perturbative) inflaton decay and nonlinear processes (preheating) (Amin *et al.*, 2014; Kofman *et al.*, 1994, 1997; Shtanov *et al.*, 1995; Traschen and Brandenberger, 1990). Reheating is said to be completed when the plasma constitutes the universe's dominant energy component. In this scenario the plasma inherits most of its energy from the inflaton, but a fraction may have arisen directly from CGPP (Passaglia *et al.*, 2021), although typically this fraction is no larger than order $H_{\text{inf}}^2/M_{\text{Pl}}^2$ and small enough to be neglected.

On the other hand, one can imagine that the inflaton's energy is depleted before it can be transferred into a plasma. For example, if the inflaton's potential minimum is locally quadratic, then its energy density redshifts down slowly like matter $\rho_\varphi \propto a^{-3}$; however, if the

inflaton's potential is flat with $V(\varphi) = 0$, then the inflaton enters a phase of kination while its energy redshifts away quickly like $\rho_\varphi \propto a^{-6}$. In this latter scenario, reheating must be accomplished without relying on energy transfer from the inflaton.

Gravitational reheating is a scenario in which the plasma's energy primarily arises from CGPP rather than from the inflaton (Ford, 1987). After the pioneering work by Ford, this idea has been explored extensively by many authors (Chun *et al.*, 2009; Copeland *et al.*, 2001; Dimopoulos and Markkanen, 2018; Feng and Li, 2003; Figueroa and Tanin, 2019; Haro *et al.*, 2019; Hashiba and Yokoyama, 2019b,c; Kamada *et al.*, 2020; Liddle and Urena-Lopez, 2003; Nishi and Kobayashi, 2016; Nishizawa and Motohashi, 2014; Opferkuch *et al.*, 2019; Sami *et al.*, 2003; Tashiro *et al.*, 2004), and frequently in the context of braneworld inflation, quintessential inflation, and curvaton scenarios. While direct reheating into the Standard Model (via the Higgs) has been considered (Figueroa and Byrnes, 2017), most studies rely on a new, heavy, and unstable particle to experience CGPP and mediate reheating into the Standard Model. A wide range of reheating temperatures are accessible as the particle's mass and (possibly) nonminimal coupling to gravity are varied.

An important constraint on gravitational reheating involves the amplification of gravitational wave radiation. Since a stiff equation of state ($w_\varphi > 1/3$) is required to rapidly deplete the inflaton's energy density, the inflationary gravitational waves develop a blue-tilted spectrum that rises toward higher frequencies (Boyle and Buonanno, 2008; Giovannini, 1998, 1999; Riazuelo and Uzan, 2000; Sahni *et al.*, 2002). The additional energy in high-frequency gravitational waves is constrained by Big Bang Nucleosynthesis and the Cosmic Microwave Background anisotropies that probe dark radiation implying $\Omega_{\text{gw}} h^2 \lesssim 10^{-6}$ (Figueroa and Tanin, 2019; Sendra and Smith, 2012). The powerful implications for gravitational reheating have been emphasized by several groups (Figueroa and Tanin, 2019; Nishi and Kobayashi, 2016; Nishizawa and Motohashi, 2014; Tashiro *et al.*, 2004), which conclude that the simplest implementations of gravitational reheating are strongly constrained. Viable gravitational reheating may be possible if there are many particle species experiencing CGPP so that the energy they collectively carry counteracts the energy carried by the two polarizations of the gravitational wave radiation.

H. Relics: baryogenesis

The cosmological excess of matter over antimatter is one of the longstanding mysteries of modern cosmology (Wilczek, 1980). It is usually assumed that this imbalance arose dynamically, through a process called baryogenesis, as a consequence of the physical laws governing

the particle content of the universe (Kolb and Wolfram, 1980). Successful baryogenesis requires particle interactions that violate certain conservation laws – namely baryon number B , charge conjugation C , and charge-parity conjugation CP – as well as a departure from thermal equilibrium (Sakharov, 1967). Since CGPP leads to the creation of particles in the early universe, it is natural to ask whether CGPP may be responsible for the origin of the matter-antimatter asymmetry.

If the interactions of particles and antiparticles with gravity respect the conservation laws B , C , and CP then baryogenesis cannot result from CGPP directly since the first two Sakharov criteria are not satisfied. On the other hand, CGPP easily provides the out of equilibrium conditions required by the third Sakharov criterion. Consequently, one can imagine a framework for CGPP Baryogenesis in which CGPP creates a population of self-conjugate X particles that decay into particles and antiparticles through interactions violating B , C , and CP , thereby generating a net baryon number (Bambi *et al.*, 2007). Similar ideas using nonthermal particle production during preheating were first developed in Kolb *et al.* (1996, 1998). Alternatively, X may decay by interactions that violate lepton number L instead, thereby generating a lepton asymmetry that is converted into a baryon asymmetry by electroweak Chern-Simons number diffusion (electroweak sphaleron) as in models of baryogenesis from leptogenesis (Fukugita and Yanagida, 1986).

Several recent studies have explored the implications of CGPP for baryogenesis (Barman *et al.*, 2022b; Bernal and Fong, 2021; Co *et al.*, 2022; Fujikura *et al.*, 2023; Hashiba and Yokoyama, 2019a). Several of these works investigate the role of CGPP for creating a heavy right-handed Majorana neutrino that is long-lived, decays out of equilibrium, and leads to baryogenesis via leptogenesis. Similar ideas for baryogenesis have been explored using noncosmological GPP via primordial black hole evaporation (Aydemir and Ren, 2021; Barman *et al.*, 2022a, 2023; Bernal *et al.*, 2022; Datta *et al.*, 2021; Hooper and Krnjaic, 2021; Perez-Gonzalez and Turner, 2021).

I. Relics: dark radiation

The universe today may contain an as-yet unseen population of dark particles that were relativistic at radiation-matter equality and may still be relativistic today or even massless. Various theories of new physics put forward different particle candidates for this dark radiation, and they offer different explanations for its origin. CGPP can contribute to the population of dark radiation in two ways: by directly producing the relativistic particles or by producing parent particles that decay into dark radiation.

For concreteness, consider a family of N massless scalar fields that are minimally coupled to gravity and otherwise

weakly coupled to one another and other particles. Suppose that the CMB-scale modes leave the horizon during inflation when $a = a_{\text{CMB}}$, that inflation ends and reheating begins when $a = a_e$, that the universe is effectively matter-dominated during reheating ($w_{\text{RH}} = 0$), that reheating completes and radiation-domination begins when $a = a_{\text{RH}}$, and that comoving entropy is subsequently conserved. In this scenario CGPP leads to a nearly scale invariant energy spectrum of radiation for modes with comoving wavenumber $k_{\text{eq}} \equiv a_{\text{eq}} H_{\text{eq}} < k < k_{\text{RH}} \equiv a_e^{3/2} H_e / a_{\text{RH}}^{1/2}$ that leave the horizon during inflation and re-enter during the radiation era before radiation-matter equality. Upon integrating this spectrum, the cosmological energy fraction today is expected to be

$$\Omega_{\text{dr}} h^2 \approx (3 \times 10^{-14}) \left(\frac{N}{1} \right) \left(\frac{H_e}{10^{14} \text{ GeV}} \right)^2 \left(\frac{\log k_{\text{RH}}/k_{\text{eq}}}{60} \right), \quad (117)$$

insensitive to the reheating temperature. Observational limits on dark radiation are at the level of $\Omega_{\text{dr}} h^2 \lesssim 0.05$, $\Omega_{\gamma} h^2 \approx 2 \times 10^{-6}$, and they derive from its would-be gravitational influence on BBN and CMB. For instance, it is customary to write $\Omega_{\text{dr}} h^2 = \Delta N_{\text{eff}} \frac{7}{8} \left(\frac{4}{11} \right)^{4/3} \Omega_{\gamma} h^2$ and *Planck* gives $\Delta N_{\text{eff}} \lesssim 0.2$ (Aghanim *et al.*, 2020). Since we have fiducialized H_e to its maximal allowed value given $r < 0.1$, achieving a detectably large $\Omega_{\text{dr}} h^2$ would require a large number of particle species ($N \gg 1$).

In other scenarios, a larger population of dark radiation could be obtained. For instance, if the cosmological equation of state during reheating were stiffer, the high- k modes would redshift differently, thereby boosting the relic abundance. See the discussion in Sec. VI.G regarding a kination-dominated phase of reheating ($w_{\text{RH}} = 1$). Alternatively dark radiation could arise indirectly via the decay of gravitationally-produced moduli fields into relativistic particles (Ema *et al.*, 2016). This scenario has more parametric freedom since one can vary the moduli mass and decay rate. While the energy is carried by the nonrelativistic moduli field it only redshifts away as a^{-3} , rather than dark radiation's a^{-4} , and if the moduli decay is sufficiently delayed, the abundance of dark radiation is correspondingly enhanced.

J. Relics: gravitational wave radiation

Cosmological inflation famously predicts a broad spectrum of primordial gravitational wave radiation (Abbott and Wise, 1984; Fabbri and Pollock, 1983; Rubakov *et al.*, 1982; Starobinsky, 1979). On an FLRW background the dispersion relation of a massless spin-2 field's transverse polarization modes ($\lambda = \pm 2$) is $\omega_k^2(\eta) = k^2 + a^2 R/6 = k^2 - a''/a$, which is familiar from studies of inflationary gravitational wave production; see Sec. V.E and Baumann (2022). This is the same dispersion relation that

one finds for a massless and minimally-coupled scalar field (12), and thus the CGPP calculation is identical up to a factor of 2 on account of the gravitational wave's two polarization modes. A calculation similar to the one that yielded Eq. (117) now gives a scale invariant spectrum of gravitational waves across the frequencies $f_{\text{eq}} < f < f_{\text{RH}}$ and with amplitude today

$$\begin{aligned} \frac{1}{\rho_c} \frac{d\rho_{\text{gw},0}}{d \ln f} h^2 &\approx 9 \times 10^{-16} \left(\frac{H_e}{10^{14} \text{ GeV}} \right)^2 \\ f_{\text{eq}} &\approx 5 \times 10^{-17} \text{ Hz} \\ f_{\text{RH}} &\approx 200 \text{ Hz} \left(\frac{T_{\text{RH}}}{10^9 \text{ GeV}} \right). \end{aligned} \quad (118)$$

This corresponds to a dimensionless strain of about $h_c(f) \approx 4 \times 10^{-26} (f/\text{Hz})^{-1} (H_e/10^{14} \text{ GeV})$. Although it is customary to say that inflationary gravitational waves arise from quantum fluctuations of the metric, it can also be said that this radiation arises from the phenomenon of CGPP due to the time-dependent dispersion relation.

Studies of gravitational wave creation via CGPP often focus on high-frequency gravitational waves (Grishchuk, 1974; Schiappacasse and Ford, 2016; Yajnik, 1990), rather than the low-frequency component that can be probed on CMB scales. Notable recent studies include (Ebadi *et al.*, 2023; Ema *et al.*, 2015, 2020, 2022; Ghiglieri *et al.*, 2020; Ghiglieri and Laine, 2015; Ghiglieri *et al.*, 2022; Ghoshal *et al.*, 2023; Nakayama and Tang, 2019; Ringwald *et al.*, 2021), which explore gravitational wave production via inflaton decay, inflaton coherent oscillations / annihilations, secondary effects, and thermal freeze-in (Weinberg, 1965).

K. Relics: primordial black holes

There are several interesting links between CGPP and primordial black holes (PBHs), particularly in regard to their formation and evaporation. Whereas astrophysical black holes form when stars collapse, primordial black holes may have formed in the early universe due to the collapse of Hubble-scale overdensities (Carr and Hawking, 1974; Niemeyer and Jedamzik, 1999). The mass scale of PBHs formed in this way depends on the amount of energy contained within a Hubble volume at the time when the overdensity enters the horizon and collapses. Although CGPP typically leads to small energy density inhomogeneities on cosmological scales, it can generate larger inhomogeneities on short scales; see Sec. IV.D. Modes on the Hubble scale at the end of inflation have $k \approx k_e \equiv a_e H_e$, and if these modes collapse soon after the end of inflation then the black hole mass is around

$$M_{\text{BH}} \approx \rho_c H_e^{-3} \approx (0.3 \text{ gram}) \left(\frac{H_e}{10^{14} \text{ GeV}} \right)^{-1}, \quad (119)$$

where $\rho_c = 3M_{\text{Pl}}^2 H_e^2$ is the cosmological critical density at the end of inflation. Such tiny black holes would emit Hawking radiation (Bekenstein, 1973; Hawking, 1974) at a temperature of $T_{\text{BH}} = M_{\text{Pl}}^2/M_{\text{BH}} = H_e/3$ and evaporate on a time scale of $\tau_{\text{BH}} \sim M_{\text{BH}}^3/M_{\text{Pl}}^4$. If the universe goes directly into radiation domination at the end of inflation (instantaneous reheating) then the black holes would survive for many Hubble times until the plasma temperature drops to $T_d \sim M_{\text{Pl}}^{5/2}/M_{\text{BH}}^{3/2} \sim (10^{11} \text{ GeV})(H_e/10^{14} \text{ GeV})^{3/2}$. Unless H_e is very small, this evaporation would complete long before BBN ($T \approx \text{MeV}$), making detectable signatures challenging to find.

Even if PBHs are not formed as a direct consequence of CGPP, the evaporation of PBHs (that form in other ways) would lead to the gravitational production of particles. Black holes emit thermal Hawking radiation into various species of particles as long as the particle masses are kinematically accessible ($m_\chi < T_{\text{BH}}$) and the interactions are not conformal. This radiation can include the known Standard Model elementary particles as well as hypothetical new particles, such as dark matter. Hooper *et al.* (2019) studied the gravitational production of dark matter via black hole evaporation, and they calculated its cosmological energy fraction finding

$$\frac{\Omega h^2}{0.1} \sim \left(\frac{m_\chi}{10^9 \text{ GeV}} \right)^{-1} \left(\frac{M_{\text{BH}}}{10^8 \text{ gram}} \right)^{-1} \left(\frac{f_{\text{BH}}}{8 \times 10^{-14}} \right), \quad (120)$$

where m_χ is the dark matter's mass, M_{BH} is the black hole's initial mass before evaporation, and $f_{\text{BH}} = \rho_{\text{BH}}/\rho_R$ is the cosmological energy fraction in black holes at 10^{10} GeV . These estimates demonstrate that the gravitational production of massive and stable particles via black hole evaporation is a viable mechanism to explain the origin of dark matter.

L. Observational: laboratory tests

The phenomenon of CGPP is not expected to have any discernible impact on the scale of laboratories in the universe today. Due to the enormous hierarchy between everyday length scales and the present cosmological horizon, the cosmological expansion plays no role. Technically speaking, the time-dependent frequency $\omega_k^2(\eta)$, for example see Eq. (12), is approximately constant on the time scales of an experiment and mode evolution remains nearly adiabatic without particle production.

Nevertheless the gravitationally-coupled relics produced via CGPP could potentially be probed by experiments on Earth (Carney *et al.*, 2022). The expected flux $F_\chi \approx \rho_\chi v_\chi/m_\chi$ of χ particles transiting a detector is

$$F_\chi \approx \left(\frac{200}{(10 \text{ cm})^2 (1 \text{ yr})} \right) \left(\frac{m_\chi}{10^{14} \text{ GeV}} \right)^{-1} f_\rho f_v. \quad (121)$$

Here the local mass density ρ_χ is assumed to be a fraction f_ρ of the fiducial local dark matter density $\rho_{\text{dm}} = 0.3 \text{ GeV/cm}^3$ and the mean velocity v_χ is assumed to be a fraction f_v of the fiducial local dark matter velocity $v_{\text{dm}} = 220 \text{ km/sec}$. At a larger mass $m_\chi = M_{\text{Pl}} = 2.4 \times 10^{18} \text{ GeV}$ the flux drops to $0.9/(100 \text{ cm})^2/\text{yr}$. These fluxes are large enough that several CGPP relics could be incident upon a meter-scale experiment over a year.

Needless to say, the challenge for such an experiment is achieving the sensitivities needed to detect particles with gravitational-strength interactions while discriminating signal from noise. It is emboldening that an experimental program has been put forward that is working to accomplish this herculean task. The Windchime Project (Attanasio *et al.*, 2022; Carney *et al.*, 2020, 2021; Monteiro *et al.*, 2020) seeks to employ optically or magnetically levitated sensors to precisely measure the location of test masses in a three-dimensional array and thereby detect the passage of dark matter as it exerts a subtle tug on the sensors. Sensitivity projections indicate that Windchime would be most sensitive to gravitationally-interacting ultraheavy dark particles with masses at or above the Planck scale $\sim 10^{19} \text{ GeV}$ (Carney *et al.*, 2020). Since CGPP is strongly suppressed above the inflaton mass, typically not much larger than 10^{14} GeV , it would be difficult to explain the origin of such heavy dark particles via CGPP. However, if the interaction is nongravitational, then Windchime's sensitivity widens to lower masses, possibly bringing gravitationally produced dark matter within reach. Opto-mechanical sensors have long been a powerful tool in precision experiments (Gonzalez-Ballesterio *et al.*, 2021), including gravitational wave detection, and they may yet offer a unique handle in searches for new physics (Moore and Geraci, 2021).

M. Observational: dark matter isocurvature

Observations of the CMB anisotropies and large scale structure are compatible a power spectrum of primordial density perturbations consisting of only an adiabatic mode, and they constrain the amplitude of isocurvature modes. In other words, the primordial dark matter inhomogeneities should align in space with the plasma inhomogeneities: overdensities with overdensities and underdensities with underdensities. For models of dark matter that is produced out of the plasma, such as thermal freeze-out or freeze-in, there is naturally a negligible isocurvature (Bellomo *et al.*, 2023). However, if the dark matter arises from a physical process that's uncorrelated with the origin of the plasma (on cosmological scales), which occurs in some models of CGPP during inflation, then there may be an unacceptably large isocurvature (Boyanovsky *et al.*, 2021; Chung *et al.*, 2005; Chung and Yoo, 2013; Chung *et al.*, 2013; Garcia *et al.*, 2023b,c; Herring and Boyanovsky, 2020; Herring *et al.*, 2020; Kolb

et al., 2023b; Ling and Long, 2021; Tenkanen, 2019). In this subsection we define isocurvature, explain how it can be calculated for models of dark matter produced via CGPP, and discuss the constraints imposed by CMB measurements.

Consider the epoch of radiation domination that followed inflation and reheating. At this time, the Universe contained various different particle species, including the Standard Model particles and dark matter, which we label with an index s . The energy density carried by particles of species s can be written as $\rho_s(\eta, \mathbf{x}) = \bar{\rho}_s(\eta) + \delta\rho_s(\eta, \mathbf{x})$ where the background energy density $\bar{\rho}_s(\eta)$ is homogeneous and the energy density perturbation $\delta\rho_s(\eta, \mathbf{x})$ has vanishing spatial average. Note that the decomposition of $\rho_s(\eta, \mathbf{x})$ into homogeneous and inhomogeneous components entails a gauge choice corresponding to selecting a mapping from the spacetime manifold to the time and space coordinates (Baumann, 2022). However, for each species, one can define a dimensionless fluid variable that is first-order gauge invariant:

$$\zeta_s(\eta, \mathbf{x}) = \frac{1}{2}(1 + 2C) - aH \frac{\delta\rho_s}{\partial_\eta \bar{\rho}_s}. \quad (122)$$

Here $C(\eta, \mathbf{x})$ is one of the scalar metric perturbations (B17). The continuity equation is $\partial_\eta \bar{\rho}_s = -3aH(1 + w_s)\bar{\rho}_s$ where $w_s = \bar{P}_s/\bar{\rho}_s$ is the equation of state.

One can define the isocurvature perturbation between species s and r as the difference of their fluid variables,

$$\mathcal{S}_{sr}(\eta, \mathbf{x}) = 3[\zeta_s(\eta, \mathbf{x}) - \zeta_r(\eta, \mathbf{x})], \quad (123)$$

which is also first-order gauge invariant. In particular, the isocurvature perturbation between dark matter (denoted by X with $w_X = 0$) and radiation (denoted by R with $w_R = 1/3$) is

$$\mathcal{S}(\eta, \mathbf{x}) = \frac{\delta\rho_X(\eta, \mathbf{x})}{\bar{\rho}_X(\eta)} - \frac{3}{4} \frac{\delta\rho_R(\eta, \mathbf{x})}{\bar{\rho}_R(\eta)}. \quad (124)$$

If only an adiabatic mode is present then $\mathcal{S}(\eta, \mathbf{x}) = 0$, and otherwise a nonzero isocurvature measures the relative inhomogeneities of the dark matter and the radiation.

Measurements of the CMB anisotropies are compatible with vanishing isocurvature. These constraints are typically expressed in terms of the dimensionless isocurvature power spectrum $\Delta_{\mathcal{S}}^2(\eta, k)$. To calculate this power spectrum, it is convenient to work in the comoving gauge, defined by the coordinate system in which the inflaton perturbations vanish. If the plasma arises from the decay of the inflaton, then the radiation perturbations also vanish in the comoving gauge. It follows that $\mathcal{S} = \delta_X^{(c)}$ where $\delta_X(\eta, \mathbf{x}) = \delta\rho_X/\bar{\rho}_X$ is the dark matter's energy density contrast and the superscript indicates comoving gauge (Chung and Yoo, 2013). Thus the isocurvature power spectrum equals the power spectrum of the dark matter's energy density contrast in the comoving gauge

$\Delta_S^2 = \Delta_\delta^2$; an expression for the latter quantity appears in Eq. (47).

Assuming that the curvature and isocurvature are uncorrelated (“axion I”), *Planck* reports a constraint of (Akrami *et al.*, 2020b)

$$\frac{\Delta_S^2}{\Delta_\xi^2 + \Delta_S^2} < 0.038 \quad \text{at 95\% CL.} \quad (125)$$

Here the power spectra are evaluated at recombination $\eta = \eta_{\text{rec}}$ for CMB-scale modes $k = 0.05 a_0 \text{ Mpc}^{-1}$ and $\Delta_\xi^2 \approx 2.1 \times 10^{-9}$ is the amplitude of the curvature power spectrum. In terms of the dark matter density contrast, Eq. (125) implies $\Delta_\delta^2 < 8.0 \times 10^{-11}$ at CMB scales.

For dark matter arising from CGPP, the scale and shape of the isocurvature power spectrum depends on the spin, mass, and gravitational coupling of particles. For instance, a conformally-coupled scalar field has $\Delta_\delta^2 \propto k^3$, which may give $O(1)$ isocurvature at small scales, but it implies a negligible isocurvature at CMB scales; see Sec. IV.D. A similar result is obtained for fields with nonzero spin, which have blue-tilted spectra; see Sec. V. Therefore, CMB limits on isocurvature are most constraining for models of minimally-coupled ($\xi = 0$) scalar dark matter. If the dark particles are light ($m \ll H_e \lesssim H_{\text{inf}}$) then the power spectrum is nearly scale invariant (see Sec. IV.D), and its amplitude at CMB scales comes into conflict with the CMB limits, but lifting the dark matter’s mass to be $m \gtrsim H_e$ tilts the power spectrum blue-ward and evades the isocurvature constraints (Chung *et al.*, 2005). Alternatively, introducing a non-minimal coupling to gravity also leads to a blue tilt and evades these constraints (Garcia *et al.*, 2023b; Kolb *et al.*, 2023b), even for $\xi = O(0.01)$. These models motivate searches for blue-tilted isocurvature in cosmological observables (Chung, 2016; Chung and Upadhye, 2017, 2018).

N. Observational: non-Gaussianity

Observations of the CMB are compatible with a spectrum of primordial curvature perturbations such that the amplitude of each Fourier mode can be modeled as an independent stochastic (random) variable with a Gaussian probability distribution centered at zero. These Gaussian initial conditions are a hallmark prediction of single-field slow-roll inflation (Mukhanov *et al.*, 1992). Their Gaussian nature follows from the fact that the inflaton is weakly coupled to itself and other fields, and a free scalar field has a Gaussian wavefunctional in its ground state (Maldacena, 2003). If the theory were extended to include non-gravitational interactions, the primordial curvature perturbations would develop a larger non-Gaussian component. This non-Gaussianity manifests in CMB anisotropy observables at the level of three-point (and higher-point) correlation functions, known as

the bispectrum (and trispectrum, so on). Measurements of the CMB anisotropies are compatible with Gaussian initial conditions and thereby constrain theories that predict appreciable non-Gaussianity (Akrami *et al.*, 2020a).

In theories that extend the inflaton sector to include additional particles at the same mass scale, known as quasi-single field inflation, an appreciable non-Gaussianity can develop in the curvature perturbations (Arkani-Hamed *et al.*, 2020; Arkani-Hamed and Maldacena, 2015; Baumann *et al.*, 2018; Baumann and Green, 2012; Chen, 2010; Chen and Wang, 2010a,b; Noumi *et al.*, 2013). In this way, inflationary observables act as a “cosmological collider” experiment to probe particles and forces whose high mass scale puts them beyond the reach of terrestrial high-energy experiments.

In theories where dark matter arises from CGPP it is natural to consider new particle species having masses around the inflationary Hubble scale $m_\chi \approx H_{\text{inf}}$. For instance, the gravitational production of spin-1/2 particles is suppressed for $m_\chi \ll H_{\text{inf}}$, since the fermion mass scale is the source of conformal symmetry breaking; see Sec. V.B. A study by Chung and Yoo (2013) [see also Chung *et al.* (2015); Hikage *et al.* (2009); and Li *et al.* (2019)] finds that the same theories in which dark matter is produced via CGPP can also lead to an appreciable CMB non-Gaussianity in the limit of the squeezed (local) triangle form. For instance, a benchmark parameter point predicts $f_{\text{NL}}^{\text{local}} \sim 30$, which is now excluded by Planck’s constraint $f_{\text{NL}}^{\text{local}} = -0.9 \pm 5.1$ (Akrami *et al.*, 2020a). CGPP can also lead to rare ‘hot spots’ in the CMB (Kim *et al.*, 2021, 2023). These examples illustrate the capability of current and future probes of CMB non-Gaussianity to test CGPP.

O. Observational: small-scale structure

If the particles that experience CGPP are going to provide a viable candidate for dark matter, then they must be sufficiently cold at radiation-matter equality. For superheavy particles with $m_\chi \approx H_e$ this is easily accomplished. Even if the spectrum after production is peaked at a very high comoving wavenumber, say $k \approx a_e H_e$ corresponding to Hubble-scale modes at the end of inflation, the characteristic velocity today is still extremely tiny:

$$v_\chi = k/a_0 m_\chi \approx 5 \times 10^{-32} \left(\frac{H_e}{10^{14} \text{ GeV}} \right)^{1/3} \times \left(\frac{T_{\text{RH}}}{10^9 \text{ GeV}} \right)^{1/3} \left(\frac{m_\chi}{10^{14} \text{ GeV}} \right)^{-1}. \quad (126)$$

For this estimate, the redshift factors are calculated by assuming a matter-dominated epoch of reheating ($w_{\text{RH}} = 0$). On the other hand, for models in which gravitational production remains efficient even for $m_\chi \ll H_e$, the velocity can be much larger. For instance, taking $m_\chi =$

10^{-12} GeV = meV gives $v_X \approx 0.5 \times 10^{-5} \approx 1.5$ km/sec.

Although $v_X \approx 10^{-5}$ still corresponds to extremely nonrelativistic particles, there is nevertheless a problem with such ‘fast’ dark matter. For successful structure formation, dark matter particles must cluster through their mutual gravitational attraction, thereby allowing overdensities to grow and form halos. However, if dark matter travels too quickly it will ‘escape’ from its initial overdensity before structures can form. In an FLRW spacetime, a free particle travels a distance

$$l_{\text{fs}}(t) = a(t) \int_0^t dt' \frac{v(t')}{a(t')} = a \int_0^a da' \frac{v(a')}{(a')^2 H(a')} \quad (127)$$

in time t , called the free-streaming length. For the values of H_e , T_{RH} , and $m_X = \text{meV}$ used in the estimate above, the free-streaming length today is $l_{\text{fs}}(t_0) \approx 20$ Mpc, and it mostly accumulates during the radiation era. The free-streaming length indicates the size of structures whose formation are inhibited by the dark matter’s speediness.

There are various probes of (cosmologically) small-scale structure in the spatial distribution of matter (Drlica-Wagner *et al.*, 2022; Tulin and Yu, 2018). For instance, observations of Lyman- α absorption due to intergalactic neutral hydrogen in the spectra of distant quasars, *i.e.*, the Lyman- α forest, are compatible with an Λ CDM-like matter power spectrum at wavenumbers below $k \approx 10 a_0 h \text{ Mpc}^{-1}$ (Viel *et al.*, 2013). These measurements place upper bounds on the free streaming length of dark matter, which are frequently used to constrain warm dark matter (Iršič *et al.*, 2017), but they also lead to constraints on m_X in the CGPP production scenario. A recent study by Garcia *et al.* (2023b) assessed the impact of Lyman- α observations on a theory of nonminimally-coupled scalar dark matter that is formed by CGPP during inflation and reheating; see also (Garcia *et al.*, 2023d; Haque and Maity, 2022). Their parameter space constraints are reproduced here as Fig. 10. Observe that gravitationally produced dark matter with mass below $m_X \sim 10^{-12}$ GeV (rising to 10^{-7} GeV for larger nonminimal coupling ξ) would be in conflict with Lyman- α observations, and is thereby ruled out.

P. Observational: signatures of late time decay

If the particles arising from CGPP are unstable but long-lived, then their late time decay into visible-sector radiation could lead to signatures in cosmological and astrophysical observables. Here we briefly remark on three possible probes of such an energy injection: nucleosynthesis, CMB spectrum and anisotropies, and cosmic rays.

The observed abundances of the light elements are compatible with the predictions of Big Bang Nucleosynthesis (BBN) (Cyburt *et al.*, 2016). The standard BBN calculation assumes the universe to be filled by a plasma of Standard Model particles at temperatures around

MeV. This good agreement between observation and theory leads to constraints on the presence of an additional particle species that decay and inject energy into the plasma (Cyburt *et al.*, 2003; Kawasaki *et al.*, 2018).

The energy spectrum of the cosmic microwave background (CMB) is observed to agree very well with a Planck (thermal blackbody) distribution (Chluba *et al.*, 2019). In the standard Λ CDM cosmology, this thermal distribution arises before recombination because photons couple to the electron-ion plasma through single-Compton and double-Compton scattering, which leads to a common temperature for all species and a vanishing chemical potential for the photon. However, double-Compton scattering goes out of equilibrium before single-Compton and during this time interval photon number is approximately conserved. Then an energy injection would lead to a nonzero photon chemical potential (spectral distortion) (Hu and Silk, 1993), which is constrained by measurements of the CMB energy spectrum by COBE/FIRAS (Fixsen *et al.*, 1996). Similarly energy injection from large-scale inhomogeneities can leave an imprint on CMB anisotropies (Acharya and Khatri, 2019; Ali-Haïmoud and Kamionkowski, 2017).

If superheavy particles are decaying in the Universe today, their visible-sector decay products would correspond to highly energetic photons, protons, electrons, positrons, and neutrinos. Of particular interest is the production of ultra-high energy cosmic ray (UHECR) protons above the Greisen-Zatsepin-Kuzmin (GZK) cut-off $E_{\text{cr}} \sim 10^{10}$ GeV (Greisen, 1966; Zatsepin and Kuzmin, 1966). Since protons scatter on CMB photons via a Δ resonance, the universe is not transparent to UHECR protons on cosmological distances. Conversely a detection of UHECR protons could be interpreted as evidence for a nearby source, such as superheavy dark matter decays within the local halo (Kuzmin and Tkachev, 1998, 1999; Kuzmin and Rubakov, 1998). More generally, searches with cosmic ray, gamma ray, and neutrino telescopes are probing long-lived superheavy dark matter (Aloisio *et al.*, 2015; Chianese *et al.*, 2021a,b; Das *et al.*, 2023; Ishiwata *et al.*, 2020; Kachelriess *et al.*, 2018).

VII. OUTLOOK

How does a strong gravitational field lead to particle creation? What are the cosmological implications of these particles and their observational signatures? For nearly the past 100 years, these questions have guided the study of cosmological gravitational particle production. Today a vibrant community of researchers are working to enrich our knowledge of CGPP as a mechanism and to explore novel applications and implications of this phenomenon. With this review, we hope to provide a tool kit that another generation of researchers can employ to pursue their own studies of CGPP, derive predictions

for cosmological relics, explore the implications for new directions beyond the Standard Model, and propose observational tests.

ACKNOWLEDGMENTS

We thank our colleagues and collaborators for feedback over the many years while this review was taking shape. We appreciate Mustafa Amin, Daniel Chung, Leah Jenks, Siyang Ling, Evan McDonough, and Sarunas Verner for taking the time to provide comments on a draft of the article. E.W.K. acknowledges the hospitality of The Institute for Theoretical Physics in Madrid where part of this work was done. The work of E.W.K. was supported in part by the US Department of Energy contract DE-FG02-13ER41958. A.J.L. is supported in part by the National Science Foundation under Award No. PHY-2114024.

Appendix A: General relativity

This appendix provides a brief refresher on general relativity (GR), the relativistic field theory of gravity that describes its interactions with radiation and matter. There are many excellent textbooks on GR including: *Gravitation and Cosmology* (Weinberg, 1972), *Gravitation* (Misner et al., 1973), *The Classical Theory of Fields* (Landau and Lifschits, 1980), *General Relativity* (Wald, 1984), *Quantum field theory in curved spacetime and black hole thermodynamics* (Wald, 1995) *Geometry, Topology, and Physics* (Nakahara, 2003), *Supergravity* (Freedman and Van Proeyen, 2012), and *Spacetime and Geometry* (Carroll, 2019).

Sign and unit conventions. Different references adopt different conventions when writing the equations of GR. A table summarizing frequently encountered sign choices is provided in Misner et al. (1973), and an appendix of Freedman and Van Proeyen (2012) includes additional signs and phases that arise in the frame-field formalism. In these appendices we follow Freedman and Van Proeyen (2012) and use the symbols $\alpha, \beta, s_*, s_1, s_2, \dots, s_8$ to simultaneously track the various sign choices; the reader is free to set $\alpha = \pm 1, \pm i, \beta = \pm 1$, and $s_i = \pm 1$. In the main body of the article we take $-\alpha = \beta = -s_* = -s_1 = s_2 = s_3 = s_4 = s_6 = s_8 = 1$; we do not use s_5 and s_7 . This corresponds to $(-, +, +)$ in notation of Misner et al. (1973). Additionally, we work in natural units, setting the speed of light c and the reduced Planck constant \hbar equal to 1.

Spacetime and metric. The coordinates of 4-dimensional spacetime are denoted by x^μ for $\mu = 0, 1, 2, 3$. Gravity is described by a type $(0, 2)$ tensor field $g_{\mu\nu}(x)$, called the metric, that may vary throughout spacetime. The

inverse metric field is denoted by $g^{\mu\nu}(x)$, and defined by $g^{\mu\nu}(x)g_{\nu\rho}(x) = \delta_\rho^\mu$ where δ_ρ^μ is the Kronecker delta symbol. The determinant of the metric is denoted by g , and appears in the factor $\sqrt{-g}$. The metric gives the differential invariant line element $(ds)^2 = g_{\mu\nu}(x)dx^\mu dx^\nu$. In Minkowski spacetime the metric is static, homogeneous, and isotropic; it can be written as

$$g_{\mu\nu}^{\text{Mink}}(x) = \eta_{\mu\nu} = s_1 \text{diag}(-1, 1, 1, 1), \quad (\text{A1})$$

and one is free to take $s_1 = \pm 1$. Its inverse is $g^{\mu\nu}_{\text{Mink}} = \eta^{\mu\nu}$.

Curvature definitions. Objects that arise in the definition of spacetime curvature include: the Levi-Civita connection (torsion-free affine connection)

$$\Gamma_{\mu\nu}^\rho(x) = \frac{1}{2}g^{\rho\lambda}(\partial_\mu g_{\nu\lambda} + \partial_\nu g_{\mu\lambda} - \partial_\lambda g_{\mu\nu}), \quad (\text{A2})$$

the Riemann curvature tensor

$$R^\rho_{\sigma\mu\nu}(x) = s_2 \left(\partial_\mu \Gamma_{\nu\sigma}^\rho - \partial_\nu \Gamma_{\mu\sigma}^\rho + \Gamma_{\mu\lambda}^\rho \Gamma_{\nu\sigma}^\lambda - \Gamma_{\nu\lambda}^\rho \Gamma_{\mu\sigma}^\lambda \right), \quad (\text{A3})$$

the Ricci tensor $R_{\mu\nu}(x) = (s_2 s_3)^{-1} R^\alpha_{\mu\alpha\nu}$, the Ricci scalar $R(x) = g^{\mu\nu} R_{\mu\nu}$, and the Einstein tensor $G_{\mu\nu}(x) = R_{\mu\nu} - \frac{1}{2}g_{\mu\nu}R$. The totally-antisymmetric Levi-Civita connection $\varepsilon_{\mu\nu\rho\sigma}$ is normalized by $\varepsilon_{0123} = s_5 = \pm 1$.

Covariant derivatives. Derivatives that transform covariantly under coordinate transformations (diffeomorphisms) are denoted by ∇_μ . Covariant derivatives of scalar, vector, and rank-2 tensor fields are defined by

$$\nabla_\sigma S = \partial_\sigma S \quad (\text{A4a})$$

$$\nabla_\sigma V^\mu = \partial_\sigma V^\mu + \Gamma_{\sigma\rho}^\mu V^\rho \quad (\text{A4b})$$

$$\nabla_\sigma V_\mu = \partial_\sigma V_\mu - \Gamma_{\sigma\mu}^\rho V_\rho \quad (\text{A4c})$$

$$\nabla_\sigma T^{\mu\nu} = \partial_\sigma T^{\mu\nu} + \Gamma_{\sigma\rho}^\mu T^{\rho\nu} + \Gamma_{\sigma\rho}^\nu T^{\mu\rho} \quad (\text{A4d})$$

$$\nabla_\sigma T^\mu_\nu = \partial_\sigma T^\mu_\nu + \Gamma_{\sigma\rho}^\mu T^\rho_\nu - \Gamma_{\sigma\rho}^\rho T^\mu_\nu \quad (\text{A4e})$$

$$\nabla_\sigma T_\mu^\nu = \partial_\sigma T_\mu^\nu - \Gamma_{\sigma\mu}^\rho T_\rho^\nu + \Gamma_{\sigma\rho}^\nu T_\mu^\rho \quad (\text{A4f})$$

$$\nabla_\sigma T_{\mu\nu} = \partial_\sigma T_{\mu\nu} - \Gamma_{\sigma\mu}^\rho T_{\rho\nu} - \Gamma_{\sigma\nu}^\rho T_{\mu\rho}, \quad (\text{A4g})$$

and the generalization to higher-rank tensors is obvious. When applied to a type (p, q) tensor with p contravariant (up) indices and q covariant (down) indices, the covariant derivative produces a type $(p, q+1)$ tensor. The Levi-Civita connection parallel transports the metric, $\nabla_\sigma g_{\mu\nu} = 0$. The d'Alembertian of a scalar field Φ is

$$\square\Phi = g^{\mu\nu}\nabla_\mu\nabla_\nu\Phi = (\sqrt{-g})^{-1}\partial_\mu(\sqrt{-g}g^{\mu\nu}\partial_\nu\Phi). \quad (\text{A5})$$

Einstein-Hilbert action and matter. The dynamics of gravity and its interactions with radiation and matter are encoded in an action S using the formalism of Lagrangian

mechanics. We treat the radiation/matter as classical fields, denoted collectively by $F_i(x)$. We study a class of theories whose actions take the form

$$S[F_i(x), g_{\mu\nu}(x)] = S_{\text{EH}}[g_{\mu\nu}(x)] + S_{\text{M}}[F_i(x), g_{\mu\nu}(x)] \quad (\text{A6})$$

where S_{EH} is the Einstein-Hilbert (EH) action and S_{M} is the radiation/matter action. The EH action is

$$S_{\text{EH}}[g_{\mu\nu}(x)] = s_1 s_3 \frac{1}{2} M_{\text{Pl}}^2 \int d^4x \sqrt{-g} R \quad (\text{A7})$$

where M_{Pl} is the reduced Planck mass, $G_N = 1/8\pi M_{\text{Pl}}^2$ is Newton's gravitational constant, and $\kappa^2 = 8\pi G_N$ is the gravitational coupling. The radiation/matter action takes the form

$$S_{\text{M}}[F_i(x), g_{\mu\nu}(x)] = \int d^4x \sqrt{-g} \mathcal{L}, \quad (\text{A8})$$

where \mathcal{L} is the radiation/matter Lagrangian density.

Einstein's equation. The equation of motion for the metric, known as Einstein's equation, is derived by applying the variational principle. Imposing $\delta S / \delta g^{\mu\nu} = 0$ leads to Einstein's equation (Einstein, 1916)

$$s_3 G_{\mu\nu} = 8\pi G_N T_{\mu\nu} = M_{\text{Pl}}^{-2} T_{\mu\nu} = \kappa^2 T_{\mu\nu}. \quad (\text{A9})$$

To evaluate the variational derivative of the Einstein-Hilbert term, the following identities prove useful:

$$\delta g^{\mu\nu} = -g^{\mu\rho} g^{\nu\sigma} \delta g_{\rho\sigma} \quad (\text{A10a})$$

$$\delta g_{\mu\nu} = -g_{\mu\rho} g_{\nu\sigma} \delta g^{\rho\sigma} \quad (\text{A10b})$$

$$\delta g = g g^{\mu\nu} \delta g_{\mu\nu} \quad (\text{A10c})$$

$$\delta \sqrt{-g} = \frac{1}{2} \sqrt{-g} g^{\mu\nu} \delta g_{\mu\nu} \quad (\text{A10d})$$

$$\begin{aligned} \delta R = & -R^{\mu\nu} \delta g_{\mu\nu} + s_3 \left(\frac{1}{2} g^{\rho\mu} g^{\sigma\nu} \right. \\ & \left. + \frac{1}{2} g^{\rho\nu} g^{\sigma\mu} - g^{\rho\sigma} g^{\mu\nu} \right) \nabla_\nu \nabla_\mu \delta g_{\rho\sigma}, \end{aligned} \quad (\text{A10e})$$

and it follows that $\delta S_{\text{EH}} / \delta g^{\mu\nu} = s_1 s_3 (\sqrt{-g}/2) M_{\text{Pl}}^2 G_{\mu\nu}$.

Stress-energy tensor. The stress-energy tensor field $T_{\mu\nu}(x)$ is defined as the variational derivative of the radiation/matter action

$$T_{\mu\nu} = -s_1 \frac{2}{\sqrt{-g}} \frac{\delta S_{\text{M}}}{\delta g^{\mu\nu}}. \quad (\text{A11})$$

Note that the stress-energy tensor is manifestly symmetric, since the inverse metric is symmetric. The scalar $T^\mu_\mu = g^{\mu\nu} T_{\nu\mu}$ is called the trace of the stress-energy tensor. For theories with fields of half-integer spin, the matter action is expressed in terms of the frame fields $e^\mu_a(x)$ (see below) rather than the metric, and the stress-energy tensor is calculated using

$$T^\mu_a = \frac{1}{e} \frac{\delta S_{\text{M}}}{\delta e^\mu_a} \quad \text{and} \quad T_{\mu\nu} = s_1 g_{\mu\rho} g_{\nu\sigma} \eta^{ab} e^\rho_a T^\sigma_b. \quad (\text{A12})$$

Perfect fluid stress-energy tensor. In many applications, the radiation/matter sector is modeled as a perfect fluid. For such systems, the stress-energy tensor takes the form

$$T_{\mu\nu} = (\rho + p) u_\mu u_\nu + s_1 p g_{\mu\nu}, \quad (\text{A13})$$

where $\rho(x)$ is the scalar energy density field, $p(x)$ is the scalar pressure field, and $u_\mu(x)$ is the vector velocity field. The vector field is normalized such that $g^{\mu\nu} u_\mu u_\nu = -s_1$. It follows that $\rho = T^{\mu\nu} u_\mu u_\nu$ and $3p = s_1 T^\mu_\mu + \rho$

Canonical stress-energy tensor. For this discussion we restrict our attention to Minkowski spacetime. If spacetime translations are a symmetry of the theory, the four Noether currents form a rank-two tensor called the canonical stress-energy tensor, which we denote by $\Theta^{\mu\nu}$. These currents may be derived by applying Noether's theorem; see Weinberg (2005) for a review. For a theory of fields $F_i(x)$ one finds

$$\Theta^{\mu\nu} = \frac{\partial \mathcal{L}}{\partial (\partial_\mu F_i)} \eta^{\nu\rho} \partial_\rho F_i - \eta^{\mu\nu} \mathcal{L}. \quad (\text{A14})$$

Although the canonical stress-energy tensor is conserved $\partial_\mu \Theta^{\mu\nu} = 0$ it need not be symmetric or even gauge invariant. However if Lorentz invariance is also a symmetry of the theory, then one can construct a conserved and symmetric tensor, the Belinfante-Rosenfeld stress-energy tensor, and denote it by $t^{\mu\nu}$. The relation takes the form $t^{\mu\nu} = \Theta^{\mu\nu} + \partial_\rho B^{\rho\mu\nu}$ where $B^{\rho\mu\nu} = -B^{\mu\rho\nu}$ is antisymmetric in its first two indices (Belinfante, 1939, 1940; Rosenfeld, 1940). In Minkowski spacetime the Belinfante-Rosenfeld stress-energy tensor $t^{\mu\nu}$ coincides with the Hilbert stress-energy tensor $T^{\mu\nu}$ defined in Eq. (A11) by varying the action with respect to the metric. While this discussion is intended to illuminate the relation between $T^{\mu\nu}$ and conserved quantities in the sense of Noether's theorem, ultimately the quantity of interest for cosmology is $T^{\mu\nu}$ that appears in Einstein's equation.

Frame-field formalism. For theories whose matter action contains particles of half-integer spin, a covariant coupling to gravity cannot be accomplished within the metric formulation of general relativity. Instead for these purposes it is customary to employ the frame-field formalism,² which is an elegant and general formulation of general relativity that allows field theory with spinors to be extended to curved spacetime. Hereafter we follow the notation of Freedman and Van Proeyen (2012).

² The frame field was originally introduced by Cartan who called them *repères mobiles* (moving frames) (Cartan, 1926); in German they are referred to as *vierbeins* (four-leg), and in the English literature they are usually called *tetrads* (Greek for "set of four"). Here we refer to them as frame fields.

At any point on the spacetime manifold, one can find a basis that locally diagonalizes the metric, and with an appropriate rescaling this yields the metric for Minkowski spacetime $\eta_{ab} = s_1 \text{diag}(-1, 1, 1, 1)$. Requiring this diagonalization to be smooth leads to the relation

$$g_{\mu\nu}(x) = e_\mu^a(x) e_\nu^b(x) \eta_{ab} , \quad (\text{A15})$$

where $e_\mu^a(x)$ for $a = 1, 2, 3, 4$ is called the frame field.³ The decomposition of metric $g_{\mu\nu}(x)$ into a pair of frame fields is not unique, and equivalent expressions are related by local Lorentz transformations $e_\mu^a(x) = (\Lambda^{-1})^a_b(x) e_\mu^b(x)$ under which the frame index transforms and the coordinate index is inert. On the other hand, under coordinate transformations (diffeomorphisms) the frame field transforms as a set of four covariant vectors $e_\mu^a(x') = (\partial x^\rho / \partial x'^\mu) e_\rho^a(x)$ while the frame index is inert. Note that $\det(e) \equiv e = \sqrt{-g}$. There exists an inverse of the frame field, denoted by $e_\mu^a(x)$, such that $e_\mu^a e_a^\nu = \delta_\mu^\nu$ and $e_a^\mu e_\mu^b = \delta_a^b$.

Spin connection. Tensor fields of arbitrary rank can be expressed in the frame-field formalism. For example a contravariant vector field $V^\mu(x)$ may be written as $V^\mu(x) = V^a(x) e_\mu^a(x)$ where $V^a(x) = e_\mu^a(x) V^\mu(x)$ are the frame components of the vector field, which transform as scalars under coordinate transformations and as a vector under local Lorentz transformations. Similarly for covariant vectors $V_\mu(x) = e_\mu^a(x) V_a(x)$ where $V_a(x) = e_\mu^a(x) V_\mu(x)$. Derivatives of frame vector fields that transform covariantly under the local Lorentz transformations are given by

$$\begin{aligned} D_\mu V^a &= \partial_\mu V^a + (s_2 s_4)^{-1} \omega_\mu^a{}_b V^b \\ D_\mu V_a &= \partial_\mu V_a - (s_2 s_4)^{-1} \omega_\mu^b{}_a V_b , \end{aligned} \quad (\text{A16})$$

where the appropriate affine connection, also known as the spin connection, is given by

$$\omega_\mu^{ab} = s_2 s_4 \left[2e^{\nu[a} \partial_{[\mu} e_{\nu]}^{b]} - e^{\nu[a} e^{b]\sigma} e_{\mu\sigma} \partial_\nu e_\sigma^c \right] . \quad (\text{A17})$$

Here $X^{[a} Y^{b]} = (X^a Y^b - X^b Y^a)/2$. The spin connection is required to be antisymmetric in its frame indices: $\omega_\mu^{ab} = -\omega_\mu^{ba}$. The derivatives $\nabla_\mu V^\nu = e_\mu^\nu D_\mu V^a$ and $\nabla_\mu V_\nu = e_\nu^\rho D_\mu V_\rho$ are covariant under coordinate transformations, transforming as type (1, 1) and (0, 2) tensors, respectively. The Levi-Civita connection is related to the spin connection by $\Gamma_{\mu\nu}^\rho = e_a^\rho \partial_\mu e_\nu^a + (s_2 s_4)^{-1} e_a^\rho \omega_\mu^a{}_b e_\nu^b$.

³ Frame indices, also called local Lorentz indices, are denoted by letters in the Latin alphabet a, b , and so on, while coordinate indices are denoted by Greek letters μ, ν , and so on. Frame indices are raised/lowered by the Minkowski metric and its inverse, η_{ab} and η^{ab} , while coordinate indices are raised/lowered by the local metric and its inverse, $g_{\mu\nu}$ and $g^{\mu\nu}$.

Spinor matrices. Let γ^a for $a = 0, 1, 2, 3$ denote the set of four complex 4×4 spinor matrices. They obey the Clifford algebra of anticommutation relations

$$\{\gamma^a, \gamma^b\} = s_6 2\eta^{ab} \mathbb{1} = (s_6/s_1) 2 \text{diag}(-1, 1, 1, 1) \mathbb{1} \quad (\text{A18})$$

where $\mathbb{1}$ is the identity matrix on the spinor indices. For instance, in the Dirac representation

$$\gamma^0 = \sqrt{\frac{-s_6}{s_1}} \begin{pmatrix} \mathbb{1} & 0 \\ 0 & -\mathbb{1} \end{pmatrix}, \quad \gamma^i = \sqrt{\frac{-s_6}{s_1}} \begin{pmatrix} 0 & \sigma^i \\ -\sigma^i & 0 \end{pmatrix} \quad (\text{A19})$$

where σ^i for $i = 1, 2, 3$ are the Pauli matrices. One may also define

$$\gamma_5 = s_7 i \gamma^0 \gamma^1 \gamma^2 \gamma^3 \quad (\text{A20a})$$

$$\gamma^{ab} = \gamma^{[a} \gamma^{b]} = \frac{1}{2} (\gamma^a \gamma^b - \gamma^b \gamma^a) \quad (\text{A20b})$$

$$\gamma^{abc} = \gamma^{[a} \gamma^b \gamma^{c]} = \frac{1}{2} (\gamma^a \gamma^b \gamma^c - \gamma^c \gamma^b \gamma^a), \quad (\text{A20c})$$

and so on; in addition $\Sigma^{ab} = \gamma^{ab}/2$. Using the frame field, one defines a set of local gamma matrices

$$\gamma^\mu(x) = e_\mu^a(x) \gamma^a, \quad (\text{A21})$$

that satisfy the Clifford algebra locally

$$\{\gamma^\mu(x), \gamma^\nu(x)\} = s_6 2g^{\mu\nu}(x) \mathbb{1}, \quad (\text{A22})$$

and from which one may construct $\gamma^{\mu\nu}(x)$ and $\gamma^{\mu\nu\rho}(x)$ in analogy with the expressions above.

Spinor fields. For spinor fields $\Psi(x)$ or vector-spinor fields $\Psi_\mu(x)$ one may define the covariant derivatives

$$D_\mu \Psi = \partial_\mu \Psi + s_2 s_4 \frac{1}{4} \omega_{\mu ab} \gamma^{ab} \Psi \quad (\text{A23a})$$

$$\nabla_\mu \Psi = D_\mu \Psi \quad (\text{A23b})$$

$$D_\mu \Psi_\nu = \partial_\mu \Psi_\nu + s_2 s_4 \frac{1}{4} \omega_{\mu ab} \gamma^{ab} \Psi_\nu \quad (\text{A23c})$$

$$\nabla_\mu \Psi_\nu = D_\mu \Psi_\nu - \Gamma_{\mu\nu}^\rho \Psi_\rho . \quad (\text{A23d})$$

All four quantities transform as spinors under local Lorentz transformations, whereas only $\nabla_\mu \Psi_\nu$ transforms as a type (0, 2) tensor under coordinate transformations.

Conjugation. The Hermitian conjugate of the spinor matrices, either γ^a or $\gamma^\mu(x)$, can be written as

$$(\gamma^a)^\dagger = (s_1 s_*/s_6) \gamma^0 \gamma^a \gamma^0 . \quad (\text{A24})$$

Then the Clifford algebra implies $(\gamma^0)^\dagger = -s_* \gamma^0$ and $(\gamma^i)^\dagger = s_* \gamma^i$ for $i = 1, 2, 3$, such that γ^0 is Hermitian for $s_* = -1$ and anti-Hermitian for $s_* = +1$. Regardless of the sign choices $(\gamma_5)^\dagger = \gamma_5$. One may define the Dirac adjoint spinors

$$\bar{\Psi} = (i/\alpha) \Psi^\dagger \gamma^0 \quad \text{and} \quad \bar{\Psi}_\mu = (i/\alpha) \Psi_\mu^\dagger \gamma^0 , \quad (\text{A25})$$

where $\gamma^0 = \gamma^a|_{a=0}$ is the constant spinor matrix, and the phase α takes values ± 1 or $\pm i$. Covariant derivative of the Dirac adjoint spinors are defined by

$$\bar{\Psi} \overleftarrow{D}_\mu = \partial_\mu \bar{\Psi} - s_2 s_4 \frac{1}{4} \omega_{\mu ab} \bar{\Psi} \gamma^{ab} \quad (\text{A26a})$$

$$\bar{\Psi} \overleftarrow{\nabla}_\mu = \bar{\Psi} \overleftarrow{D}_\mu \quad (\text{A26b})$$

$$\bar{\Psi}_\nu \overleftarrow{D}_\mu = \partial_\mu \bar{\Psi}_\nu - s_2 s_4 \frac{1}{4} \omega_{\mu ab} \bar{\Psi}_\nu \gamma^{ab} \quad (\text{A26c})$$

$$\bar{\Psi}_\nu \overleftarrow{\nabla}_\mu = \bar{\Psi}_\nu \overleftarrow{D}_\mu - \Gamma_{\mu\nu}^\rho \bar{\Psi}_\rho \quad (\text{A26d})$$

Bilinear products. A final sign ambiguity arises in the complex conjugation of spinor products. If χ_1 and χ_2 are two anticommuting variables, such as components of a spinor field Ψ , then $\chi_1 \chi_2 = -\chi_2 \chi_1$. The complex conjugate of their product may be evaluated as $(\chi_1 \chi_2)^* = -\beta \chi_1^* \chi_2^* = \beta \chi_2^* \chi_1^*$ where the sign $\beta = \pm 1$ controls whether complex conjugation also exchanges order. For example the bilinear product of two spinors complex conjugates to $(\bar{\psi} \chi)^* = s_8 \bar{\chi} \psi$ where $s_8 \equiv \beta s_* \alpha / \alpha^* = \pm 1$. If $s_8 = +1$ then $\bar{\psi} \psi$ is real, *i.e.*, complex conjugates to itself, but if $s_8 = -1$ then $\bar{\psi} \psi$ is imaginary and an additional factor of $i = \sqrt{s_8}$ must be added when constructing the Lagrangian mass term. A similar argument applies for kinetic terms.

Radiation/matter action. The frame-field formalism may be used to study radiation/matter sectors containing fields of either integer or half-integer spin, but we will only employ it in the study of spinor fields. The radiation/matter action for free massive fields of spin $s = 0, 1/2, 1$, and $3/2$ may be written as

$$S_M = \int d^4x \sqrt{-g} \sum_s \mathcal{L}^{(s)} \quad (\text{A27})$$

$$\mathcal{L}^{(0)} = -s_1 \frac{1}{2} g^{\mu\nu} \nabla_\mu \Phi \nabla_\nu \Phi - \frac{1}{2} m^2 \Phi^2 - s_1 s_3 \frac{1}{2} \xi R \Phi^2$$

$$\mathcal{L}^{(1/2)} = \sqrt{s_8 s_*} \left(\frac{1}{4} \bar{\Psi} \gamma^\mu \nabla_\mu \Psi - \frac{1}{4} \bar{\Psi} \overleftarrow{\nabla}_\mu \gamma^\mu \Psi \right) - \sqrt{s_8} \frac{1}{2} m \bar{\Psi} \Psi$$

$$\mathcal{L}^{(1)} = -\frac{1}{2} g^{\mu\rho} g^{\nu\sigma} F_{\mu\nu} F_{\rho\sigma} - s_1 \frac{1}{2} m^2 g^{\mu\nu} A_\mu A_\nu$$

$$\mathcal{L}^{(3/2)} = \sqrt{s_8 s_*^3} \left(\frac{1}{4} \bar{\Psi}_\mu \gamma^{\mu\nu\rho} \nabla_\nu \Psi_\rho - \frac{1}{4} \bar{\Psi}_\mu \overleftarrow{\nabla}_\nu \gamma^{\mu\nu\rho} \Psi_\rho \right) - \sqrt{s_8 s_*^2} \frac{1}{2} m \bar{\Psi}_\mu \gamma^{\mu\nu} \Psi_\nu$$

where m^2 , m , and ξ are real parameters, and where

$$\nabla_\mu \Phi = \partial_\mu \Phi \quad (\text{A28a})$$

$$\nabla_\mu \Psi = \partial_\mu \Psi + s_2 s_4 \frac{1}{4} \omega_{\mu ab} \gamma^{ab} \Psi \quad (\text{A28b})$$

$$\bar{\Psi} = (i/\alpha) \Psi^\dagger \gamma^0 \quad (\text{A28c})$$

$$\bar{\Psi} \overleftarrow{\nabla}_\mu = \partial_\mu \bar{\Psi} - s_2 s_4 \frac{1}{4} \omega_{\mu ab} \bar{\Psi} \gamma^{ab} \quad (\text{A28d})$$

$$F_{\mu\nu} = \nabla_\mu A_\nu - \nabla_\nu A_\mu \quad (\text{A28e})$$

$$\nabla_\mu A_\nu = \partial_\mu A_\nu - \Gamma_{\mu\nu}^\rho A_\rho \quad (\text{A28f})$$

$$\nabla_\mu \Psi_\nu = \partial_\mu \Psi_\nu + s_2 s_4 \frac{1}{4} \omega_{\mu ab} \gamma^{ab} \Psi_\nu - \Gamma_{\mu\nu}^\rho \Psi_\rho \quad (\text{A28g})$$

$$\bar{\Psi}_\mu = (i/\alpha) \Psi_\mu^\dagger \gamma^0 \quad (\text{A28h})$$

$$\bar{\Psi}_\mu \overleftarrow{\nabla}_\nu = \partial_\nu \bar{\Psi}_\mu - s_2 s_4 \frac{1}{4} \omega_{\mu ab} \bar{\Psi}_\nu \gamma^{ab} - \Gamma_{\mu\nu}^\rho \bar{\Psi}_\rho \quad (\text{A28i})$$

Note that the $\Gamma_{\mu\nu}^\rho$ terms in $\nabla_\mu A_\nu$ and $\nabla_\mu \Psi_\nu$ do not contribute to the Lagrangian, since the symmetric Levi-Civita connection is contracted with an antisymmetric tensor. In the main body of the article we take $-i\alpha = \beta = -s_* = -s_1 = s_2 = s_3 = s_4 = s_6 = s_8 = 1$.

Appendix B: FLRW spacetime

This appendix summarizes key relations that arise frequently in the FLRW spacetime. We provide expressions using both coordinate time t and conformal time η so that the reader can move between these two conventions. We only consider the spatially flat FLRW spacetime ($k = 0$).

Metric. The differential spacetime interval for the homogeneous and isotropic FLRW spacetime (Friedmann, 1922; Friedmann, 1924; Lemaitre, 1931; Robertson, 1935a,b, 1936; Walker, 1937) may be written as

$$\begin{aligned} (ds)^2 &= s_1 [-(dt)^2 + a^2(t) |d\mathbf{x}|^2] \quad \text{or} \\ (ds)^2 &= s_1 [-a^2(\eta) (d\eta)^2 + a^2(\eta) |d\mathbf{x}|^2] \end{aligned} \quad (\text{B1})$$

We call t the time coordinate, η the conformal time coordinate, \mathbf{x} the comoving spatial coordinate, and a the scale factor. Note that $dt = a(\eta) d\eta$ and $d\eta = dt/a(t)$, as well as $\partial_t = a^{-1}(\eta) \partial_\eta$ and $\partial_\eta = a(t) \partial_t$. In other words, the nonzero components of the metric are

$$\begin{aligned} g_{00}(t) &= -s_1 \quad \text{or} \quad g_{00}(\eta) = -s_1 a^2(\eta) \\ g_{ii}(t) &= s_1 a^2(t) \quad \text{or} \quad g_{ii}(\eta) = s_1 a^2(\eta) \end{aligned} \quad (\text{B2})$$

for $i = 1, 2, 3$ (no sum). The metric determinant gives

$$\sqrt{-g} = a^3(t) \quad \text{or} \quad \sqrt{-g} = a^4(\eta) \quad (\text{B3})$$

When using conformal time, the FLRW metric can be written compactly as $g_{\mu\nu}(\eta) = a^2(\eta) \eta_{\mu\nu}$ where $\eta_{\mu\nu}$ is the Minkowski metric. Hence, the (spatially flat) FLRW spacetime is conformally related to Minkowski spacetime. The components of the corresponding frame fields are

$$\begin{aligned} e_\mu^0(t) &= \delta_\mu^0 \quad \text{or} \quad e_\mu^0(\eta) = a(\eta) \delta_\mu^0 \\ e_\mu^i(t) &= a(t) \delta_\mu^i \quad \text{or} \quad e_\mu^i(\eta) = a(\eta) \delta_\mu^i \end{aligned} \quad (\text{B4})$$

for $\mu = 0, 1, 2, 3$ and $i = 1, 2, 3$.

Hubble parameter. Evolution of the scale factor is measured with the Hubble parameter H , which is defined equivalently by either of the following relations:

$$H(t) = \frac{\dot{a}(t)}{a(t)} \quad \text{or} \quad H(\eta) = \frac{a'(\eta)}{a^2(\eta)} \quad (\text{B5})$$

Here dots denote derivative with respect to t and primes denote derivatives with respect to η . One may also define the comoving Hubble parameter $\mathcal{H}(\eta) = a'(\eta)/a(\eta)$. The

value of the Hubble parameter today, also known as the Hubble constant (Hubble, 1929), is denoted by H_0 . It is customary to write $H_0 = 100h \text{ km sec}^{-1} \text{ Mpc}^{-1}$ where the dimensionless factor $h \approx 0.7 \simeq 1/\sqrt{2}$.

Distances. The distance between any two points in the expanding universe changes in time in proportion to the scale factor a . If at some time the scale factor is a_1 and the physical distance between two points is $l_{\text{phys},1}$, then at some other time when the scale factor is a , the distance will be $l_{\text{phys}}(a) = l_{\text{phys},1}(a/a_1)$. It is often useful to consider a *comoving* distance $l = l_{\text{phys}}/a$; the comoving distance is constant in expansion. Similarly, the momentum of a particle redshifts in expansion as $\mathbf{p}_{\text{phys}}(a) = \mathbf{p}_{\text{phys},1}(a_1/a)$, and it is useful to define a *comoving* momentum $\mathbf{p} = a\mathbf{p}_{\text{phys}}$. Analogous relations arise when spatially varying fields are represented in Fourier space. A Fourier mode with *comoving* wavevector \mathbf{k} and comoving wavenumber $k = |\mathbf{k}|$ corresponds to a comoving wavelength of $\lambda = 2\pi/k$, and it corresponds to physical wavelength of $\lambda_{\text{phys}} = 2\pi a/k$. We define the comoving Hubble length scale as

$$d_H(t) = \frac{2\pi}{a(t)H(t)} \quad \text{or} \quad d_H(\eta) = \frac{2\pi}{a(\eta)H(\eta)}. \quad (\text{B6})$$

Modes with comoving wavelength λ and comoving wavenumber $k = 2\pi/\lambda$ are said to ‘cross’ the Hubble scale (*i.e.*, ‘enter’ or ‘leave’ the horizon) when $k = aH$, corresponding to $\lambda = d_H$.

GR tensors. In the FLRW spacetime, the only nonzero components of the Levi-Civita connection $\Gamma_{\mu\nu}^\rho$ are

$$\begin{aligned} \Gamma_{00}^0(t) = 0 \quad \text{or} \quad \Gamma_{00}^0(\eta) = aH \\ \Gamma_{ii}^0(t) = a^2 H \quad \text{or} \quad \Gamma_{ii}^0(\eta) = aH \\ \Gamma_{0i}^i(t) = H \quad \text{or} \quad \Gamma_{0i}^i(\eta) = aH \\ \Gamma_{i0}^i(t) = H \quad \text{or} \quad \Gamma_{i0}^i(\eta) = aH, \end{aligned} \quad (\text{B7})$$

for $i = 1, 2, 3$ (no summation). Similarly the nonzero components of the spin connection ω_μ^{ab} are

$$\begin{aligned} \frac{s_1}{s_2 s_4} \omega_i^{0i}(t) = aH \quad \text{or} \quad \frac{s_1}{s_2 s_4} \omega_i^{0i}(\eta) = aH \\ \frac{s_1}{s_2 s_4} \omega_i^{i0}(t) = -aH \quad \text{or} \quad \frac{s_1}{s_2 s_4} \omega_i^{i0}(\eta) = -aH. \end{aligned} \quad (\text{B8})$$

The nonzero components of the Ricci tensor are

$$\begin{aligned} s_3 R_{00}(t) = -3\frac{\ddot{a}}{a} \quad \text{or} \quad s_3 R_{00}(\eta) = -3\frac{a''}{a} + 3\frac{a'^2}{a^2} \\ s_3 R_{ii}(t) = a\ddot{a} + 2\dot{a}^2 \quad \text{or} \quad s_3 R_{ii}(\eta) = \frac{a''}{a} + \frac{a'^2}{a^2} \end{aligned} \quad (\text{B9})$$

for $i = 1, 2, 3$ (no summation). The Ricci scalar is

$$s_1 s_3 R(t) = 6\frac{\ddot{a}}{a} + 6\frac{\dot{a}^2}{a^2} \quad \text{or} \quad s_1 s_3 R(\eta) = 6\frac{a''}{a^3}. \quad (\text{B10})$$

The nonzero components of the Einstein tensor are

$$s_3 G_{00}(t) = 3\frac{\dot{a}^2}{a^2} \quad \text{or} \quad s_3 G_{00}(\eta) = 3\frac{a'^2}{a^2} \quad (\text{B11})$$

$$s_3 G_{ii}(t) = -2a\ddot{a} - \dot{a}^2 \quad \text{or} \quad s_3 G_{ii}(\eta) = -2\frac{a''}{a} + \frac{a'^2}{a^2}$$

for $i = 1, 2, 3$ (no summation). For a perfect fluid with energy density ρ and pressure p , the stress-energy tensor in the fluid’s rest frame can be written as

$$\begin{aligned} T_{00}(t) = \rho \quad \text{or} \quad T_{00}(\eta) = a^2 \rho \\ T_{ii}(t) = a^2 p \quad \text{or} \quad T_{ii}(\eta) = a^2 p \end{aligned} \quad (\text{B12})$$

for $i = 1, 2, 3$ (no summation). The diagonal entries of Einstein’s equation give

$$\begin{aligned} \frac{\dot{a}^2}{a^2} = \frac{1}{3M_{\text{Pl}}^2} \rho \quad \text{or} \quad \frac{a'^2}{a^4} = \frac{1}{3M_{\text{Pl}}^2} \rho \\ \frac{\ddot{a}}{a} = -\frac{1}{6M_{\text{Pl}}^2}(\rho + 3p) \quad \text{or} \quad \frac{a''}{a^3} = \frac{1}{6M_{\text{Pl}}^2}(\rho - 3p), \end{aligned} \quad (\text{B13})$$

which are Friedmann’s first and second equations. Differentiating the first equation gives the continuity equation

$$\dot{\rho} + 3H(\rho + p) = 0 \quad \text{or} \quad \rho' + 3aH(\rho + p) = 0, \quad (\text{B14})$$

which expresses energy non-conservation due to the cosmological expansion $H \neq 0$. Note that Friedmann’s equations allow the Ricci scalar to be written as

$$s_1 s_3 R = M_{\text{Pl}}^{-2}(\rho - 3p), \quad (\text{B15})$$

which holds using either coordinate or conformal time.

Constant equation of state. Although the energy density ρ and pressure p may vary in time, it is often the case that their ratio, the equation of state $w = p/\rho$, is a constant. In that case the continuity equation is solved to find

$$\begin{aligned} \rho(a) = \rho_1 (a/a_1)^{-3(1+w)} \\ p(a) = p_1 (a/a_1)^{-3(1+w)} \\ H(a) = H_1 (a/a_1)^{-3(1+w)/2}, \end{aligned} \quad (\text{B16})$$

where $p_1 = w\rho_1$. Frequently encountered equations of state include:

- *Kination*: $w = 1$, $\rho \propto a^{-6}$, and $H \propto a^{-3}$.
- *Radiation*: $w = 1/3$, $\rho \propto a^{-4}$, and $H \propto a^{-2}$.
- *Matter*: $w = 0$, $\rho \propto a^{-3}$, and $H \propto a^{-3/2}$.
- *Dark energy*: $w = -1$, $\rho \propto a^0$, and $H \propto a^0$.

The cases labeled as “radiation” and “matter” refer more generally to relativistic and nonrelativistic particles.

Perturbations on FLRW. The FLRW spacetime models an

idealized homogeneous and isotropic universe, and describing our messy Universe requires a departure from FLRW. Provided that this departure is small, it can be treated perturbatively. Excellent introductions to cosmological perturbation theory are available in several textbooks and review articles; we follow [Baumann \(2022\)](#). Allowing for perturbations on the FLRW metric, the spacetime interval may be written as

$$(ds)^2 = s_1 a^2 \left[-(1 + 2A)(d\eta)^2 + 2B_i dx^i d\eta + (\delta_{ij} + 2E_{ij}) dx^i dx^j \right] \quad (B17)$$

where $B_i = \partial_i B + \hat{B}_i$
and $E_{ij} = C\delta_{ij} + \partial_{(i} \partial_{j)} E + \partial_{(i} \hat{E}_{j)} + \hat{E}_{ij}$,

where we've defined $\partial_{(i} \partial_{j)} E = (\partial_i \partial_j - \frac{1}{3} \delta_{ij} \nabla^2) E$. The functions $A(\eta, \mathbf{x})$, $B(\eta, \mathbf{x})$, $C(\eta, \mathbf{x})$, and $E(\eta, \mathbf{x})$ are called the scalar metric perturbations; $\hat{B}_i(\eta, \mathbf{x})$ and $\hat{E}_i(\eta, \mathbf{x})$ are called the vector metric perturbations; and $\hat{E}_{ij}(\eta, \mathbf{x})$ is called the tensor metric perturbation. The vector and tensor perturbations obey the transverse and traceless conditions: $\partial^i \hat{B}_i = \partial^i \hat{E}_i = \partial^i \hat{E}_{ij} = \hat{E}^i_i = 0$.

Coordinate transformations. Under a general coordinate transformation

$$x^\mu \mapsto x^\mu + \xi^\mu(x) \quad (B18)$$

where we can write $\xi^0 = T$ and $\xi^i = \partial^i L + \hat{L}^i$. The functions $T(\eta, \mathbf{x})$ and $L(\eta, \mathbf{x})$ parametrize the two scalar gauge freedoms, and the function $\hat{L}^i(\eta, \mathbf{x})$ parametrizes the single vector gauge freedom. Invariance of the spacetime interval to linear order in ξ^μ implies the following transformation rules for the metric perturbations:

$$A \mapsto A - T' - \mathcal{H}T \quad (B19a)$$

$$B \mapsto B + T - L' \quad (B19b)$$

$$C \mapsto C - \mathcal{H}T - \frac{1}{3} \nabla^2 L \quad (B19c)$$

$$E \mapsto E - L \quad (B19d)$$

$$\hat{B}_i \mapsto \hat{B}_i - \hat{L}'_i \quad (B19e)$$

$$\hat{E}_i \mapsto \hat{E}_i - \hat{L}_i \quad (B19f)$$

$$\hat{E}_{ij} \mapsto \hat{E}_{ij} \quad (B19g)$$

Note that the tensor perturbations remain invariant.

Gauge fixing. A judicious choice of the scalar transformation parameters, $T(\eta, \mathbf{x})$ and $L(\eta, \mathbf{x})$, may be used to remove some of the scalar metric perturbations; this procedure is known as gauge fixing. Popular gauge choices have special names; for example, Newtonian gauge sets $B = E = 0$, synchronous gauge sets $A = B = 0$, and spatially flat gauge sets $C = E = 0$.

Appendix C: de Sitter spacetime

This appendix contains expressions for solutions of the mode equations in de Sitter spacetime, a discussion of why CGPP does not take place in a de Sitter universe, and a discussion of applications to CGPP in an inflationary cosmology. This appendix is partly adapted from [Birrell and Davies \(1984\)](#).

de Sitter spacetime. The de Sitter spacetime ([de Sitter, 1916a,b, 1917](#)) is defined as the set of points $(z_0, z_1, z_2, z_3, z_4)$ that lie on the 4-dimensional hyperboloid $z_0^2 - z_1^2 - z_2^2 - z_3^2 - z_4^2 = -1/H^2$ that is embedded in 5-dimensional Minkowski spacetime with length element

$$(ds)^2 = s_1 \left[-(dz_0)^2 + \sum_{i=1}^4 (dz_i)^2 \right]. \quad (C1)$$

Points in de Sitter space can be written as

$$\begin{aligned} z_0 &= (2\eta)^{-1}(\eta^2 - x_1^2 - x_2^2 - x_3^2 - 1/H^2) \\ z_1 &= -(H\eta)^{-1}x_1 \\ z_2 &= -(H\eta)^{-1}x_2 \\ z_3 &= -(H\eta)^{-1}x_3 \\ z_4 &= (2\eta)^{-1}(x_1^2 + x_2^2 + x_3^2 - \eta^2 - 1/H^2) \end{aligned} \quad (C2)$$

using the 4-dimensional coordinates $\eta, x_1, x_2, x_3 \in (-\infty, \infty)$, and the metric is

$$(ds)^2 = \frac{s_1}{H^2 \eta^2} \left[-(d\eta)^2 + \sum_{i=1}^3 (dx_i)^2 \right]. \quad (C3)$$

For $\eta \in (-\infty, 0)$ the distance between points of fixed comoving separation is growing like $-1/H\eta$ as η increases; at $\eta = 0$ there is a coordinate singularity; and for $\eta \in (0, \infty)$ the distance is shrinking. The dS spacetime metric takes the same form as the spatially flat FLRW metric Eq. (B1) with $a(\eta) = -1/H\eta$. One can verify that the Hubble parameter and Ricci scalar are constant: $H = a'/a^2$ and $s_1 s_3 R = 12H^2$.

Mode functions. In de Sitter spacetime with Hubble parameter H , the scalar field's mode equation (11) becomes

$$\chi_k''(\eta) + \omega_k^2(\eta) \chi_k(\eta) = 0 \quad \text{where} \quad \omega_k^2(\eta) = k^2 + (m^2/H^2 - 2 + 12\xi)/\eta^2. \quad (C4)$$

There is an infinite one-parameter family of models with $m^2/H^2 - 2 + 12\xi = 0$ for which the dispersion relation is independent of time $\omega_k^2 = k^2$, the mode functions are the usual $\chi_k \propto e^{\mp i k \eta}$ of Minkowski spacetime, and no particle production occurs. To study solutions for general parameters, it is convenient to first put this equation into a familiar form by defining $x = k\eta \in (-\infty, \infty)$,

$y = \chi_k(\eta)/\sqrt{k\eta}$, and

$$\nu = \sqrt{\frac{9}{4} - \frac{m^2}{H^2} - 12\xi}. \quad (\text{C5})$$

With these substitutions, the mode equation is recast in the form of Bessel's equation

$$x^2 y''(x) + x y'(x) + (x^2 - \nu^2) y(x) = 0. \quad (\text{C6})$$

Its solutions are linear combinations of Bessel functions of the first and second kind, $J_\nu(x)$ and $Y_\nu(x)$. In particular we focus on Hankel functions of the first and second kind $H_\nu^{(1,2)}(x) = J_\nu(x) \pm iY_\nu(x)$, and write the solutions as

$$\begin{aligned} \chi_k(\eta) = & C_1 \sqrt{-k\eta} H_\nu^{(1)}(-k\eta) \\ & + C_2 \sqrt{-k\eta} H_\nu^{(2)}(-k\eta). \end{aligned} \quad (\text{C7})$$

Note that both the square root function and the Hankel functions are double-valued in the complex $k\eta$ -plane with a single branch point at $k\eta = 0$, and we can orient their branch cuts to lie along the positive real axis, $k\eta \in \mathbb{R}^{>0}$. Similarly, as m/H and ξ are analytically continued into the complex plane, ν is interpreted as the double-valued square-root function, and the Hankel functions may be evaluated with complex index. It is also useful to note that Hankel functions satisfy the relation $H_{-\nu}^{(1,2)}(z) = e^{\pm i\pi\nu} H_\nu^{(1,2)}(z)$ for $z, \nu \in \mathbb{C}$.

Bunch-Davies vacuum condition. The IN and OUT mode functions, $\chi_k^{\text{IN}}(\eta)$ and $\chi_k^{\text{OUT}}(\eta)$, correspond to the solutions that have the asymptotic forms in Eq. (26). The complex integration constants, C_1 and C_2 , can be chosen to yield the IN mode function $\chi_k^{\text{IN}}(\eta)$. Hankel functions are asymptotic to (Abramowitz and Stegun, 1964)

$$\begin{aligned} H_\nu^{(1)}(z) &\sim \sqrt{\frac{2}{\pi z}} e^{i(z - \nu\pi/2 - \pi/4)} \quad \text{as } |z| \rightarrow \infty \\ H_\nu^{(2)}(z) &\sim \sqrt{\frac{2}{\pi z}} e^{-i(z - \nu\pi/2 - \pi/4)} \quad \text{as } |z| \rightarrow \infty \end{aligned} \quad (\text{C8})$$

for $\arg(z)$ throughout the first sheet, and for fixed ν . Choosing $C_1 = \sqrt{\pi/4k} e^{i(\nu\pi/2 + \pi/4)}$ and $C_2 = 0$ gives

$$\chi_k^{\text{IN}}(\eta) = \sqrt{\frac{\pi}{4k}} \sqrt{-k\eta} H_\nu^{(1)}(-k\eta) e^{i(\nu\pi/2 + \pi/4)}, \quad (\text{C9})$$

which is asymptotic to

$$\chi_k^{\text{IN}}(\eta) \sim \frac{1}{\sqrt{2k}} e^{-ik\eta} \quad \text{as } k\eta \rightarrow -\infty \quad (\text{C10})$$

at early times for any value of ν . For $k\eta \in (0, \infty)$ we evaluate these functions above the cut on the first Riemann sheet. These mode functions solve the scalar field's equation of motion in de Sitter spacetime along with the Bunch-Davies initial condition.

Special cases. For models involving a massless scalar, or

more generally $m \ll H$, the mode functions simplify. Here we regain expressions that are familiar from studies of scalar inflaton perturbations during inflation (Bau-mann, 2022). For the massless and conformally coupled scalar, setting $m = 0$ and $\xi = 1/6$ yields

$$\chi_k^{\text{IN}}(\eta) = i \sqrt{\frac{\pi}{4k}} \sqrt{z} H_{1/2}^{(1)}(z) = \frac{1}{\sqrt{2k}} e^{iz}, \quad (\text{C11})$$

whereas for the massless and minimally coupled scalar, setting $m = 0$ and $\xi = 0$ yields

$$\chi_k^{\text{IN}}(\eta) = -\sqrt{\frac{\pi}{4k}} \sqrt{z} H_{3/2}^{(1)}(z) = \frac{1}{\sqrt{2k}} \left(1 + \frac{i}{z}\right) e^{iz} \quad (\text{C12})$$

where $z \equiv -k\eta$. As expected, the massless and conformally coupled scalar's mode functions are equivalent to the positive-frequency mode functions in Minkowski spacetime; see the discussion in Sec. V.A. On the other hand, the minimally coupled scalar's mode functions grow relatively by a factor of $1/k\eta$ as modes leave the horizon and $-1 \ll k\eta < 0$.

Connection to inflation. During the epoch of inflation, the Hubble parameter varies slowly ($\epsilon = -H'/aH^2 \ll 1$), and the expanding branch of de Sitter is a good approximation for the spacetime. Consequently the de Sitter mode functions (C9) are a good approximation to the evolution of the spectator field. At early times, they are compatible with the Bunch-Davies initial condition (C10). At late times, they go to

$$\chi_k^{\text{IN}}(\eta_e) = \sqrt{\frac{\pi}{4a_e H_e}} H_\nu^{(1)}(k/a_e H_e) e^{i(\nu\pi/2 + \pi/4)} \quad (\text{C13a})$$

$$|\chi_k^{\text{IN}}(\eta_e)| = \frac{1}{\sqrt{2k}} \quad \text{for } m = 0, \xi = 1/6 \quad (\text{C13b})$$

$$|\chi_k^{\text{IN}}(\eta_e)| = \frac{1}{\sqrt{2k}} \sqrt{1 + \frac{a_e^2 H_e^2}{k^2}} \quad \text{for } m = 0, \xi = 0. \quad (\text{C13c})$$

where we've defined the 'end of inflation' as $\eta_e = -1/a_e H_e$. Although the Hubble parameter begins to vary significantly at the end of inflation, invalidating the de Sitter solution, these expressions typically provide reliable approximations that can be used as initial conditions for the mode equations during reheating after inflation.

Appendix D: JWKB Method

This appendix contains a brief review of the Jeffreys-Wentzel-Kramers-Brillouin method (Brillouin, 1926; Jeffreys, 1925; Kramers, 1926; Wentzel, 1926). The JWKB method may be applied to derive approximate solutions to equations of the form

$$y''(x) + Q(x) y(x) = 0 \quad (\text{D1})$$

where $Q(x)$ is differentiable function. See [Bender and Orszag \(1999\)](#) for an excellent introduction to asymptotic methods and perturbation theory, and see [Parker and Toms \(2009\)](#) for applications of JWKB to QFT in curved spacetime (*e.g.*, adiabatic subtraction, trace anomaly).

Motivation. Equations of this form arise in the description of both classical and quantum physical systems. In classical mechanics, the displacement of a one-dimensional harmonic oscillator with time-dependent natural frequency is governed by $d^2x/dt^2 + \omega^2(t)x(t) = 0$. In quantum mechanics, the wavefunction of a nonrelativistic mass moving in a one-dimensional static potential is governed by $d^2\psi/dx^2 + (2m/\hbar^2)[E - V(x)]\psi(x) = 0$. In quantum field theory, the Fourier mode amplitudes of a free scalar field in an FLRW spacetime are governed by $\chi_k''(\eta) + \omega_k^2(\eta)\chi_k(\eta) = 0$, which we encountered in Eq. (11). Similar second-order linear equations appear in the study of free fields with spin (see Sec. V).

Strategy. The JWKB method draws upon perturbation theory and asymptotic series to tackle equations of the form in Eq. (D1) (as well as more general equations). To appreciate the strategy, note that if $Q(x) = q^2$ were a constant, one could immediately identify the four-dimensional space of solutions $y(x) = C_1 e^{-iqx} + C_2 e^{iqx}$ for arbitrary complex coefficients $C_1, C_2 \in \mathbb{C}$. This observation motivates one to seek a solution for general $Q(x)$ using perturbation theory, with the constant case taken as the expansion point. The JWKB method entails the construction of a power series. With the exception of special cases, such as the constant $Q(x) = q^2$, the resultant power series is divergent. However the first few terms in this series typically provide a good approximation to the desired solution. In this appendix we focus on explaining the conceptual underpinnings of the JWKB method and remark upon its application to QFT in curved spacetime.

Adiabatic parameter. Since Eq. (D1) is easily solved for constant $Q(x)$, it suggests that approximate solutions should be available for slowly-varying $Q(x)$ with small time derivatives. To seek out such solutions, introduce an expansion parameter $\varepsilon \in \mathbb{R}$ at each appearance of a derivative: $\partial_x \rightarrow \varepsilon \partial_x$. In principle $Q(x)$ may be constructed from derivatives as well, so we should write $Q(x) = \sum_{n=0}^{\infty} \varepsilon^n Q_n(x)$. With these substitutions, one

obtains an infinite one-parameter family of equations:⁴

$$\varepsilon^2 y''(x; \varepsilon) + \sum_{n=0}^{\infty} \varepsilon^n Q_n(x) y(x; \varepsilon) = 0. \quad (\text{D2})$$

Once these equations are solved, the desired solution is $y(x; 1)$. Since ε tracks time derivatives, it is called the adiabatic parameter (or $T = \varepsilon^{-1}$ the slowness parameter), and $O(\varepsilon^n)$ terms are called n^{th} adiabatic order.

JWKB ansatz. Since the equation with constant $Q(x)$ is solved by an exponential function, this observation motivates searching for solutions that can be written as

$$\tilde{y}(x; \varepsilon) = \exp\left(\frac{1}{\varepsilon} \sum_{n=0}^{\infty} \varepsilon^n S_n(x)\right). \quad (\text{D3})$$

It may not be the case that solutions of Eq. (D2) can be written in this form. Nevertheless, it's valuable to search for such solutions, since even if they don't solve the equation, they may provide a good approximation to the desired solution. Putting this ansatz into the equation for $y(x; \varepsilon)$, and solving order-by-order in powers of ε yields

$$\begin{aligned} [S'_0(x)]^2 &= -Q_0(x) \\ 2S'_0(x)S'_1(x) &= -Q_1(x) - S''_0(x) \\ 2S'_0(x)S'_2(x) &= -Q_2(x) - S'_1(x) - [S'_1(x)]^2, \end{aligned} \quad (\text{D4})$$

and so on. Note that there are two solution branches corresponding to $S_0(x) = \mp \int^x dx' \sqrt{-Q_0(x')}$.

Discussion. If the series $\tilde{y}(x; \varepsilon)$ is convergent at $\varepsilon = 1$, then $y(x) = \tilde{y}(x; 1)$ is the desired solution to the original equation. However, for the situations of interest, the series typically diverges for any nonzero ε . In that case, the formal series should be understood as an asymptotic expansion of the solution at small adiabatic parameter:

$$y(x; \varepsilon) \sim \tilde{y}(x; \varepsilon) \quad \text{as } \varepsilon \rightarrow 0. \quad (\text{D5})$$

This outcome may seem like a failure, since the goal was to solve the equation with $\varepsilon = 1$, but Eq. (D5) gives the asymptotic form of the solution as $\varepsilon \rightarrow 0$. Nevertheless, it is often the case that an asymptotic series, when truncated to a low order provides a good approximation. For instance, truncating the series at $O(\varepsilon^N)$ and taking $\varepsilon = 1$

⁴ It may appear that introducing ε has made the problem more difficult, since rather than needing to solve the single equation (D1) it is now necessary to solve an infinite family of equations. However, if we assume that solutions of Eq. (D2) can be expressed as a Taylor series in powers of the arbitrary ε , then we can solve order-by-order in powers of ε . In this way, perturbation theory substitutes one hard problem for an infinite number of easy problems ([Bender and Orszag, 1999](#)).

gives the function

$$y^{(N)}(x) = \exp\left(\sum_{n=0}^N S_n(x)\right). \quad (\text{D6})$$

To be concrete, suppose that $Q_0(x) = [q(x)]^2$ and $Q_n(x) = 0$ for $n \geq 1$. Then for $N = 1$ we have

$$y^{(1)}(x) = \frac{1}{\sqrt{2q(x)}} \exp\left(-i \int^x dx' q(x')\right), \quad (\text{D7})$$

which is the leading order JWKB approximation. Although $y^{(1)}(x)$ is not a solution of Eq. (D1) (except for special cases like constant $q(x)$), it typically provides a good approximation. Adding a few more terms in the asymptotic series will typically improve the approximation, but eventually adding more terms will expose the divergence of the series, and cause the approximation to degrade. The onset of the divergence is controlled by the magnitude of the derivatives of $q(x)$: since $y^{(1)}(x)$ is an exact solution for constant $q(x)$, one expects $y^{(1)}(x)$ to be a good approximation when $q(x)$ is slowly varying, *i.e.*, adiabatic. It is customary to define a dimensionless measure of the adiabaticity of the system as

$$A(x) = |q'(x)/q(x)^2|, \quad (\text{D8})$$

which corresponds to the fraction by which $q(x)$ changes during each oscillation cycle. Smaller $A(x)$ corresponds to a more adiabatic system, and $y^{(1)}(x)$ provides a better approximation to the desired solution.

Applications to QFT in curved spacetime. In the remainder of this appendix, we focus on applications of the JWKB method to studies of QFT in curved spacetime. For concreteness we use the scalar field in FLRW spacetime as an example. The scalar field's Fourier mode amplitudes $\chi_k(\eta)$ obey the second-order, linear differential equation (11). Upon introducing the adiabatic parameter ε , the equation of motion becomes

$$\varepsilon^2 \chi''(\eta; \varepsilon) + \omega^2(\eta; \varepsilon) \chi(\eta; \varepsilon) = 0 \quad \text{with} \quad (\text{D9})$$

$$\omega^2(\eta; \varepsilon) = [k^2 + a^2(\eta)m^2] + [(\tfrac{1}{6} - \xi)a^2(\eta)R(\eta)] \varepsilon^2,$$

where we have dropped the subscript k to simplify the notation. Since the Ricci scalar $R(\eta)$ involves two time derivatives, this term develops a factor of ε^2 . For studies of QFT in curved spacetime, it is customary to write the JWKB ansatz as (Birrell and Davies, 1984)

$$\tilde{\chi}(\eta; \varepsilon) = \frac{1}{\sqrt{2W(\eta; \varepsilon)}} \exp\left(-\frac{i}{\varepsilon} \int^\eta d\eta' W(\eta'; \varepsilon)\right) \quad (\text{D10})$$

where the power series $W(\eta; \varepsilon) = \sum_{n=0}^\infty \varepsilon^n W_n(\eta)$ satisfies

$$[W(\eta, \varepsilon)]^2 = \omega^2(\eta; \varepsilon) - \frac{\varepsilon^2}{2} \left[\frac{W''(\eta; \varepsilon)}{W(\eta; \varepsilon)} - \frac{3}{2} \left(\frac{W'(\eta; \varepsilon)}{W(\eta; \varepsilon)} \right)^2 \right]. \quad (\text{D11})$$

Equating order-by-order in powers of ε yields

$$\begin{aligned} [W_0(\eta)]^2 &= k^2 + a^2(\eta)m^2 \equiv [\omega_0(\eta)]^2 \\ 2W_0(\eta)W_2(\eta) &= (\tfrac{1}{6} - \xi)a^2(\eta)R(\eta) \\ &\quad + \tfrac{3}{4} \left(\frac{W_0'(\eta)}{W_0(\eta)} \right)^2 - \tfrac{1}{2} \frac{W_0''(\eta)}{W_0(\eta)}, \end{aligned} \quad (\text{D12})$$

and $W_n(\eta) = 0$ for odd n . Once again there are two solutions branches with $W_0(\eta) = \pm\omega_0(\eta)$, corresponding to positive- and negative-frequency modes, respectively. The N^{th} -order JWKB approximation is obtained by truncating the series at $O(\varepsilon^N)$ and setting $\varepsilon = 1$:

$$\chi^{(N)}(\eta) = \frac{\exp\left(-i \int^\eta d\eta' \sum_{n=0}^N W_n(\eta')\right)}{\sqrt{2 \sum_{n=0}^N W_n(\eta)}}. \quad (\text{D13})$$

For instance, the leading-order JWKB approximation is

$$\chi^{(0)}(\eta) = \frac{\exp\left(-i \int^\eta d\eta' \sqrt{k^2 + a^2(\eta')m^2}\right)}{[2\sqrt{k^2 + a(\eta)^2 m^2}]^{1/2}}. \quad (\text{D14})$$

Adiabatic vacuum. One application of the JWKB method for QFT in curved spacetime is the definition of the adiabatic vacuum (Birrell and Davies, 1984; Mukhanov and Winitzki, 2007). Although the JWKB approximation isn't a solution of the original equation, it can be used as an initial condition at conformal time η_0 to define an exact solution:

$$\chi(\eta_0) = \chi^{(N)}(\eta_0) \quad \text{and} \quad \chi'(\eta_0) = \frac{d\chi^{(N)}}{d\eta} \Big|_{\eta=\eta_0}. \quad (\text{D15})$$

The solution consistent with these initial conditions is known as the N^{th} -order adiabatic mode function at time η_0 . The vacuum state annihilated by the corresponding ladder operators is known as the N^{th} -order adiabatic vacuum, $|0_{\text{ad}, \eta_0}\rangle$. If the system is strongly adiabatic at early times, *i.e.*, $\omega'(\eta)/\omega^2(\eta) \rightarrow 0$ as $\eta \rightarrow -\infty$, then all the vacuum prescriptions agree asymptotically, thereby providing a naturally unique vacuum state.

Adiabatic regularization. The construction of adiabatic orders through the JWKB method, also proves useful for handling UV divergences through the technique of adiabatic regularization (Parker and Toms, 2009). Calculating observables that are nonlinear in the fields, such as expectation values of the stress-energy tensor, generally lead to UV divergences. Adiabatic regularization entails expressing the observable as a power series in the adiabatic parameter ε , and removing all the terms at a given order if any of those terms contain a UV divergence. To give a schematic example, suppose that we're calculating an observable and finding that it can be written as $O = (a_0)\varepsilon^0 + (a_2 + b_2 + c_2)\varepsilon^2 + (a_4 + b_4)\varepsilon^4 + \dots$ where

the coefficients represent momentum integrals. Suppose that a_0 and b_2 are integrals with UV divergences while the other terms are finite. Then adiabatic regularization requires the removal of all terms at ε^0 and ε^2 , leaving only $O_{\text{reg}} = (a_4 + b_4)\varepsilon^4 + \dots$. Adiabatic regularization proves useful in several derivations, including the conformal anomaly in the trace of the stress-energy tensor.

Extensions. Whereas this discussion has focused on the JWKB method for equations of the form in Eq. (D1), which arise in bosonic field theories (Ferreiro *et al.*, 2023; Ferreiro and Torrenti, 2023; Marañón González and Navarro-Salas, 2023), a similar method is available for the linear, coupled equations that arise in theories of fermions. See Hashiba *et al.* (2022) as well as Corbà and Sorbo (2023); Dabrowski and Dunne (2014, 2016); Dumlu and Dunne (2010); Durrer *et al.* (2009); Enomoto and Matsuda (2021, 2022); Landete *et al.* (2013, 2014); del Rio *et al.* (2014); and Sou *et al.* (2021).

REFERENCES

- Abbott, L. F., and M. B. Wise (1984), Nucl. Phys. B **244**, 541.
- Abramowitz, M., and I. A. Stegun (1964), *Handbook of Mathematical Functions with Formulas, Graphs, and Mathematical Tables*, ninth dover printing, tenth gpo printing ed. (Dover, New York).
- Acharya, S. K., and R. Khatri (2019), JCAP **12**, 046, arXiv:1910.06272 [astro-ph.CO].
- Ade, P. A. R., *et al.* (BICEP, Keck) (2021), Phys. Rev. Lett. **127** (15), 151301, arXiv:2110.00483 [astro-ph.CO].
- Aghanim, N., *et al.* (Planck) (2020), Astron. Astrophys. **641**, A6, [Erratum: Astron. Astrophys. 652, C4 (2021)], arXiv:1807.06209 [astro-ph.CO].
- Ahmed, A., B. Grzadkowski, and A. Socha (2020), JHEP **08**, 059, arXiv:2005.01766 [hep-ph].
- Akrami, Y., *et al.* (Planck) (2020a), Astron. Astrophys. **641**, A9, arXiv:1905.05697 [astro-ph.CO].
- Akrami, Y., *et al.* (Planck) (2020b), Astron. Astrophys. **641**, A10, arXiv:1807.06211 [astro-ph.CO].
- Albrecht, A., P. Ferreira, M. Joyce, and T. Prokopec (1994), Phys. Rev. D **50**, 4807, arXiv:astro-ph/9303001.
- Alexander, S., L. Jenks, and E. McDonough (2021), Phys. Lett. B **819**, 136436, arXiv:2010.15125 [hep-ph].
- Alexander, S. H.-S., M. E. Peskin, and M. M. Sheikh-Jabbari (2006), Phys. Rev. Lett. **96**, 081301, arXiv:hep-th/0403069.
- Ali-Haïmoud, Y., and M. Kamionkowski (2017), Phys. Rev. D **95** (4), 043534, arXiv:1612.05644 [astro-ph.CO].
- Aloisio, R., S. Matarrese, and A. V. Olinto (2015), JCAP **08**, 024, arXiv:1504.01319 [astro-ph.HE].
- Amin, M. A., M. P. Hertzberg, D. I. Kaiser, and J. Karouby (2014), Int. J. Mod. Phys. D **24**, 1530003, arXiv:1410.3808 [hep-ph].
- Amin, M. A., and M. Mirbabayi (2022), arXiv:2211.09775 [hep-ph].
- Antoniadis, I., K. Benakli, and W. Ke (2021), JHEP **11**, 063, arXiv:2105.03784 [hep-th].
- Aoki, K., and S. Mukohyama (2016), Phys. Rev. D **94** (2), 024001, arXiv:1604.06704 [hep-th].
- Aragone, C., and S. Deser (1979), Phys. Lett. B **86**, 161.
- Arkani-Hamed, N., D. Baumann, H. Lee, and G. L. Pimentel (2020), JHEP **04**, 105, arXiv:1811.00024 [hep-th].
- Arkani-Hamed, N., and J. Maldacena (2015), arXiv:1503.08043 [hep-th].
- Armendariz-Picon, C., and A. Diez-Tejedor (2023), JCAP **11**, 030, arXiv:2305.16293 [gr-qc].
- Arvanitaki, A., S. Dimopoulos, M. Galanis, D. Racco, O. Simon, and J. O. Thompson (2021), JHEP **11**, 106, arXiv:2108.04823 [hep-ph].
- Attanasio, A., *et al.* (Windchime) (2022), in *Snowmass 2021*, arXiv:2203.07242 [hep-ex].
- Audretsch, J., and G. Schaefer (1978), J. Phys. A **11**, 1583.
- Aydemir, U., and J. Ren (2021), Chin. Phys. C **45** (7), 075103, arXiv:2011.13154 [hep-ph].
- Babichev, E., L. Marzola, M. Raidal, A. Schmidt-May, F. Urban, H. Veermäe, and M. von Strauss (2016a), Phys. Rev. D **94** (8), 084055, arXiv:1604.08564 [hep-ph].
- Babichev, E., L. Marzola, M. Raidal, A. Schmidt-May, F. Urban, H. Veermäe, and M. von Strauss (2016b), JCAP **09**, 016, arXiv:1607.03497 [hep-th].
- Bambi, C., A. D. Dolgov, and K. Freese (2007), JCAP **04**, 005, arXiv:hep-ph/0612018.
- Barman, B., and N. Bernal (2021), JCAP **06**, 011, arXiv:2104.10699 [hep-ph].
- Barman, B., D. Borah, S. Das Jyoti, and R. Roshan (2022a), JCAP **08**, 068, arXiv:2204.10339 [hep-ph].
- Barman, B., D. Borah, S. Jyoti Das, and R. Roshan (2023), Phys. Rev. D **107** (9), 095002, arXiv:2212.00052 [hep-ph].
- Barman, B., S. Cléry, R. T. Co, Y. Mambrini, and K. A. Olive (2022b), JHEP **12**, 072, arXiv:2210.05716 [hep-ph].
- Basso, E., D. J. H. Chung, E. W. Kolb, and A. J. Long (2022), JHEP **12**, 108, arXiv:2209.01713 [gr-qc].
- Basso, E. E., and D. J. H. Chung (2021), JHEP **11**, 146, arXiv:2108.01653 [hep-ph].
- Bastero-Gil, M., and A. Mazumdar (2000), Phys. Rev. D **62**, 083510, arXiv:hep-ph/0002004.
- Baumann, D. (2022), *Cosmology* (Cambridge University Press).
- Baumann, D., G. Goon, H. Lee, and G. L. Pimentel (2018), JHEP **04**, 140, arXiv:1712.06624 [hep-th].
- Baumann, D., and D. Green (2012), Phys. Rev. D **85**, 103520, arXiv:1109.0292 [hep-th].
- Bekenstein, J. D. (1973), Phys. Rev. **D7**, 2333.
- Belinfante, F. J. (1939), Physica **6**, 887.
- Belinfante, F. J. (1940), Physica **7**, 449.
- Bellazzini, B., F. Riva, J. Serra, and F. Sgarlata (2019), JHEP **10**, 189, arXiv:1903.08664 [hep-th].
- Bellomo, N., K. V. Berghaus, and K. K. Boddy (2023), JCAP **11**, 024, arXiv:2210.15691 [astro-ph.CO].
- Bender, C. M., and S. A. Orszag (1999), *Advanced mathematical methods for scientists and engineers* (Springer-Verlag New York, Inc) originally published: New York : McGraw-Hill, c1978.
- Bernal, N., M. Dutra, Y. Mambrini, K. Olive, M. Peloso, and M. Pierre (2018), Phys. Rev. D **97** (11), 115020, arXiv:1803.01866 [hep-ph].
- Bernal, N., and C. S. Fong (2021), JCAP **06**, 028, arXiv:2103.06896 [hep-ph].
- Bernal, N., C. S. Fong, Y. F. Perez-Gonzalez, and J. Turner (2022), Phys. Rev. D **106** (3), 035019, arXiv:2203.08823 [hep-ph].
- Birrell, N. D., and P. C. W. Davies (1984), *Quantum Fields in Curved Space*, Cambridge Monographs on Mathematical

- Physics (Cambridge Univ. Press, Cambridge, UK).
- Boyanovsky, D., M. Rai, and L. Chen (2021), Phys. Rev. D **104** (12), 123552, arXiv:2110.15488 [gr-qc].
- Boyle, L., K. Finn, and N. Turok (2022), Annals Phys. **438**, 168767, arXiv:1803.08930 [hep-ph].
- Boyle, L. A., and A. Buonanno (2008), Phys. Rev. D **78**, 043531, arXiv:0708.2279 [astro-ph].
- Brillouin, L. (1926), Compt. Rend. Hebd. Seances Acad. Sci. **183** (1), 24.
- de Broglie, L. (1922), J. Phys. Radium **3**, 422.
- de Broglie, L. (1934), C. R. Acad. Sci. **198**, 135.
- Bunch, T. S., and P. C. W. Davies (1978), Proc. Roy. Soc. Lond. **A360**, 117.
- Capanelli, C., L. Jenks, E. W. Kolb, and E. McDonough (2023), arXiv:2309.02485 [hep-ph].
- Caputo, A., A. J. Millar, C. A. J. O'Hare, and E. Vitagliano (2021), Phys. Rev. D **104** (9), 095029, arXiv:2105.04565 [hep-ph].
- Carney, D., S. Ghosh, G. Krnjaic, and J. M. Taylor (2020), Phys. Rev. D **102** (7), 072003, arXiv:1903.00492 [hep-ph].
- Carney, D., *et al.* (2021), Quantum Sci. Technol. **6**, 024002, arXiv:2008.06074 [physics.ins-det].
- Carney, D., *et al.* (2022), 10.21468/SciPostPhysCore.6.4.075, arXiv:2203.06508 [hep-ph].
- Carr, B. J., and S. W. Hawking (1974), Mon. Not. Roy. Astron. Soc. **168**, 399.
- Carroll, S. M. (2019), *Spacetime and Geometry: An Introduction to General Relativity* (Cambridge University Press).
- Cartan, E. (1926), Acta Mathematica **48** (1-2), 1.
- Casagrande, G., E. Dudas, and M. Peloso (2023), arXiv:2310.14964 [hep-th].
- Castellano, A., A. Font, A. Herraez, and L. E. Ibáñez (2021), JHEP **08**, 092, arXiv:2104.10181 [hep-th].
- Cembranos, J. A. R., L. J. Garay, A. Parra-López, and J. M. Sánchez Velázquez (2023), arXiv:2310.07515 [gr-qc].
- Cembranos, J. A. R., L. J. Garay, and J. M. Sánchez Velázquez (2020), JHEP **06**, 084, arXiv:1910.13937 [hep-ph].
- Chen, X. (2010), Adv. Astron. **2010**, 638979, arXiv:1002.1416 [astro-ph.CO].
- Chen, X., and Y. Wang (2010a), Phys. Rev. D **81**, 063511, arXiv:0909.0496 [astro-ph.CO].
- Chen, X., and Y. Wang (2010b), JCAP **04**, 027, arXiv:0911.3380 [hep-th].
- Chianese, M., D. F. G. Fiorillo, R. Hajjar, G. Miele, S. Morisi, and N. Saviano (2021a), JCAP **05**, 074, arXiv:2103.03254 [hep-ph].
- Chianese, M., D. F. G. Fiorillo, R. Hajjar, G. Miele, and N. Saviano (2021b), JCAP **11**, 035, arXiv:2108.01678 [hep-ph].
- Chianese, M., B. Fu, and S. F. King (2020), JCAP **06**, 019, arXiv:2003.07366 [hep-ph].
- Chianese, M., B. Fu, and S. F. King (2021c), JCAP **01**, 034, arXiv:2009.01847 [hep-ph].
- Chluba, J., *et al.* (2019), Bull. Am. Astron. Soc. **51** (3), 184, arXiv:1903.04218 [astro-ph.CO].
- Chun, E. J., S. Scopel, and I. Zaballa (2009), JCAP **07**, 022, arXiv:0904.0675 [hep-ph].
- Chung, D. J. H. (2003), Phys. Rev. **D67**, 083514, arXiv:hep-ph/9809489 [hep-ph].
- Chung, D. J. H. (2016), Phys. Rev. D **94** (4), 043524, arXiv:1509.05850 [astro-ph.CO].
- Chung, D. J. H., P. Crotty, E. W. Kolb, and A. Riotto (2001), Phys. Rev. **D64**, 043503, arXiv:hep-ph/0104100 [hep-ph].
- Chung, D. J. H., L. L. Everett, H. Yoo, and P. Zhou (2012), Phys. Lett. **B712**, 147, arXiv:1109.2524 [astro-ph.CO].
- Chung, D. J. H., E. W. Kolb, and A. J. Long (2019), JHEP **01**, 189, arXiv:1812.00211 [hep-ph].
- Chung, D. J. H., E. W. Kolb, and A. Riotto (1998a), Phys. Rev. Lett. **81**, 4048, arXiv:hep-ph/9805473 [hep-ph].
- Chung, D. J. H., E. W. Kolb, and A. Riotto (1998b), Phys. Rev. **D59**, 023501, arXiv:hep-ph/9802238 [hep-ph].
- Chung, D. J. H., E. W. Kolb, and A. Riotto (1999), Phys. Rev. **D60**, 063504, arXiv:hep-ph/9809453 [hep-ph].
- Chung, D. J. H., E. W. Kolb, A. Riotto, and L. Senatore (2005), Phys. Rev. **D72**, 023511, arXiv:astro-ph/0411468 [astro-ph].
- Chung, D. J. H., and A. Upadhye (2017), Phys. Rev. **D95** (2), 023503, arXiv:1610.04284 [astro-ph.CO].
- Chung, D. J. H., and A. Upadhye (2018), Phys. Rev. D **98** (2), 023525, arXiv:1711.06736 [astro-ph.CO].
- Chung, D. J. H., and H. Yoo (2013), Phys. Rev. **D87**, 023516, arXiv:1110.5931 [astro-ph.CO].
- Chung, D. J. H., H. Yoo, and P. Zhou (2013), Phys. Rev. **D87**, 123502, arXiv:1303.6024 [astro-ph.CO].
- Chung, D. J. H., H. Yoo, and P. Zhou (2015), Phys. Rev. **D91** (4), 043516, arXiv:1306.1966 [astro-ph.CO].
- Clery, S., Y. Mambrini, K. A. Olive, A. Shkerin, and S. Verner (2022a), Phys. Rev. D **105** (9), 095042, arXiv:2203.02004 [hep-ph].
- Clery, S., Y. Mambrini, K. A. Olive, and S. Verner (2022b), Phys. Rev. D **105** (7), 075005, arXiv:2112.15214 [hep-ph].
- Co, R. T., Y. Mambrini, and K. A. Olive (2022), Phys. Rev. D **106** (7), 075006, arXiv:2205.01689 [hep-ph].
- Coleman, S. R., and J. Mandula (1967), Phys. Rev. **159**, 1251.
- Comelli, D., M. Crisostomi, K. Koyama, L. Pilo, and G. Tasinato (2015), JCAP **04**, 026, arXiv:1501.00864 [hep-th].
- Copeland, E. J., A. R. Liddle, and J. E. Lidsey (2001), Phys. Rev. D **64**, 023509, arXiv:astro-ph/0006421.
- Corbà, S. P., and L. Sorbo (2023), JCAP **07**, 005, arXiv:2209.14362 [hep-th].
- Criado, J. C., N. Koivunen, M. Raidal, and H. Veermäe (2020), Phys. Rev. D **102** (12), 125031, arXiv:2010.02224 [hep-ph].
- Cribiori, N., D. Lust, and M. Scalisi (2021), JHEP **06**, 071, arXiv:2104.08288 [hep-th].
- Cyburt, R. H., J. R. Ellis, B. D. Fields, and K. A. Olive (2003), Phys. Rev. D **67**, 103521, arXiv:astro-ph/0211258.
- Cyburt, R. H., B. D. Fields, K. A. Olive, and T.-H. Yeh (2016), Rev. Mod. Phys. **88**, 015004.
- Dabrowski, R., and G. V. Dunne (2014), Phys. Rev. D **90** (2), 025021, arXiv:1405.0302 [hep-th].
- Dabrowski, R., and G. V. Dunne (2016), Phys. Rev. D **94** (6), 065005, arXiv:1606.00902 [hep-th].
- Das, S., K. Murase, and T. Fujii (2023), Phys. Rev. D **107** (10), 103013, arXiv:2302.02993 [astro-ph.HE].
- Datta, S., A. Ghosal, and R. Samanta (2021), JCAP **08**, 021, arXiv:2012.14981 [hep-ph].
- Dimopoulos, K. (2006), Phys. Rev. D **74**, 083502, arXiv:hep-ph/0607229.
- Dimopoulos, K., and T. Markkanen (2018), JCAP **06**, 021, arXiv:1803.07399 [gr-qc].
- Dirac, P. A. M. (1928), Proc. Roy. Soc. Lond. A **117**, 610.
- Dolgov, A. D. (1981), Sov. Phys. JETP **54**, 223.
- Drlica-Wagner, A., *et al.* (2022), arXiv:2209.08215 [hep-ph].
- Dudas, E., M. A. G. Garcia, Y. Mambrini, K. A. Olive, M. Peloso, and S. Verner (2021), Phys. Rev. D **103**,

- 123519, arXiv:2104.03749 [hep-th].
- Dumlu, C. K., and G. V. Dunne (2010), Phys. Rev. Lett. **104**, 250402, arXiv:1004.2509 [hep-th].
- Durrer, R., G. Marozzi, and M. Rinaldi (2009), Phys. Rev. D **80**, 065024, arXiv:0906.4772 [astro-ph.CO].
- Ebadi, R., S. Kumar, A. McCune, H. Tai, and L.-T. Wang (2023), arXiv:2307.01248 [astro-ph.CO].
- Einstein, A. (1916), Annalen Phys. **49** (7), 769, [Annalen Phys.354,no.7,769(1916)].
- Ellis, J. R., J. S. Hagelin, D. V. Nanopoulos, K. A. Olive, and M. Srednicki (1984a), Nucl. Phys. B **238**, 453.
- Ellis, J. R., J. E. Kim, and D. V. Nanopoulos (1984b), Phys. Lett. B **145**, 181.
- Ema, Y., R. Jinno, K. Mukaida, and K. Nakayama (2015), JCAP **05**, 038, arXiv:1502.02475 [hep-ph].
- Ema, Y., R. Jinno, K. Mukaida, and K. Nakayama (2016), Phys. Rev. D **94** (6), 063517, arXiv:1604.08898 [hep-ph].
- Ema, Y., R. Jinno, and K. Nakayama (2020), JCAP **09**, 015, arXiv:2006.09972 [astro-ph.CO].
- Ema, Y., K. Mukaida, and K. Nakayama (2022), JHEP **05**, 087, arXiv:2112.12774 [hep-ph].
- Ema, Y., K. Nakayama, and Y. Tang (2018), JHEP **09**, 135, arXiv:1804.07471 [hep-ph].
- Ema, Y., K. Nakayama, and Y. Tang (2019), JHEP **07**, 060, arXiv:1903.10973 [hep-ph].
- Enomoto, S., and T. Matsuda (2021), JHEP **03**, 090, arXiv:2010.14835 [hep-ph].
- Enomoto, S., and T. Matsuda (2022), JHEP **02**, 131, arXiv:2104.02312 [hep-th].
- Fabbri, R., and M. d. Pollock (1983), Phys. Lett. B **125**, 445.
- Fairbairn, M., K. Kainulainen, T. Markkanen, and S. Nurmi (2019), JCAP **04**, 005, arXiv:1808.08236 [astro-ph.CO].
- Falkowski, A., G. Isabella, and C. S. Machado (2021), SciPost Phys. **10** (5), 101, arXiv:2011.05339 [hep-ph].
- Fasiello, M., and A. J. Tolley (2012), JCAP **11**, 035, arXiv:1206.3852 [hep-th].
- Fasiello, M., and A. J. Tolley (2013), JCAP **12**, 002, arXiv:1308.1647 [hep-th].
- Feng, B., and M.-z. Li (2003), Phys. Lett. B **564**, 169, arXiv:hep-ph/0212213.
- Ferreiro, A., S. Monin, and F. Torrenti (2023), arXiv:2311.08986 [gr-qc].
- Ferreiro, A., and F. Torrenti (2023), Phys. Lett. B **840**, 137868, arXiv:2212.01078 [gr-qc].
- Fierz, M., and W. Pauli (1939), Proc. Roy. Soc. Lond. **A173**, 211.
- Figueroa, D. G., and C. T. Byrnes (2017), Phys. Lett. B **767**, 272, arXiv:1604.03905 [hep-ph].
- Figueroa, D. G., and E. H. Tanin (2019), JCAP **10**, 050, arXiv:1811.04093 [astro-ph.CO].
- Fixsen, D. J., E. S. Cheng, J. M. Gales, J. C. Mather, R. A. Shafer, and E. L. Wright (1996), Astrophys. J. **473**, 576, arXiv:astro-ph/9605054.
- Ford, L. H. (1987), Phys. Rev. D **35**, 2955.
- Ford, L. H. (2021), Rept. Prog. Phys. **84** (11), 10.1088/1361-6633/ac1b23, arXiv:2112.02444 [gr-qc].
- Ford, L. H., and L. Parker (1977a), Phys. Rev. D **16**, 245.
- Ford, L. H., and L. Parker (1977b), Phys. Rev. D **16**, 1601.
- Ford, L. H., and L. Parker (1978), Phys. Rev. D **17**, 1485.
- Freedman, D. Z., and A. Van Proeyen (2012), *Supergravity* (Cambridge Univ. Press, Cambridge, UK).
- Friedmann, A. (1922), Zeitschrift für Physik **10**, 377.
- Friedmann, A. (1924), Zeitschrift für Physik **21** (1), 326.
- Frolov, V. M., S. G. Mamaev, and V. M. Mostepanenko (1976), Phys. Lett. **A55**, 389.
- Fujikura, K., S. Hashiba, and J. Yokoyama (2023), Phys. Rev. D **107** (6), 063537, arXiv:2210.05214 [hep-ph].
- Fukugita, M., and T. Yanagida (1986), Phys. Lett. B **174**, 45.
- Fulling, S. A., and L. Parker (1974), Annals Phys. **87**, 176.
- Fulling, S. A., L. Parker, and B. L. Hu (1974), Phys. Rev. D **10**, 3905.
- Garcia, M. A. G., K. Kaneta, W. Ke, Y. Mambrini, K. A. Olive, and S. Verner (2023a), arXiv:2311.14794 [hep-ph].
- Garcia, M. A. G., K. Kaneta, Y. Mambrini, K. A. Olive, and S. Verner (2022), JCAP **03** (03), 016, arXiv:2109.13280 [hep-ph].
- Garcia, M. A. G., Y. Mambrini, K. A. Olive, and S. Verner (2020), Phys. Rev. D **102** (8), 083533, arXiv:2006.03325 [hep-ph].
- Garcia, M. A. G., M. Pierre, and S. Verner (2023b), arXiv:2305.14446 [hep-ph].
- Garcia, M. A. G., M. Pierre, and S. Verner (2023c), Phys. Rev. D **107** (12), 123508, arXiv:2303.07359 [hep-ph].
- Garcia, M. A. G., M. Pierre, and S. Verner (2023d), Phys. Rev. D **107** (4), 043530, arXiv:2206.08940 [hep-ph].
- Garny, M., A. Palessandro, M. Sandora, and M. S. Sloth (2018), JCAP **02**, 027, arXiv:1709.09688 [hep-ph].
- Garny, M., A. Palessandro, M. Sandora, and M. S. Sloth (2019), JCAP **01**, 021, arXiv:1810.01428 [hep-ph].
- Garny, M., M. Sandora, and M. S. Sloth (2016), Phys. Rev. Lett. **116** (10), 101302, arXiv:1511.03278 [hep-ph].
- Ghiglieri, J., G. Jackson, M. Laine, and Y. Zhu (2020), JHEP **07**, 092, arXiv:2004.11392 [hep-ph].
- Ghiglieri, J., and M. Laine (2015), JCAP **07**, 022, arXiv:1504.02569 [hep-ph].
- Ghiglieri, J., J. Schütte-Engel, and E. Speranza (2022), arXiv:2211.16513 [hep-ph].
- Ghoshal, A., R. Samanta, and G. White (2023), Phys. Rev. D **108** (3), 035019, arXiv:2211.10433 [hep-ph].
- Giovannini, M. (1998), Phys. Rev. D **58**, 083504, arXiv:hep-ph/9806329.
- Giovannini, M. (1999), Phys. Rev. D **60**, 123511, arXiv:astro-ph/9903004.
- Giudice, G. F., E. W. Kolb, and A. Riotto (2001), Phys. Rev. D **64**, 023508, arXiv:hep-ph/0005123 [hep-ph].
- Giudice, G. F., A. Riotto, and I. Tkachev (1999a), JHEP **11**, 036, arXiv:hep-ph/9911302.
- Giudice, G. F., I. Tkachev, and A. Riotto (1999b), JHEP **08**, 009, arXiv:hep-ph/9907510.
- Golkar, S., D. X. Nguyen, M. M. Roberts, and D. T. Son (2016), Phys. Rev. Lett. **117** (21), 216403, arXiv:1602.08499 [cond-mat.mes-hall].
- Golovnev, A., V. Mukhanov, and V. Vanchurin (2008), JCAP **06**, 009, arXiv:0802.2068 [astro-ph].
- Gondolo, P., and G. Gelmini (1991), Nucl. Phys. B **360**, 145.
- Marañón González, F. J., and J. Navarro-Salas (2023), Phys. Rev. D **108** (12), 125001, arXiv:2310.11860 [gr-qc].
- Gonzalez-Ballester, C., M. Asplmeyer, L. Novotny, R. Quidant, and O. Romero-Isart (2021), Science **374** (6564), eabg3027, arXiv:2111.05215 [quant-ph].
- Gorji, M. A. (2023), JCAP **11**, 081, arXiv:2305.13381 [astro-ph.CO].
- Graham, P. W., J. Mardon, and S. Rajendran (2016), Phys. Rev. D **93** (10), 103520, arXiv:1504.02102 [hep-ph].
- Greisen, K. (1966), Phys. Rev. Lett. **16**, 748.
- Grib, A. A., S. G. Mamaev, and V. M. Mostepanenko (1976), Gen. Rel. Grav. **7**, 535.

- Grib, A. A., S. G. Mamayev, and V. M. Mostepanenko (1994), *Vacuum quantum effects in strong fields* (Friedmann Laboratory Publishing, St.Petersburg).
- Griest, K., and M. Kamionkowski (1990), Phys. Rev. Lett. **64**, 615.
- Grishchuk, L. P. (1974), Zh. Eksp. Teor. Fiz. **67**, 825.
- Gross, C., S. Karamitsos, G. Landini, and A. Strumia (2021), JHEP **03**, 174, arXiv:2012.12087 [hep-ph].
- Gumrukcuoglu, A. E., L. Heisenberg, S. Mukohyama, and N. Tanahashi (2015), JCAP **04**, 008, arXiv:1501.02790 [hep-th].
- Hall, L. J., K. Jedamzik, J. March-Russell, and S. M. West (2010), JHEP **03**, 080, arXiv:0911.1120 [hep-ph].
- Haque, M. R., and D. Maity (2022), Phys. Rev. D **106** (2), 023506, arXiv:2112.14668 [hep-ph].
- Haro, J., W. Yang, and S. Pan (2019), JCAP **01**, 023, arXiv:1811.07371 [gr-qc].
- Hasegawa, F., K. Mukaida, K. Nakayama, T. Terada, and Y. Yamada (2017), Phys. Lett. B **767**, 392, arXiv:1701.03106 [hep-ph].
- Hashiba, S., S. Ling, and A. J. Long (2022), JHEP **09**, 216, arXiv:2206.14204 [hep-th].
- Hashiba, S., and Y. Yamada (2021), JCAP **05**, 022, arXiv:2101.07634 [hep-th].
- Hashiba, S., and J. Yokoyama (2019a), Phys. Lett. B **798**, 135024, arXiv:1905.12423 [hep-ph].
- Hashiba, S., and J. Yokoyama (2019b), Phys. Rev. D **99** (4), 043008, arXiv:1812.10032 [hep-ph].
- Hashiba, S., and J. Yokoyama (2019c), JCAP **01**, 028, arXiv:1809.05410 [gr-qc].
- Hassan, S. F., and R. A. Rosen (2012), JHEP **02**, 126, arXiv:1109.3515 [hep-th].
- Hawking, S. W. (1974), Nature **248**, 30.
- Heisenberg, W., and H. Euler (1936), Z. Phys. **98** (11-12), 714, arXiv:physics/0605038 [physics].
- Herring, N., and D. Boyanovsky (2020), Phys. Rev. D **101** (12), 123522, arXiv:2005.00391 [astro-ph.CO].
- Herring, N., D. Boyanovsky, and A. R. Zentner (2020), Phys. Rev. D **101** (8), 083516, arXiv:1912.10859 [gr-qc].
- Higuchi, A. (1987), Nucl. Phys. B **282**, 397.
- Hikage, C., K. Koyama, T. Matsubara, T. Takahashi, and M. Yamaguchi (2009), Mon. Not. Roy. Astron. Soc. **398**, 2188, arXiv:0812.3500 [astro-ph].
- Himmetoglu, B., C. R. Contaldi, and M. Peloso (2009), Phys. Rev. Lett. **102**, 111301, arXiv:0809.2779 [astro-ph].
- Hinterbichler, K. (2012), Rev. Mod. Phys. **84**, 671, arXiv:1105.3735 [hep-th].
- Hook, A., G. Marques-Tavares, and D. Racco (2021), JHEP **02**, 117, arXiv:2010.03568 [hep-ph].
- Hooper, D., and G. Krnjaic (2021), Phys. Rev. D **103** (4), 043504, arXiv:2010.01134 [hep-ph].
- Hooper, D., G. Krnjaic, and S. D. McDermott (2019), JHEP **08**, 001, arXiv:1905.01301 [hep-ph].
- Hu, W., and J. Silk (1993), Phys. Rev. Lett. **70**, 2661.
- Hubble, E. (1929), Proc. Nat. Acad. Sci. **15**, 168.
- Iršič, V., *et al.* (2017), Phys. Rev. D **96** (2), 023522, arXiv:1702.01764 [astro-ph.CO].
- Ishiwata, K., O. Macias, S. Ando, and M. Arimoto (2020), JCAP **01**, 003, arXiv:1907.11671 [astro-ph.HE].
- Jeffreys, H. (1925), Proc. Lond. Math. Soc. **23**, 428.
- Jenks, L., E. W. Kolb, A. J. Long, and K. Thyme (2024), In preparation.
- Jenks, L., K. Koutrolikos, E. McDonough, S. Alexander, and S. J. Gates, Jr. (2023), Phys. Lett. B **842**, 137956, arXiv:2212.07442 [hep-ph].
- Kachelriess, M., O. E. Kalashev, and M. Y. Kuznetsov (2018), Phys. Rev. D **98** (8), 083016, arXiv:1805.04500 [astro-ph.HE].
- Kallosh, R., L. Kofman, A. D. Linde, and A. Van Proeyen (2000), Phys. Rev. **D61**, 103503, arXiv:hep-th/9907124 [hep-th].
- Kallosh, R., and A. Linde (2013), JCAP **10**, 033, arXiv:1307.7938 [hep-th].
- Kallosh, R., and A. D. Linde (2004), JHEP **12**, 004, arXiv:hep-th/0411011.
- Kamada, K., J. Kume, Y. Yamada, and J. Yokoyama (2020), JCAP **01**, 016, arXiv:1911.02657 [hep-ph].
- Kamionkowski, M., and E. D. Kovetz (2016), Ann. Rev. Astron. Astrophys. **54**, 227, arXiv:1510.06042 [astro-ph.CO].
- Kaneta, K., W. Ke, Y. Mambrini, K. A. Olive, and S. Verner (2023), arXiv:2309.15146 [hep-ph].
- Kaneta, K., S. M. Lee, and K. ya Oda (2022), Journal of Cosmology and Astroparticle Physics **2022** (09), 018.
- Kaneta, K., Y. Mambrini, and K. A. Olive (2019), Phys. Rev. D **99** (6), 063508, arXiv:1901.04449 [hep-ph].
- Kannike, K., A. Racioppi, and M. Raidal (2017), Nucl. Phys. B **918**, 162, arXiv:1605.09378 [hep-ph].
- Karam, A., M. Raidal, and E. Tomberg (2021), JCAP **03**, 064, arXiv:2007.03484 [astro-ph.CO].
- Kawasaki, M., K. Kohri, T. Moroi, and Y. Takaesu (2018), Phys. Rev. D **97** (2), 023502, arXiv:1709.01211 [hep-ph].
- Kawasaki, M., and T. Moroi (1995), Prog. Theor. Phys. **93**, 879, arXiv:hep-ph/9403364.
- Khlopov, M. Y., and A. D. Linde (1984), Phys. Lett. B **138**, 265.
- Kim, J. H., S. Kumar, A. Martin, and Y. Tsai (2021), JHEP **11**, 158, arXiv:2107.09061 [hep-ph].
- Kim, T., J. H. Kim, S. Kumar, A. Martin, M. Münchmeyer, and Y. Tsai (2023), Phys. Rev. D **108** (4), 043525, arXiv:2303.08869 [hep-ph].
- Kodama, H., and M. Sasaki (1984), Prog. Theor. Phys. Suppl. **78**, 1.
- Kofman, L., A. D. Linde, and A. A. Starobinsky (1994), Phys. Rev. Lett. **73**, 3195, arXiv:hep-th/9405187.
- Kofman, L., A. D. Linde, and A. A. Starobinsky (1997), Phys. Rev. D **56**, 3258, arXiv:hep-ph/9704452.
- Kolb, E. W., D. J. H. Chung, and A. Riotto (1999a), in *Proceedings, 2nd International Heidelberg Conference on Dark matter in astrophysics and particle physics (DARK 1998): Heidelberg, Germany, July 20-25, 1998*, edited by H. V. Klapdor-Kleingrothaus and L. Baudis (IOP, Bristol, UK).
- Kolb, E. W., D. J. H. Chung, and A. Riotto (1999b), AIP Conf. Proc. **484** (1), 91, arXiv:hep-ph/9810361.
- Kolb, E. W., A. D. Linde, and A. Riotto (1996), Phys. Rev. Lett. **77**, 4290, arXiv:hep-ph/9606260.
- Kolb, E. W., S. Ling, A. J. Long, and R. A. Rosen (2023a), JHEP **05**, 181, arXiv:2302.04390 [astro-ph.CO].
- Kolb, E. W., and A. J. Long (2017), Phys. Rev. **D96** (10), 103540, arXiv:1708.04293 [astro-ph.CO].
- Kolb, E. W., and A. J. Long (2021), JHEP **03**, 283, arXiv:2009.03828 [astro-ph.CO].
- Kolb, E. W., A. J. Long, and E. McDonough (2021a), Phys. Rev. D **104** (7), 075015, arXiv:2102.10113 [hep-th].
- Kolb, E. W., A. J. Long, and E. McDonough (2021b), Phys. Rev. Lett. **127** (13), 131603, arXiv:2103.10437 [hep-th].
- Kolb, E. W., A. J. Long, E. McDonough, and G. Payeur (2023b), JHEP **02**, 181, arXiv:2211.14323 [hep-th].
- Kolb, E. W., A. Riotto, and I. I. Tkachev (1998), Phys. Lett.

- B **423**, 348, arXiv:hep-ph/9801306.
- Kolb, E. W., and M. S. Turner (1990), *The Early Universe* (CRC Press, Boca Raton, FL).
- Kolb, E. W., and S. Wolfram (1980), Nucl. Phys. B **172**, 224, [Erratum: Nucl.Phys.B 195, 542 (1982)].
- Kramers, H. A. (1926), Z. Phys. **39** (10), 828.
- Krauss, L. M. (1983), Nucl. Phys. B **227**, 556.
- Kuo, C.-I., and L. H. Ford (1993), Phys. Rev. D **47**, 4510, arXiv:gr-qc/9304008.
- Kuzmin, V., and I. Tkachev (1998), JETP Lett. **68**, 271, [Pisma Zh. Eksp. Teor. Fiz.68,255(1998)], arXiv:hep-ph/9802304 [hep-ph].
- Kuzmin, V., and I. Tkachev (1999), Phys. Rev. **D59**, 123006, arXiv:hep-ph/9809547 [hep-ph].
- Kuzmin, V. A., and V. A. Rubakov (1998), Phys. Atom. Nucl. **61**, 1028, arXiv:astro-ph/9709187.
- Landau, L. D., and E. M. Lifschits (1980), *The Classical Theory of Fields*, 4th ed., Course of Theoretical Physics, Vol. Volume 2 (Pergamon Press, Oxford).
- Landete, A., J. Navarro-Salas, and F. Torrenti (2013), Phys. Rev. D **88**, 061501, arXiv:1305.7374 [gr-qc].
- Landete, A., J. Navarro-Salas, and F. Torrenti (2014), Phys. Rev. D **89**, 044030, arXiv:1311.4958 [gr-qc].
- Lee, H., D. Baumann, and G. L. Pimentel (2016), JHEP **12**, 040, arXiv:1607.03735 [hep-th].
- Lemaître, A. G. (1931), Monthly Notices of the Royal Astronomical Society **91** (5), 483, <https://academic.oup.com/mnras/article-pdf/91/5/483/3079971/mnras91-0483.pdf>.
- Li, L., T. Nakama, C. M. Sou, Y. Wang, and S. Zhou (2019), JHEP **07**, 067, arXiv:1903.08842 [astro-ph.CO].
- Liddle, A. R., and A. Mazumdar (2000), Phys. Rev. **D61**, 123507, arXiv:astro-ph/9912349 [astro-ph].
- Liddle, A. R., and L. A. Urena-Lopez (2003), Phys. Rev. D **68**, 043517, arXiv:astro-ph/0302054.
- Linde, A. D. (1983), Phys. Lett. B **129**, 177.
- Ling, S., and A. J. Long (2021), Phys. Rev. D **103** (10), 103532, arXiv:2101.11621 [astro-ph.CO].
- Lue, A., L.-M. Wang, and M. Kamionkowski (1999), Phys. Rev. Lett. **83**, 1506, arXiv:astro-ph/9812088.
- Maldacena, J. M. (2003), JHEP **05**, 013, arXiv:astro-ph/0210603.
- Mamaev, S. G., V. M. Mostepanenko, and A. A. Starobinsky (1976), Zh. Eksp. Teor. Fiz. **70**, 1577.
- Mambrini, Y., and K. A. Olive (2021), Phys. Rev. D **103** (11), 115009, arXiv:2102.06214 [hep-ph].
- Mambrini, Y., K. A. Olive, and J. Zheng (2022), JCAP **10**, 055, arXiv:2208.05859 [hep-ph].
- Mambrini, Y., S. Profumo, and F. S. Queiroz (2016), Phys. Lett. B **760**, 807, arXiv:1508.06635 [hep-ph].
- Markkanen, T., and S. Nurmi (2017), JCAP **02**, 008, arXiv:1512.07288 [astro-ph.CO].
- Markkanen, T., and A. Rajantie (2017), JHEP **01**, 133, arXiv:1607.00334 [gr-qc].
- Martin, J. (2008), Lect. Notes Phys. **738**, 193, arXiv:0704.3540 [hep-th].
- Martin, J., C. Ringeval, and V. Vennin (2014), Phys. Dark Univ. **5-6**, 75, arXiv:1303.3787 [astro-ph.CO].
- Misner, C. W., K. S. Thorne, and J. A. Wheeler (1973), *Gravitation* (W. H. Freeman, San Francisco).
- Monteiro, F., G. Afek, D. Carney, G. Krnjaic, J. Wang, and D. C. Moore (2020), Phys. Rev. Lett. **125** (18), 181102, arXiv:2007.12067 [hep-ex].
- Moore, D. C., and A. A. Geraci (2021), Quantum Sci. Tech. nol. **6**, 014008, arXiv:2008.13197 [quant-ph].
- Mukhanov, V. (2005), *Physical Foundations of Cosmology* (Cambridge University Press, Oxford).
- Mukhanov, V., and S. Winitzki (2007), *Introduction to quantum effects in gravity* (Cambridge University Press).
- Mukhanov, V. F. (1988), Sov. Phys. JETP **67**, 1297, [Zh. Eksp. Teor. Fiz.94N7,1(1988)].
- Mukhanov, V. F., and G. V. Chibisov (1981), JETP Lett. **33**, 532.
- Mukhanov, V. F., H. A. Feldman, and R. H. Brandenberger (1992), Phys. Rept. **215**, 203.
- Nakahara, M. (2003), *Geometry, topology and physics* (Taylor & Francis).
- Nakayama, K., and Y. Tang (2019), Phys. Lett. B **788**, 341, arXiv:1810.04975 [hep-ph].
- Nanopoulos, D. V., K. A. Olive, and M. Srednicki (1983), Phys. Lett. B **127**, 30.
- Niemeyer, J. C., and K. Jedamzik (1999), Phys. Rev. **D59**, 124013, arXiv:astro-ph/9901292 [astro-ph].
- Nilles, H. P., M. Peloso, and L. Sorbo (2001a), JHEP **04**, 004, arXiv:hep-th/0103202.
- Nilles, H. P., M. Peloso, and L. Sorbo (2001b), Phys. Rev. Lett. **87**, 051302, arXiv:hep-ph/0102264.
- Nishi, S., and T. Kobayashi (2016), JCAP **04**, 018, arXiv:1601.06561 [hep-th].
- Nishizawa, A., and H. Motohashi (2014), Phys. Rev. D **89** (6), 063541, arXiv:1401.1023 [astro-ph.CO].
- Noumi, T., M. Yamaguchi, and D. Yokoyama (2013), JHEP **06**, 051, arXiv:1211.1624 [hep-th].
- Olive, K. A., D. N. Schramm, and M. Srednicki (1985), Nucl. Phys. B **255**, 495.
- Opferkuch, T., P. Schwaller, and B. A. Stefanek (2019), JCAP **07**, 016, arXiv:1905.06823 [gr-qc].
- Özsoy, O., and G. Tasinato (2023), arXiv:2310.03862 [astro-ph.CO].
- Parker, L. (1965), *The Creation of Particles in an Expanding Universe*, Ph.D. thesis (Harvard U.).
- Parker, L. (1968), Phys. Rev. Lett. **21**, 562.
- Parker, L. (1969), Phys. Rev. **183**, 1057.
- Parker, L. (1971), Phys. Rev. **D3**, 346, [Erratum: Phys. Rev.D3,2546(1971)].
- Parker, L. (1972), Phys. Rev. Lett. **28**, 705, [Erratum: Phys. Rev. Lett.28,1497(1972)].
- Parker, L., and S. A. Fulling (1974), Phys. Rev. **D9**, 341.
- Parker, L. E., and D. Toms (2009), *Quantum Field Theory in Curved Spacetime: Quantized Field and Gravity*, Cambridge Monographs on Mathematical Physics (Cambridge University Press).
- Passaglia, S., W. Hu, A. J. Long, and D. Zegeye (2021), Phys. Rev. D **104** (8), 083540, arXiv:2108.00962 [hep-ph].
- Perez-Gonzalez, Y. F., and J. Turner (2021), Phys. Rev. D **104** (10), 103021, arXiv:2010.03565 [hep-ph].
- Proca, A. (1936), J. Phys. Radium **7**, 347.
- Rarita, W., and J. Schwinger (1941), Phys. Rev. **60**, 61.
- Redi, M., A. Tesi, and H. Tillim (2021), JHEP **05**, 010, arXiv:2011.10565 [hep-ph].
- de Rham, C. (2014), Living Rev. Rel. **17**, 7, arXiv:1401.4173 [hep-th].
- de Rham, C., L. Heisenberg, and R. H. Ribeiro (2015), Class. Quant. Grav. **32**, 035022, arXiv:1408.1678 [hep-th].
- Riazuelo, A., and J.-P. Uzan (2000), Phys. Rev. D **62**, 083506, arXiv:astro-ph/0004156.
- Ringwald, A., J. Schütte-Engel, and C. Tamarit (2021),

- JCAP **03**, 054, arXiv:2011.04731 [hep-ph].
- del Rio, A., J. Navarro-Salas, and F. Torrenti (2014), Phys. Rev. D **90** (8), 084017, arXiv:1407.5058 [gr-qc].
- Robertson, H. P. (1935a), Astrophys. J. **82**, 284.
- Robertson, H. P. (1935b), Astrophys. J. **83**, 187.
- Robertson, H. P. (1936), Astrophys. J. **83**, 257.
- Rosenfeld, L. (1940), Mémoires Acad. Roy. de Belgique **18** (6), 1.
- Rubakov, V. A., M. V. Sazhin, and A. V. Veryaskin (1982), Phys. Lett. B **115**, 189.
- Sagnotti, A. (2013), J. Phys. A **46**, 214006, arXiv:1112.4285 [hep-th].
- Sahni, V., M. Sami, and T. Souradeep (2002), Phys. Rev. D **65**, 023518, arXiv:gr-qc/0105121.
- Sakharov, A. D. (1967), Pisma Zh. Eksp. Teor. Fiz. **5**, 32.
- de Salas, P. F., M. Lattanzi, G. Mangano, G. Miele, S. Pastor, and O. Pisanti (2015), Phys. Rev. D **92** (12), 123534, arXiv:1511.00672 [astro-ph.CO].
- Sami, M., N. Dadhich, and T. Shiromizu (2003), Phys. Lett. B **568**, 118, arXiv:hep-th/0304187.
- Sasaki, M. (1983), Prog. Theor. Phys. **70**, 394.
- Sauter, F. (1931), Z. Phys. **69**, 742.
- Schiappacasse, E. D., and L. H. Ford (2016), Phys. Rev. D **94** (8), 084030, arXiv:1602.08416 [gr-qc].
- Schrödinger, E. (1939), PHYSICA **6** (7–12), 899.
- Schwinger, J. S. (1951), Phys. Rev. **82**, 664, [116(1951)].
- Sendra, I., and T. L. Smith (2012), Phys. Rev. D **85**, 123002, arXiv:1203.4232 [astro-ph.CO].
- Shtanov, Y., J. H. Traschen, and R. H. Brandenberger (1995), Phys. Rev. D **51**, 5438, arXiv:hep-ph/9407247.
- de Sitter, W. (1916a), Mon. Not. Roy. Astron. Soc. **76**, 699.
- de Sitter, W. (1916b), Mon. Not. Roy. Astron. Soc. **77**, 155.
- de Sitter, W. (1917), Mon. Not. Roy. Astron. Soc. **78**, 3.
- Sou, C. M., X. Tong, and Y. Wang (2021), JHEP **06**, 129, arXiv:2104.08772 [hep-th].
- Starobinsky, A. A. (1979), JETP Lett. **30**, 682.
- Suen, W. M., and P. R. Anderson (1987), Phys. Rev. D **35**, 2940.
- Tang, Y., and Y.-L. Wu (2016), Phys. Lett. B **758**, 402, arXiv:1604.04701 [hep-ph].
- Tang, Y., and Y.-L. Wu (2017), Phys. Lett. B **774**, 676, arXiv:1708.05138 [hep-ph].
- Tashiro, H., T. Chiba, and M. Sasaki (2004), Class. Quant. Grav. **21**, 1761, arXiv:gr-qc/0307068.
- Tenkanen, T. (2019), Phys. Rev. Lett. **123** (6), 061302, arXiv:1905.01214 [astro-ph.CO].
- Terada, T. (2021), Phys. Rev. D **103** (12), 125022, arXiv:2104.05731 [hep-th].
- Traschen, J. H., and R. H. Brandenberger (1990), Phys. Rev. D **42**, 2491.
- Tulin, S., and H.-B. Yu (2018), Phys. Rept. **730**, 1, arXiv:1705.02358 [hep-ph].
- Turner, M. S., and L. M. Widrow (1988), Phys. Rev. D **37**, 3428.
- Viel, M., G. D. Becker, J. S. Bolton, and M. G. Haehnelt (2013), Phys. Rev. D **88**, 043502, arXiv:1306.2314 [astro-ph.CO].
- Vilenkin, A. (1985), Phys. Rev. D **32**, 2511.
- Wald, R. M. (1984), *General Relativity* (Chicago Univ. Pr., Chicago, USA).
- Wald, R. M. (1995), *Quantum Field Theory in Curved Space-Time and Black Hole Thermodynamics*, Chicago Lectures in Physics (University of Chicago Press, Chicago, IL).
- Walker, A. G. (1937), Proceedings of the London Mathematical Society **s2-42** (1), 90.
- Weinberg, S. (1964), Phys. Rev. **135**, B1049.
- Weinberg, S. (1965), Phys. Rev. **140**, B516.
- Weinberg, S. (1972), *Gravitation and Cosmology: Principles and Applications of the General Theory of Relativity* (John Wiley and Sons, New York).
- Weinberg, S. (2005), *The Quantum theory of fields. Vol. 1: Foundations* (Cambridge University Press).
- Weinberg, S., and E. Witten (1980), Phys. Lett. B **96**, 59.
- Wentzel, G. (1926), Z. Phys. **38** (6), 518.
- Weyl, H. (1929), Z. Phys. **56**, 330.
- Wilczek, F. (1980), Sci. Am. **243N6**, 60.
- Yajnik, U. A. (1990), Phys. Lett. **B234**, 271.
- Yu, Z., C. Fu, and Z.-K. Guo (2023), arXiv:2307.03120 [gr-qc].
- Zatsepin, G. T., and V. A. Kuzmin (1966), JETP Lett. **4**, 78.
- Zel'dovich, Y. B. (1970), JETP Lett. **12**, 307.
- Zel'dovich, Y. B., and A. A. Starobinsky (1977), JETP Lett. **26** (5), 252, [Pis'ma Zh. Eksp. Teor. Fiz.26,no.5,373(1977)].
- Zeldovich, Ya. B., and A. A. Starobinsky (1972), Sov. Phys. JETP **34**, 1159, [Zh. Eksp. Teor. Fiz.61,2161(1971)].
- Zhang, R., Z. Xu, and S. Zheng (2023), JCAP **07**, 048, arXiv:2305.02568 [hep-ph].
- Zhang, R., and S. Zheng (2023), arXiv:2311.14273 [hep-ph].